# THERMAL ANALYSIS OF STEEL COLUMNS EXPOSED TO LOCALISED FIRES

Author: Gonçalo Ferraz

Supervisors: Professor Aldina Maria da Cruz Santiago
Professor João Paulo Correia Rodrigues

University: University of Coimbra

European Commission
ERASMUS MUNDUS

University: University of Coimbra

Date: 13.01.2014

# ACKNOWLEDGEMENTS

The author would like to express his gratitude to Professor Aldina Santiago, for the excellent supervision, guidance and support through this thesis, but also for solving all the scientific, technical and institutional problems. The opinions from his second supervisor, Professor João Paulo Correia Rodrigues, were extremely appreciated, having great value in the development of this thesis. To Engineer Pedro Barata, a special word of appreciation, for his measureless help during the fire tests, despite of the tight schedule of his own work.

The assistance provided by the technical staff of ISISE Research Institute, in particular Luis Gaspar, was appreciated for their advices, comments and commitment during the experimental work.

The author would like to acknowledge CBS Fire Fighting Unit (*Companhia de Bombeiros Sapadores*) of Coimbra for the provided services.

Special acknowledgments are addressed to the Erasmus Mundus SUSCOS_M Consortium, for the Consortium Grant. The author acknowledges, as well, the financial support from FEDER and OE - *Ministério da Educação e da Ciência (Fundação para a Ciência e Tecnologia)* under research project *PTDC/ECM/110807/2009*.

Finally, the support of the author's family, girlfriend and friends was deeply rewarding.

## ABSTRACT

Fire design plays an essential role in the design of steel structures. The most common method for fire design of steel structures is to design the building for ambient temperature and to protect the structural members using passive fire protection materials to ensure that a specific temperature is not exceeded. The main limitation of this approach is that it often assumes that the steel members fire resistance time in standard fire tests is the same as their resistance time in a real fire, which can be more or less severe than the standard fire test depending on the characteristics of the fire enclosure. The temperature-time curve ISO 834, used in standard fire tests, is intended for relatively small compartments where flashover is likely to occur but in large compartments like car parks, airport terminals and big industrial halls, distributed temperatures characteristics of post-flashover stages are totally unlikely to occur. In these cases, the thermal actions of a localised fire must be taken into account. Concerning the localised fire effect in exposed steel members, considerable studies have been conducted regarding the flame heating of steel beams subjected to localised fires and EN 1991-1-2 (2002) presents a simplified model to calculate temperatures in a ceiling slab and in the beams supporting the slab. However, no simplified model to calculate the heat transfer to vertical elements, such as columns, is yet available. Therefore, there is an urgent need to investigate the effects of localised fires in building compartments and especially on exposed steel columns. For this purpose, this dissertation is focused in thermal analysis of steel columns exposed to localised fires. This work presents full-scale experiments on steel columns exposed to pool fires. Different fire loads, fire position and ventilation conditions were tested in order to establish heat transfer correlations. Experimental results were analysed and validated by analytic and numerical methods. As main conclusion, it was establish that localised fire leads a steel column an asymmetric distribution of temperatures along the total column height is verified. Concerning the relative position between the column and the localised fire, the thermal gradient in the cross sections is significant for short distances, whereas for larger distances it becomes less significant. The ventilation conditions within a compartment have great influence in the thermal exposure associated to a localised fire.

## KEY WORDS

Localised fire, steel columns, thermal analysis, experimental evaluation

## RESUMO

O dimensionamento ao fogo é um requisito fundamental no projeto de estruturas metálicas. O método mais utilizado para o dimensionamento ao fogo das estruturas em aço consiste em realizar o dimensionamento para a temperatura ambiente e revestir os elementos estruturais com materiais de proteção ao fogo para garantir que a temperatura no aço não atinge um valor máximo estabelecido, na eventualidade da ocorrência de incêndio. A principal limitação deste método prende-se com a assunção, de que o tempo de resistência ao fogo dos elementos estruturais obtido nos ensaios de resistência ao fogo é idêntico ao tempo de resistência a um fogo real, o qual poderá ser mais ou menos severo que o ensaio de resistência ao fogo. A curva ISO 834, a mais utilizada nos ensaios de resistência ao fogo, adequa-se a compartimentos relativamente pequenos, em que a probabilidade de ocorrência do fenómeno de flashover é alta; no entanto, em grandes compartimentos, como parques de estacionamento, terminais de aeroporto e grandes edifícios industriais, temperaturas distribuídos características de estágios de pós-flashover são totalmente improvável de ocorrer. Nos últimos anos, diversas investigações têm sido realizadas no âmbito do comportamento de vigas metálicas submetidas a fogos localizados e a EN 1991-1-2 (2002) apresenta métodos simplificados para o cálculo das temperaturas em lajes e vigas de teto numa situação de incêndio localizado. No entanto, não existem ainda modelos para o cálculo das temperaturas em colunas de aço. Neste sentido, é urgente o estudo dos efeitos dos fogos localizados em compartimentos e, especificamente, em colunas de aço. Esta investigação debruça-se sobre a análise térmica de colunas de aço expostas a fogos localizados. Este trabalho apresenta ensaios experimentaias de grande escala em colunas de aço expostas a incêndios localizados. Diferentes cargas térmicas, posições do fogo e condições de ventilação foram testados de modo a estabelecer correlações de transferência de calor. Os resultados experimentais foram analisados e validados por métodos analíticos e numéricos. Conclui-se que um incêndio localizado leva uma coluna de aço a uma distribuição assimétrica das temperaturas. Relativamente à posição relativa entre a coluna e o incêndio localizado, o gradiente térmico nas secções transversais é significativo para distâncias curtas, e menos significativo para maiores distancias. As condições de ventilação de um compartimento têm grande influência na duração de um fogo localised.

## PALAVRAS-CHAVE

Fogo localizado, colunas de aço, análise térmica, avaliação experimental.

# TABLE OF CONTENTS

# FIGURE INDEX

# TABLE INDEX

# NOTATIONS

| | |
|---|---|
| $A_f$ | is horizontal burning area of the fire source [$m^2$] |
| $A_m$ | lateral surface area of the steel profile exposed to fire [$m^2$] |
| $A_p$ | area of the inner surface of the fire protection material per unit length of the member [$m^2$] |
| $A_t$ | total area of enclosure (walls, ceiling and floor, including openings) [$m^2$] |
| $A_v$ | total area of vertical openings on all walls [$m^2$] |
| $A_v$ | area of window "i" [$m^2$] |
| b | thermal absorptivity for the total enclosure |
| c | specific heat [J/Kg.K] |
| $c_a$ | specific heat of steel [J/Kg.K] |
| $d_p$ | thickness of fire protection material [m] |
| D | diameter of burning area [m] |
| D | depth of the fire compartment [m] |
| $E_g$ | internal energy of gas [J] |
| H | distance between the fire source and the ceiling [m] |
| $h_{eq}$ | weighted average of window heights on all walls [m] |
| $\dot{h}$ | heat flux [$kW/m^2$] |
| $\dot{h}_{net}$ | net heat flux [$kW/m^2$] |
| $\dot{h}_{net,c}$ | convective component of net heat flux [$kW/m^2$] |
| $h_{net,d}$ | design value of the net heat flux [$W/m^2$] |
| $\dot{h}_{net,r}$ | radiative component of net heat flux [$kW/m^2$] |
| $k_{sh}$ | correction factor for the shadow effect |
| kβ | empirical constant [$m^{-1}$] |
| l | length at 20 °C [m] |
| $L_c$ | length of the core [m] |
| $L_f$ | flame length along axis [m] |
| $L_h$ | horizontal flame length [m] |
| m | non-dimensional combustion factor |
| $\dot{m}$ | burning rate [kg/sec] |
| $\dot{m}$” | burning rate per unit area per unit time [$kg/m^2$-sec] |
| $\dot{m}”_\infty$ | maximum burning rate per unit area per unit time [$kg/m^2$-sec] |
| $\dot{m}_{in}$ | rate of gas mass coming in through the openings [kg/sec] |
| $\dot{m}_{out}$ | rate of gas mass going out through the openings [kg/sec] |

| | |
|---|---|
| $\dot{m}_{fi}$ | rate of pyrolysis products generated [kg/sec] |
| O | opening factor of the fire compartment |
| $P_{int}$ | internal pressure [N/m$^2$] |
| $q_{f,d}$ | design fire load density related to the floor area $A_f$ [MJ/m$^2$] |
| $q_{f,k}$ | characteristic fire load density related to the surface area $A_f$ [MJ/m$^2$] |
| $q_{t,d}$ | design fire load density related to the surface area $A_t$ [MJ/m$^2$] |
| Q | heat release rate [MW] |
| $Q_c$ | convective part of the heat release rate [W], with $Q_c$ = 0.8 Q by default |
| $Q_{in}$ | heat release rate entering through openings by gas flow [W] |
| $Q_{out}$ | heat release rate lost through openings by gas flow [W] |
| $Q_{rad}$ | heat release rate lost by radiation through openings [W] |
| $Q_{wall}$ | heat release rate lost by radiation and convection to the surfaces of the compartment [W] |
| $Q_H^*$ | non-dimensional heat release rate |
| R | ideal gas constant (= 287 [J/kgK]) |
| r | horizontal distance from the vertical flame axis to the point along the ceiling [m] |
| T | temperature [K] |
| t | time in fire exposure [h] |
| $t_{lim}$ | time for maximum gas temperature in case of fuel controlled fire [h] |
| $t_{max}$ | time for maximum gas temperature [h] |
| V | volume [m$^3$] |
| W | width of wall containing window(s) [m] |
| $W_c$ | width of the core [m] |
| $W_1$ | width of the wall 1, assumed to contain the greatest window area [m] |
| $W_2$ | width of the wall of the fire compartment, perpendicular to wall $W_1$ [m] |
| $w_t$ | sum of window widths on all walls [m] |
| z | virtual origin of the axis [m] |
| z | height along the flame axis [m] |
| z' | vertical position of the virtual heat source [m] |
| $\alpha_c$ | coefficient of heat transfer by convection [W/m$^2$K] |
| $\rho_a$ | unit mass of steel [Kg/m3] |
| $\delta_{n,i}$ | factor accounting for the existence of a specific fire fighting measure i |
| $\delta_{q,1}$ | factor taking into account the fire activation risk due to the size of the compartment |
| $\delta_{q,2}$ | factor taking into account the fire activation risk due to the type of occupancy |
| $\Delta H_c$ | heat of combustion [kJ/kg] |
| $\Delta H_{c,eff}$ | effective heat of combustion [kJ/kg] |
| $\Delta l$ | temperature induced expansion [m] |

| | |
|---|---|
| $\Delta t$ | time interval [s] |
| $\varepsilon_f$ | emissivity of the fire |
| $\varepsilon_m$ | emissivity of the member [=1] |
| $\Theta_r$ | effective radiation temperature of the fire environment [°C] |
| $\Theta_g$ | gas temperature in the vicinity of the fire exposed member [ºC] |
| $\Theta_m$ | surface temperature of the member [°C] |
| $\lambda$ | thermal conductivity [W/mK] |
| $\rho$ | liquid fuel density [kg/m$^3$] |
| $\sigma$ | Stefan-Boltzmann Constant [=5.67x10$^{-11}$ kW/ s$^2$K$^4$] |
| $\upsilon$ | regression rate [m/sec] |
| $\phi$ | configuration factor |
| $\Gamma$ | time factor function of the opening factor O and the thermal absorptivity b |
| $\chi$ | efficiency of combustion |

## ABBREVIATIONS

| | |
|---|---|
| CFD | Computational Fluid Dynamics |
| EC | Eurocode |
| EN | European Norm |
| FCTUC | Faculdade de Ciências e Tecnologia da Universidade de Coimbra |
| FDS | Fire Dynamics Simulator |
| FEM | Finite Element Method |
| SIF | Structures in fire |
| TC | Thermocouple |
| SUSCOS | Sustainable Construction under natural hazards and catastrophic events |
| ISO | International Standard Organization |
| dia. | Diameter |

# 1 INTRODUCTION

## 1.1 Overview

With the development of new techniques and construction methods, steel construction has become essential for the process of industrialization and globalization of construction. Nowadays, large structural members may be pre-fabricated in industrial processes and assembled on site. Furthermore, the possibility of exportation enhances the attractiveness of steel construction market. Emerging economies namely China, Brazil and Angola are growing at incredible rates and their demands on construction industry are huge. Consequently, these markets provide multiple opportunities for companies facing reductions on domestic demands.

Within the design of structures, the use of steel provides high strength to weight ratio, a characteristic that allows steel structural systems to withstand large spans and support tall buildings whilst maintaining cost-effectiveness. For this reasons, steel is being used in large span structures, as industrial halls, and tall structures, as skyscrapers. Within the inherent properties of steel, its high thermal conductivity is another intrinsic property worth mentioning; when a steel structural member is heated in a fire, the temperature of the member will be increased into the member itself. Furthermore, steel strength decreases as the temperature increases beyond 400 ºC and it melts around 1500 °C (Franssen & Vila Real, 2010). However, unlike other structural materials such as wood, in which the loss of strength in fire situation is due to a reduction of cross sectional area, in steel structural elements the failure occurs due to the degradation of its mechanical properties in the presence of elevated temperatures. The steel strength reduction at elevated temperatures and the development of additional stresses due to the thermal expansion, make the current design of steel elements for ambient temperature inaccurate in a fire situation. Therefore, fire design plays a very important role in the design of steel structures.

Considered a landmark in the history of fire engineering, The Great Fire, which occurred in London in 1666, triggered a series of measures in order to decrease the risk of fires in buildings. Through these measures, the first regulations with respect to fire safety were prepared, which later contributed to the creation of the current standards for fire safety. In the mid-nineteenth century, decisive factors such as the industrial revolution, advances in

scientific fields namely in structural and mechanical engineering, in addition to the increasing migration to urban areas, contributed to the development of fire safety technology. In the last 30 years scientific investigation related to fire safety has gained emphasis, leading to the development of fire safety regulations, and of strategies and technologies aimed to minimize losses resulting from fires and to increasing knowledge about the behaviour of materials against fire, as well as the phenomena associated with it (Buchanan, 2008). Through these studies, it became possible to analyse the impact of fire in structures. Professionals and researchers began to be aware that the effects of fires can be evaluated and estimated in terms of some parameters, such as the fire load density, the opening factors of compartments and the boundary characteristics of enclosure.

The European Union has spent several years developing unified rules for the design of structures. In 1975, the European Commission launched a program responsible to establish a set of European standards, later called Eurocodes. In fire situation, the combinations of actions are different from those at ambient temperature. EN 1990 (2009) gives the combinations for accidental fire exposure. Fire actions are given in EN 1991-1-2 (2002), and the fire design of structures can be assessed using the part 1-2 of the Eurocodes (EC). Concerning the steel structures design, EN 1993-1-2 (2005) gives the rules for calculating the temperature development in the steel structures, the mechanical and thermal properties, and the rules for design of steel structures in fire.

According to EN 1991-1-2 (2002), the development of a fire can be reproduced through nominal curves, parametric curves, localised fires, zone models and Computational Fluid Dynamics models (CFD). EN 1991-1-2 (2002) presents three nominal curves: the standard temperature-time curve (ISO 834), the external fire curve and the hydrocarbon fire curve. These curves do not represent real fires but only a simplification since they do not consider the decay stage of a fire (cooling strains are ignored). Fire resistance of structural components (with or without thermal protection) is usually determined by the standard temperature-time curve ISO 834, for a specified time. In current fire design, parametric curves such as the ones specified in Annex A of EN 1991-1-2 (2002), may be applied instead of nominal curves (Byström et al., 2012). However, all these design fire curves are intended for relatively small compartments where flashover is likely to occur. Flashover is a stage of fire development, where the radiation from the burning flame and the hot smoke layer will cause an instant ignition of unburned materials, leading fire to the fully developed phase, with uniform temperatures, as represented in Figure 1.

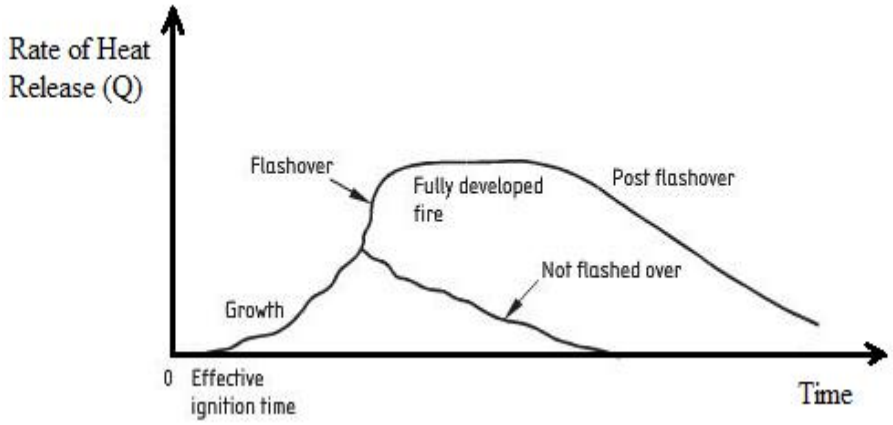


Figure 1- Phases of development of the fire (PD 7974-1, 2003)

According to EN 1991-1-2 (2002), in a natural fire "where flash-over is unlikely to occur, thermal actions of a localised fire should be taken into account". According to this statement, a localised fire may be considered as a not flashed over fire, where fully developed phase do not happen (Figure 1). There are many examples where structural elements are submitted only to a localised a fire. In large compartments like car parks, airport terminals, big industrial halls, or even at open spaces, uniformly distributed temperatures characteristics of post-flashover stages are totally unlikely to occur (Kamikawa et al., 2003).

Annex C of EN 1991-1-2 (2002) provides a simple calculation approach for determining localised fires of compartments. According to this method, the temperatures in the fire plume and the surrounding gas are not uniform and need to be determined separately. This is the main difference between a localised and a post-flashover fire (temperature is assumed to be uniform within the fire compartment). In order to estimate localised fire loads density, Annex E of EN 1991-1-2 (2002) proposes an evaluation of heat release rate in fire growing phase according to compartment occupancy. However, the use of average temperatures may not be safe to verify localised fire occurrence. If only a limited part of a structure is exposed to fire, its fire resistance may be significantly different from that obtained assuming uniform temperature distribution. This can lead to very conservative or even incorrect fire design. Moreover, beams and columns heated from one side usually develop an important temperature gradient across the cross-section, which will lead to the deflection of the member towards the heat source. The overall thermal expansion will also lead to the development of restraint forces at the ends of the member. This will cause additional normal moments and subsequently also second-order moments into the member (Outinen et al., 2010). Annex C and Annex E of EN 1991-1-2 (2002) have been contested, and its use was refused in United Kingdom (PD 6688-1-2, 2007) and Germany National Annex.

Concerning the localised fire effect in exposed steel members, considerable studies have been conducted regarding the flame heating of steel beams subjected to localised fires (Hasemi, 1986; Haremza et al., 2013; Zhang et al., 2013). EN 1991-1-2 (2002) presents a simplified model based on the experimental works performed by Hasemi (Hasemi, 1986), that is used to calculate temperatures in a ceiling slab and in the beams that eventually support the slab. However, no simplified model to calculate the heat transfer to vertical elements, such as columns, is available. Therefore, there is an urgent need to investigate the effects of localised fires in building compartments and especially on exposed steel columns.

## 1.2 Purpose and scope of this research

The main goal of this thesis is to improve the existing knowledge on the effects of localised fires in a building compartment, especially on steel columns. For this purpose the thermal impact from localised fires, determined according to the Annex C of EN 1991-1-2 (2002), is studied. This informative annex is based on plume theories: Hesketad method was adapted in order to model smaller or open-air fires, while Hasemi method was used to model larger fires impacting the ceiling (Karlsson & Quintiere, 2000). However, these theories were mainly developed for the determination of plume temperatures and flame heights, and not so much for thermal exposures on structural elements. Following Hasemi method, an equation is presented in order to assess the temperature of horizontal elements at the level of the ceiling, at a given distance from the fire source. However, no solution is yet presented to assess the steel temperature or the heat transfer to vertical elements such as columns. For this purpose, this dissertation is focused in thermal analysis of steel columns exposed to localised fires, in order to develop heat transfer correlations.

The research review concerning this subject showed that little experimental research has been carried out in the localised fire effect on columns. However, columns, as load-bearing elements, require careful examination because asymmetric fires may lead structural elements into buckling phenomenon. Also, columns can be heated directly by any nearby burning object in the event of a fire, while the heating of a beam is significant only when the flame becomes large enough to reach the beam. Although some studies have been carried out on the flame heating of steel columns, most of such works were not conclusive because the heat flux calculation in large fire compartments is still very difficult, mostly due to the complexity on the assessment of the radiative heat flux.

The design of steel structures for the accidental situation of a localised fire requires very detailed data concerning the steel temperature development. To be able to design for non-flashover fires there is a need for experimental data on real scale structures exposed to localised fires. This work presents full-scale experiments on steel columns exposed to pool

fires. The CHS 245 x 10 steel columns was exposed to a total of height fire tests, each of them simulating a distinct localised fire scenario. Different fire loads, fire position and ventilations conditions were tested in order to establish heat transfer correlations. Experimental results were analysed and validated by analytic and numerical methods.

## 1.3 Organization of the thesis

This thesis is organised in seven chapters. In the following paragraphs, a brief description of the contents of each is presented:

**Chapter 1 – Introduction**

Chapter 1 is an introduction to the research work presented in this thesis. The motivation for this work is also mentioned in this chapter, as well as its main goals.

**Chapter 2 – Thermal analysis of steel elements according to Eurocodes**

Chapter 2 presents the general procedure to evaluate thermal behaviour steel columns subjected to localised fires, according to EN 1991-1-2 (2002) and EN 1993-1-2 (2005). The thermal and mechanical properties of steel are mentioned. Thermal actions for temperature analysis are also described. The calculation of temperatures in structural elements is described.

**Chapter 3 – State-of-the-art on localised fires**

In Chapter 3 a brief review of the State-of-the-art is presented, concerning the thermal behaviour of steel columns exposed to localised fires.

**Chapter 4 – Estimation of heat release characteristics in localised fire scenario**

In Chapter 4, burning characteristics of fuel materials are presented. Heat release rate measurement methods are described and the concept of burning rate is introduced. Pool fires are introduced as a localised fire action.

**Chapter 5 –Experimental evaluation of heat transfer in localised fire scenario**

This chapter presents the full description of an experimental investigation on the heat transfer phenomenon into steel columns subjected to localised fires. Experimental result are presented and analysed within this chapter.

**Chapter 6 – Validation of experimental results**

Based on the analytical estimations and numerical tools available in literature, this chapter intends to provide a proper validation and understanding of the experimental results.

**Chapter 7 – Conclusions and future works**

Conclusions and future works are presented in Chapter 7. A great deal of conclusions was possible to draw, concerning the different kind of tests on the steel columns.

# 2 THERMAL ANALYSIS OF STEEL ELEMENTS ACCORDING TO EUROCODES

The specific procedures in EN 1991-1-2 (2002) and EN 1993-1-2 (2005) were used in the present research. EN 1991-1-2 (2002) describes the thermal and mechanical actions for the structural design of buildings exposed to fire, while EN 1993-1-2 (2005) deals with the design of steel structures for the accidental fire exposure, presenting the rules for the determination of temperature development in steel members and for the design of steel structures at elevated temperatures, establishing all the relevant mechanical and thermal properties of steel to be used in fire analyses. Relevant information on the scope of localised fire actions and thermal analysis of steel elements are presented in this chapter.

## 2.1 Steel thermal properties

The thermal conductivity (Figure 11a), the specific heat (Figure 11b) and the thermal elongation (Figure 12) of carbon steel are defined in EN 1993-1-2 (2005) as a function of temperature, according to the following graphs:

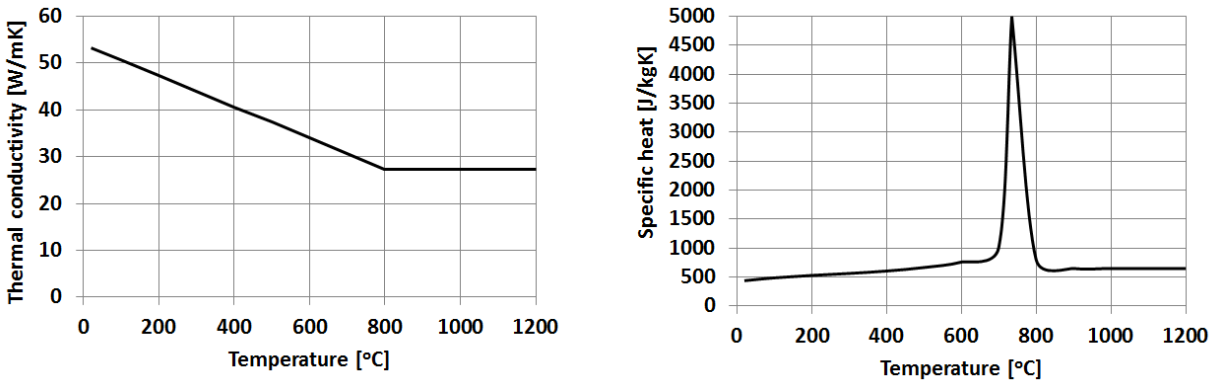


(a) (b)

Figure 2- (a) Thermal conductivity of carbon steel as function of the temperature; (b) Specific heat of carbon steel as function of the temperature (EN 1993-1-2, 2005)

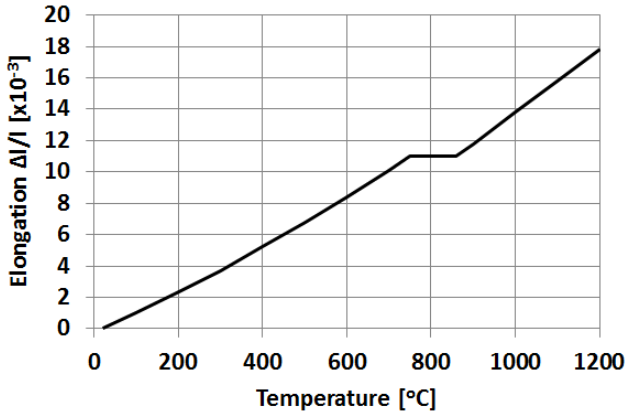


Figure 3- Relative elongation of carbon steel as function of temperature (EN 1993-1-2, 2005)

The thermal conductivity of steel varies according to the temperature as shown in Figure 2 (a), reducing linearly from 54 W/mK at 20 ºC to 27.3 W/mK at 800 ºC. The specific heat of steel varies according to temperature, as shown in Figure 2 (b), where the peak results from a metallurgical change about 730 ºC (Santiago, 2008). The relative elongation of carbon steel increases linearly according to temperature, as shown in Figure 3, and a discontinuity occurs between 750 and 860 ºC. For calculation purposes, these parameters may be calculated according to equations presented in EN 1993-1-2 (2005).

## 2.2 Thermal actions for temperature analysis – EN 1991-1-2 (2002) approach

### 2.2.1 Introduction

A thermal action represents the action of a fire on a structure and it is quantified by the net heat flux ($\dot{h}_{\text{net}}$) transmitted to the surface of a structural member. In accordance to EN 1991-1-2 (2002), the net heat flux should be determined on the fire exposed surfaces considering heat transfer by convection and radiation:

$$\dot{h}_{net} = \dot{h}_{net,c} + \dot{h}_{net,r} \tag{2.1}$$

Where:

$\dot{h}_{net,c}$ is the heat transfer by convection, given by equation (3.2);
$\dot{h}_{net,r}$ is the heat transfer by radiation, given by equation (3.3).

The convective component of net heat flux ($\dot{h}_{net,c}$) is given by the Newton law of cooling present in the EN 1991-1-2 (2002) as:

$$\dot{h}_{net,c} = \alpha_c . (\Theta_g - \Theta_m) \quad (2.2)$$

Where:

$\alpha_c$ is the coefficient of heat transfer by convection [W/m$^2$K];
$\Theta_g$ is the gas temperature in the vicinity of the fire exposed member [ºC];
$\Theta_m$ is the surface temperature of the member [ºC].

The radiative component of net heat flux is given by the Stefan–Boltzmann law present in the EN 1991-1-2 (2002) as:

$$\dot{h}_{net,r} = \Phi . \varepsilon_m . \varepsilon_f . \sigma . [(\Theta_r + 273)^4 - (\Theta_m + 273)^4] \quad (2.3)$$

Where:

$\Phi$ is the configuration factor;
$\varepsilon_m$ is the surface emissivity of the member;
$\varepsilon_f$ is the emissivity of the fire;
$\sigma$ is the Stephan Boltzmann constant [5.67×10$^{-8}$ W/m$^2$K$^4$];
$\Theta_r$ is the effective radiation temperature of the fire environment [°C];
$\Theta_m$ is the surface temperature of the member [°C].

The values of the emissivity of the member and the fire are given in the fire parts of the Eurocodes and may be taken, in ordinary situations, $\varepsilon_m$ = 0.7 for steel, 0.4 for stainless steel and 0.8 for other materials and $\varepsilon_f$ = 1.0 for fire. The configuration factor, Φ, is a geometric parameter that takes into account the size and relative position between the emission source and the sensing element. EN 1991-1-2 (2002) suggests that, if no specific data is given in EN 1993-1-2 (2005), the configuration factor should be taken as Φ = 1, meaning all the energy released in the form of radiation covers the exposed member, which is not a very realistic assumption. Therefore, a lower value may be chosen to take into account the so called position and shadow effects. As the fire progresses and the fire load consumes, the density of heat flow varies. Except for the temperatures and the gases in the compartment, all other parameters in equation (2.3) can be considered constant.

There are different ways to define the thermal action. One possibility consists on establishing time-temperature relationships that can be used to determine the net heat flux together with appropriate boundary conditions. Another possibility consists on using relationships to directly obtain the net heat flux. EN 1991-1-2 (2002) presents two major groups of fire models: nominal fire curves and natural fire models, in accordance to Figure 4.

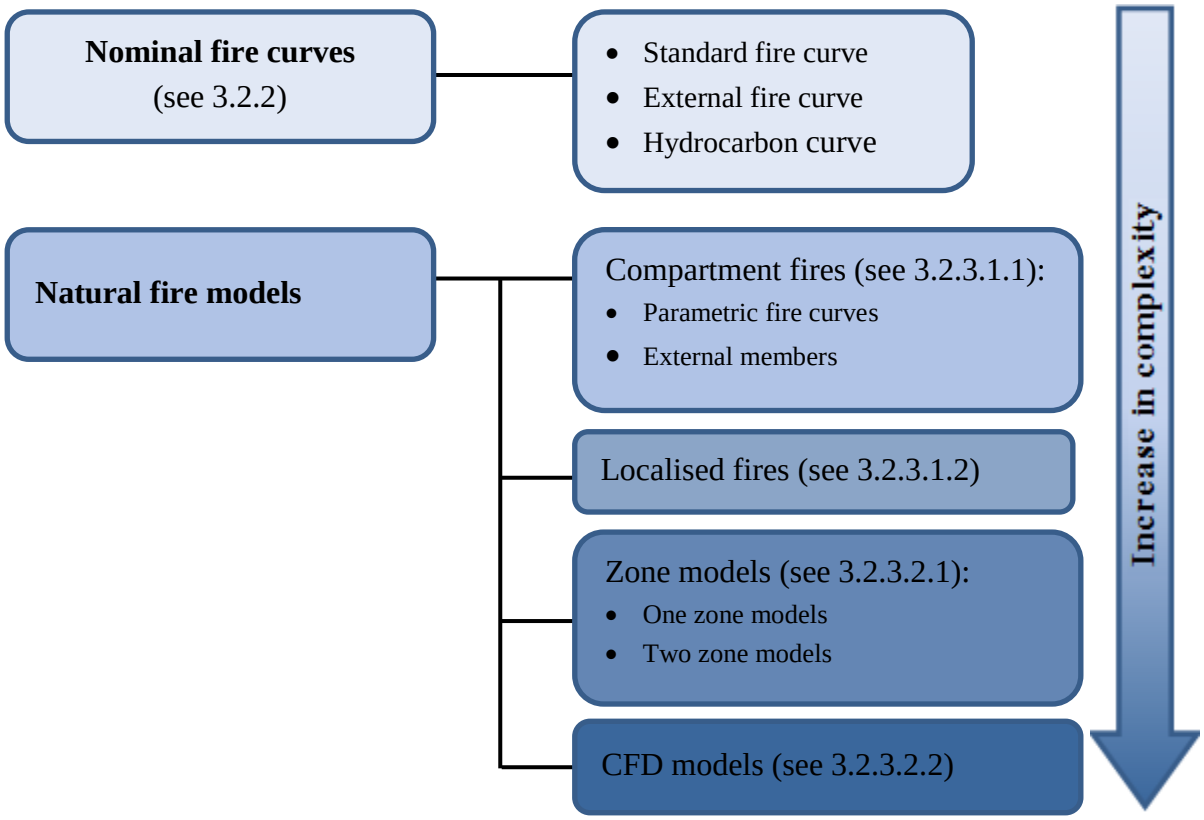


Figure 4-Options for fire modelling in compartments

The level of complexity increases from simple nominal fire curves to Computational Fluid Dynamics models (CFD), as shown in Figure 4. The nominal temperature-time curves, the parametric curves and the methods given for localised fires can be considered as simplified models, whereas the zone and CFD models belong to the group of advanced models, which require very detailed input data and considerable computational effort.

In simple fire models, the gas temperature of a compartment is defined as uniform and represented by a temperature-time relationship. In these models, the smoke movement and fire spread cannot be consider and therefore they are especially suitable for modelling post-flashover fires. Nominal fires are conventional fires which are assumed to be identical

regardless of the specific characteristics of the building. Parametric fire curves, on the other hand, are fire curves based on a consideration of the physical parameters specific to a particular building.

The advanced fire models, such as the zone and Computational Fluid Dynamics models, are theoretical computer models that simulate the heat and mass transfer processes associated with a compartment fire. They can predict compartment gas temperatures in much more detail since smoke movement and fire spread may be taken into account in the analyses. In a one zone model it is assumed that the whole compartment is fully involved in the fire at the same time and the same temperature applies in the whole compartment. In two zone models it is considered that the height of the compartment is separated into two gaseous layers each one of them with its own thermal characteristics. Computational Fluid Dynamics models can be used to analyse fires in which there are no definite boundaries to the gaseous state, a type of analysis that is often used to model smoke movement and that is suitable for very large compartments such as airport terminals and sports stadia (Tom Lennon, 2008).

Following, a more detailed description of the fire models for compartments is presented in accordance with EN 1991-1-2 (2002).

### 2.2.2 Nominal fire curves

Nominal fires are representative fires that can be expressed by a simple formula and are used for purposes of classification of fire resistance, but bear no relationship to the specific characteristics (fire load, thermal properties of compartment linings, ventilation condition) of the building considered. Nominal fire curves given in EN 1991-1-2 (2002) are the standard fire ISO 834, the hydrocarbon fire and the external fire curve.

#### 2.2.2.1 Standard fire curve

The international standard fire curve ISO 834 is widely used to test the fire resisting properties of building components. This curve, represented in Figure 5, is suitable for cellulosic materials but has very limited similarity to the temperatures in real compartment fires. Although its lack of physical reality, the use of this curve allows to standardize the thermal processes in the furnace tests enabling the comparison of experimental results of fire resistance tests in laboratories all over the world. In EN 1991-1-2 (2002) the gas temperature $\theta_g$ is given by expression (2.4).

$$\theta_g = 20 + 345 log_{10}(8t + 1) \qquad (2.4)$$

Where:

$\Theta_g$ is the gas temperature in the fire compartment [°C];
t is the time [min].

When using the ISO 834 curve to determine the evolution of temperatures within the compartment, the coefficient of heat transfer by convection should be taken as $\alpha_c$ = 25 W/m$^2$K.

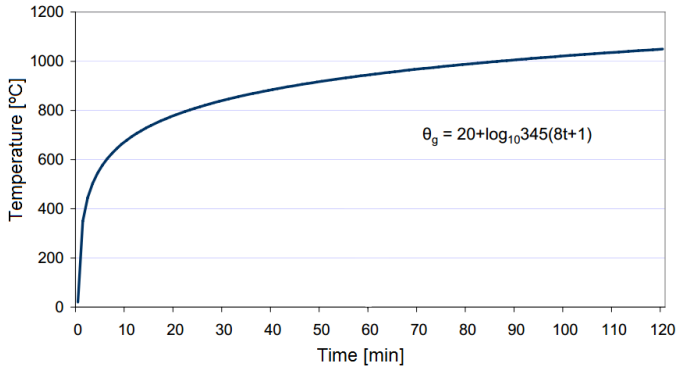


Figure 5 - Standard fire curve ISO 834

#### 2.2.2.2 External fire curve

The time-temperature curve depicted in Figure 6 is used for the outside surface of separating external walls, which are exposed to fire from different parts of the façade. This curve should not be used for calculating the effects of a fire on an external load bearing structure, for example external steel beams and columns of a building (Franssen & Vila Real, 2010). The external fire curve is given in EN 1991-1-2 (2002) by formula (2.26).

$$\theta_g = 660(1 - 0.687e^{-0.32t} - 0.313e^{-3.8t}) + 20 \qquad (2.5)$$

Where:

$\Theta_g$ is the gas temperature near the member [°C];
t is the time [min].

When this curve is used, the coefficient of heat transfer by convection must be taken as $\alpha_c$ = 25 W/m$^2$K.

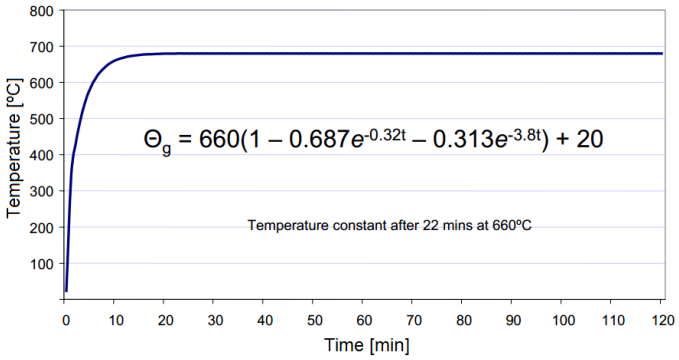


Figure 6 - External fire curve

#### 2.2.2.3 Hydrocarbon curve

The hydrocarbon fire curve is used for representing the effects of a hydrocarbon type fire. This curve is applicable where small petroleum fires might occur, i.e., car fuel, tanks, petrol or oil tankers, etc. As it can be seen in Figure 7, this curve is more severe than the others presented in Figure 5 and Figure 6. In fact, while the hydrocarbon curve increases very quickly and reaches a constant value of 1100ºC after half an hour, the ISO 834 fire curve increases more progressively but keeps on increasing with time (Franssen & Vila Real, 2010). The hydrocarbon curve is given in EN 1991-1-2 (2002) by formula (2.6).

$$\theta_g = 1080(1 - 0.325e^{-0.167t} - 0.675e^{-2.5t}) + 20 \qquad (2.6)$$

Where:

$\Theta_g$ is the gas temperature near the member [ºC];
t is the time [min].

In this case, the coefficient of heat transfer by convection must be taken $\alpha_c$ = 50 W/m$^2$K.

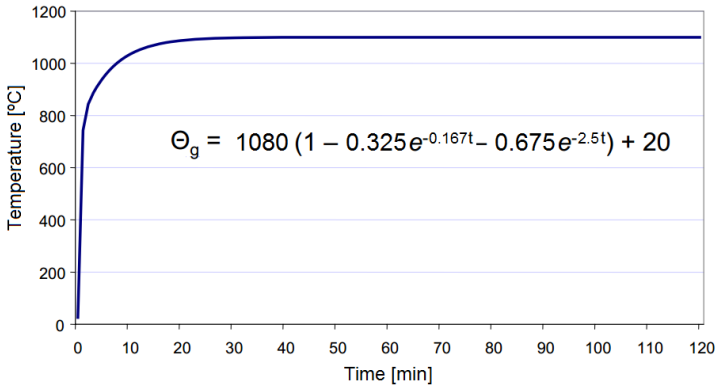


Figure 7- Hydrocarbon curve

### 2.2.3 Natural fire models

#### 2.2.3.1 Simplified fire models

Natural fire models are based on specific physical parameters with a limited field of application. The temperature is determined from compartment fire models or from localised fires models, which depend, among other parameters, on the fire load and characteristics of the compartment in fire. For compartment fires it is generally assumed a uniform temperature distribution as a function of time, whereas for localised fires is assumed a non-uniform temperature distribution.

The value of fire load can be calculated accurately taking into account the distribution of combustible material in the floor surface of the compartment and the variation of the quantity of material with time of fire exposure. Annex E of EN 1991-1-2 (2002) presents a method for calculating design fire load densities based on characteristic values from survey data for different occupancies. The characteristic values are modified according to the risk of fire ignition and the consequence of failure related to occupancy and compartment floor area. In this method, active fire safety measures are taken into account through a reduction in the design fire load density.

According to Annex E of EN 1991-1-2 (2002), the design value of the fire load density is given by:

$$q_{f,d} = q_{f,k} m \delta_{q1} \delta_{q2} \delta_n \ [MJ/m^2] \qquad (2.7)$$

Where:

m is the combustion factor;

$\delta_{q,1}$ is a factor taking into account the fire activation risk due to the size of the compartment;

$\delta_{q,2}$ is a factor taking into account the fire activation risk due to the type of occupancy;

$q_{f,k}$ is the characteristic fire load density per unit floor area [MJ/m$^2$];

$\delta_n = \prod_{i=1}^{10} \delta_{ni}$ is a factor taking into account the different active fire fighting measures (sprinkler, smoke detection, automatic alarm transmission, firemen, etc.).

According to the Portuguese National Annex of EN 1992-1-2 (2002), Annex E can only be applied in Portugal if some modifications are considered, namely the equation (2.7) must be replaced by:

$$q_{f,d} = q_{f,k} m \ [MJ/m^2] \qquad (2.8)$$

Where the value of the characteristic fire load density per unit floor area [MJ/m$^2$] related to compartment occupancy may be taken from Table 1; also, the value of the combustion factor depends on the combustion conditions that should be considered according to the compartment occupancy and the fire load type. In the absence of specific information on the combustion conditions, the combustion factor may be assumed as m = 1.

Table 1- Fire load densities for different occupancies [MJ/m$^2$]

| Occupancy | Average | 80% Fractile |
|---|---|---|
| Dwelling | 780 | 948 |
| Hospital (room) | 230 | 280 |
| Hotel (room) | 310 | 377 |
| Library | 1500 | 1824 |
| Office | 420 | 511 |
| Classroom of a school | 285 | 347 |
| Shopping centre | 600 | 730 |
| Theatre (cinema) | 300 | 365 |
| Transport (public space) | 100 | 122 |
| **NOTE** Gumbel distribution is assumed for the 80% fractile. | | |

When using the simplified fire methods, the coefficient of heat transfer by convection should be taken as $\alpha_c$ = 35 W/m$^2$K.

#### *2.2.3.1.1 Compartment fires*

In compartment fire models, the gas temperature depends, among other parameters, on the density of fire load and ventilation conditions. In EN 1991-1-2 (2002) two methods are presented for modelling these fires: the parametric fire curves for inside (Annex A) and the method for the evaluation of temperatures outside the fire compartment (Annex B).

**Parametric fire curves** – these curves define the evolution of gas temperature as a function of time, based on parameters that influence the development of the fire in a compartment. The parametric temperature-time curve described in Annex A of EN 1991-1-2 (2002) is valid for fire compartments up to 500 m$^2$ of floor area, without openings in the roof and for a maximum compartment height of 4 m and are based on the assumption that the fire load of the compartment is completely burnt out.

These curves have a heating phase followed by a cooling phase which distinguishes them from the nominal curves. The heating phase is given by:

$$\Theta_g = 20 + 1325(1 - 0.324e^{-0.2t^*} - 0.204e^{-1.7t^*} - 0.472e^{-19t^*}) \quad (2.9)$$

Where:

$\Theta_g$ is the gas temperature in the fire compartment [ºC];
$t^* = t \cdot \Gamma$ [h];
t is the time [h];
$\Gamma = [O/b]^2 / (0.04/1160)^2$ is a time factor function of the opening factor O and the thermal absorptivity b;
$b = \sqrt{(\rho c \lambda)}$ [J/m$^2$s$^{1/2}$K] is a parameter which accounts for the thermal properties of the enclosure. It is related to the faculty of the boundaries of the compartment (walls, floor and ceiling) to absorb part of the energy released by the fire and has the following limits: $100 \leq b \leq 2200$;
ρ is the density of the enclosure boundary [kg/m$^3$];
c is the specific heat of the enclosure boundary [J/kgK];
λ is the thermal conductivity of the enclosure boundary [W/mK];
$O = A_v\sqrt{h_{eq}}/A_t$ [m$^{1/2}$] is the opening factor, a parameter that accounts for the openings in the vertical walls. The value of this parameter has to be in the range 0.02 to 0.20 for the model of EN 1991-1-2 (2002) to be applicable;
$A_v$ is the total area of vertical openings on all walls [m$^2$];
$h_{eq}$ is the weighted average of window heights on all walls [m];
$A_t$ is the total area of enclosure (walls, ceiling and floor, including openings [m$^2$].

The maximum temperature in the heating phase occurs for:

$$t^*_{max} = t_{max} \cdot \Gamma \; [h] \quad (2.10)$$

With:

$$t_{max} = \max\left[\left(0.2 \cdot 10^{-3} \cdot q_{t,d}/O\right); t_{lim}\right] \; [h] \quad (2.11)$$

Where:

$q_{t,d}$ is the design value of the fire load density related to the total surface area $A_f$ of the enclosure whereby $q_{t,d} = q_{f,d} \cdot A_f/A_t$ [MJ/m$^2$], with the following limits: $50 \leq q_{t,d} \leq 1000$ [MJ/m$^2$];

$q_{f,d}$ is the design value of the fire load density related to the surface area $A_f$ of the floor [MJ/m$^2$], calculated according to Annex E of EN 1991-1-2 as explained at §2.2.3.1;
$t_{lim}$ is the time dependent on the speed of fire spreading depending on the occupation of the fire compartment [h]. In case of slow fire growth rate, $t_{lim}$ = 25 min; in case of medium fire growth rate, $t_{lim}$ = 20 min and in case of fast fire growth rate, $t_{lim}$ = 15 min.

The time $t_{max}$ corresponding to the maximum temperature is given by $t_{lim}$ in case of fires controlled by the fire load. In other cases, $t_{lim}$ is given by $(0.2 \cdot 10^{-3} \cdot q_{t,d}/O)$ and the fire is controlled by ventilation.

When $t_{max} = t_{lim}$, $t^*$ must be replaced by:

$$t^* = t \cdot \Gamma_{lim}\ [h] \tag{2.12}$$

With:

$$\Gamma_{lim} = [O_{lim}/b]^2/(0.04/1160)^2 \tag{2.13}$$

Where:

$$O_{lim} = 0.1 \cdot 10^{-3} \cdot q_{t,d}/t_{lim} \tag{2.14}$$

If $\left(O > 0.04\ and\ q_{t,d} < 75\ and\ b < 1160\right)$, $\Gamma_{lim}$ has to be multiplied by k:

$$k = 1 + \left(\frac{O - 0.04}{0.04}\right)\left(\frac{q_{t,d} - 75}{75}\right)\left(\frac{1160 - b}{1160}\right) \tag{2.15}$$

In the cooling phase, the time-temperature curves are given by:

$$\theta_g = \theta_{max} - 625(t^* - t^*_{max} \cdot x)\ if\ t^*_{max} \leq 0.5 \tag{2.16}$$

$$\theta_g = \theta_{max} - 250(3 - t^*_{max})(t^* - t^*_{max} \cdot x)\ if\ 0.5 < t^*_{max} < 2 \tag{2.17}$$

$$\theta_g = \theta_{max} - 250(t^* - t^*_{max} \cdot x)\ if\ t^*_{max} \geq 2 \tag{2.18}$$

Where:

$$x = 1 \; if \; t_{max} > t_{lim} \tag{2.19}$$

$$x = t_{lim} \cdot \Gamma / t^*_{max} \; if \; t_{max} = t_{lim} \tag{2.20}$$

With:

$$t^*_{max} = \left(0.2 \cdot 10^{-3} \cdot q_{t,d}/O\right) \cdot \Gamma \tag{2.21}$$

When a parametric fire model is used, the coefficient of convection $\alpha_c$ must be taken as 35 W/m$^2$K.

**Thermal actions for external members** – Annex B of EN 1991-1-2 (2002) provides a simplified calculation method for determining the thermal actions on external elements to the compartment fire. The method can only be applied for fire loads higher than 200 MJ/m$^2$ and the size of the compartment should not exceed 70 m in length, 18 m in width and 5 m in height. This method assumes a steady state situation of a fully developed compartment fire and does not consider the fire pre-flashover and cooling down phases.

The application of the method begins with the calculation of D/W ratio which depends on the number of compartment walls with windows, the number of windows in the walls and the presence of a core in the compartment.

When there are windows in only wall 1, referred in EN 1991-1-2 (2002) as the wall that contains the greatest window area, and there is no core in the fire compartment, the ratio D/W is given by equation (2.22) where $W_2$ is the width of the wall perpendicular to wall 1 in the fire compartment, and $w_t$ is the sum of window widths.

$$D/W = \frac{W_2}{w_t} \tag{2.22}$$

When there are windows on more than one wall, the ratio D/W must be obtained from equation (2.23) where $W_1$ is the width of the wall 1, $A_v$ is the total area of vertical openings and $A_{v1}$ is the sum of window areas on wall 1.

$$D/W = \frac{W_2}{W_1}\frac{A_{v1}}{A_v} \tag{2.23}$$

When there is a core in the fire compartment, the ratio D/W has to be obtained according to equation (2.24), where $L_c$ and $W_c$ are the length and width of the core and $W_1$ and $W_2$ are the length and width of the fire compartment, respectively.

$$D/W = \frac{W_2 - L_c}{W_1 - W_c}\frac{A_{v1}}{A_v} \tag{2.24}$$

All the parts of an external wall that do not have the required fire resistance for the stability of the building have to be considered as window areas.

If the total window area exceeds 50% of the wall area, two situations should be considered for calculation: firstly the total area and secondly 50% of the area of the relevant external wall of the compartment. When using 50% of the area of the external wall, the location and geometry of the open surfaces should be chosen so that the most severe case for the structural elements is considered.

Annex B of EN 1992-1-2 (2002) also considers the effects of the wind on the model. According to this Annex, the flames can leave the fire compartment through the windows either perpendicular to the façade or at a horizontal angle of 45° to the façade as shown in Figure 8.

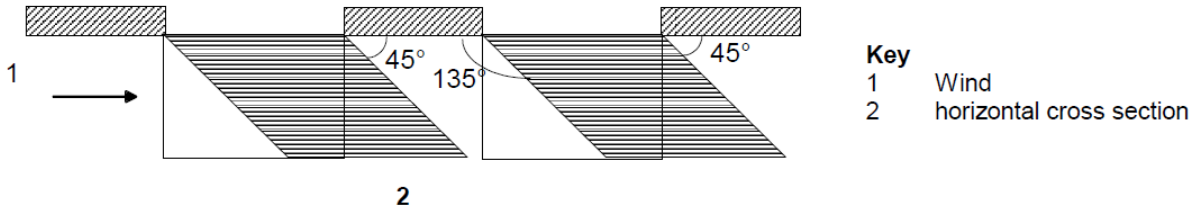


Figure 8 - Deflection on flame by wind (EN 1992-1-2 (2002))

If there are openings on opposite sides of the fire compartment, or if additional air is being fed to the fire from other source than windows, the calculation shall be done with forced draught conditions. Otherwise, the calculation is done with no forced draught conditions. This method gives equations for the determination of the maximum temperatures of a compartment fire, the size and temperatures of the flame from openings and the radiation and convection parameters both with forced and no forced draught conditions.

#### *2.2.3.1.2 Localised fires*

EN 1991-1-2 (2002) provides a simple approach for determining the thermal action of localised fires in Annex C (informative). Depending on the height of the fire flame relative to the ceiling of the compartment, a localised fire can be defined as either a small fire or a large fire For a small fire, a design formula is given to calculate the temperature in the plume along the vertical flame axis. For a big fire, some simple steps have been developed to give the heat flux received by the fire exposed surfaces at the ceiling level.

The limitations of the approach include:

- The diameter of fire: $D \leq 10$ m;
- The heat release rate or the fire: $Q \leq 50$ MW.

However, the approach can be applied to the cases of two localised fires:

- Smaller Fires or Open-Air Fires;
- Larger Fires Impacting Ceiling;

**Smaller fires** - In a localised fire, as shown in Figure 9, the highest temperature is at the vertical flame axis, decreasing toward the edge of the plume. The flame axis temperature changes with height. It is roughly constant in the continuous flame region and represents the mean flame temperature. The temperature decreases sharply above the flames as an increasing amount of ambient air is entrained into the plume (Karlsson & Quintiere, 2000). EN 1991-1-2 (2002) provides a design formula to calculate the temperature in the plume of a small localised fire, based on the fire flume model developed by Heskestad (Hesketad, 1998). It can be applied to open-air fires as well. Considering a localised fire as shown in Figure 9, the flame height $L_f$ of the fire is given by:

$$L_f = -1.02D + 0.0148Q^{2/5} \tag{2.25}$$

Where:

*D* is the diameter of the fire [m];
*Q* is the heat release rate of the fire [W];
*H* is the distance between the fire source and the ceiling [m].

In case of fire do not impinge on the ceiling of the compartment when $L_f < H$, or fire in open spaces, the temperature $\Theta_{(z)}$ in the plume along the symmetric vertical flame axis is given by:

$$\Theta_{(z)} = 20 + 0.35 Q_c^{\frac{2}{3}} (z - z_0)^{-5/3} \leq 900 \quad (2.26)$$

With:

$$z_0 = -1.02D + 0.00524 Q^{2/5} \quad (2.27)$$

Where:

$Q_c$ is the convective part of the heat release rate [W], with $Q_c = 0.8\ Q$ by default;
$z$ is the height along the flame axis [m];
$z_0$ is the virtual origin of the axis [m].

The virtual origin $z_0$ depends on the diameter of the fire and the heat release rate. This empirical equation has been derived from experimental data. The value of $z_0$ may be negative and locate beneath the fuel source, indicating that the area of the fuel source is large compared to the energy being released over that area. For fire sources where the fuel releases high energy over a small area, $z_0$ may be positive and locate above the fuel source.

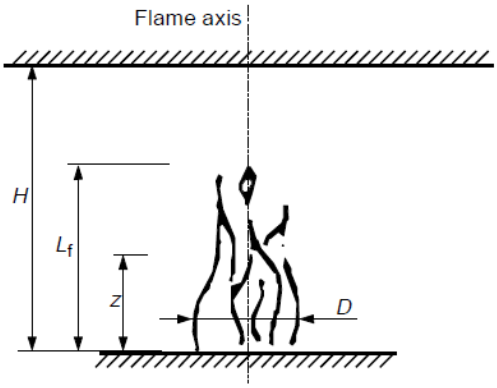


Figure 9- Schematic diagram for small localised fires (EN 1991-1-2, 2002).

**Larger Fires Impacting Ceiling** - When a localised fire becomes large enough with $L_f \geq H$, the fire flame will impinge on the ceiling of the compartment. The ceiling surface will cause the flame to turn and move horizontally beneath the ceiling. EN 1991-1-2 (2002) presents some design formulas, based on the fire plume model developed by Hasemi (Hasemi, 1986). Figure 10 shows a schematic diagram of a localised fire impacting on the ceiling with the ceiling jet flowing beneath an unconfined ceiling. As the ceiling jet moves radially outward, it loses heat to the cooler ambient air being entrained into the flow, as well as the heat transfer

to the ceiling. Generally, the maximum temperature occurs relatively close to the ceiling (Karlsson & Quintiere, 2000).

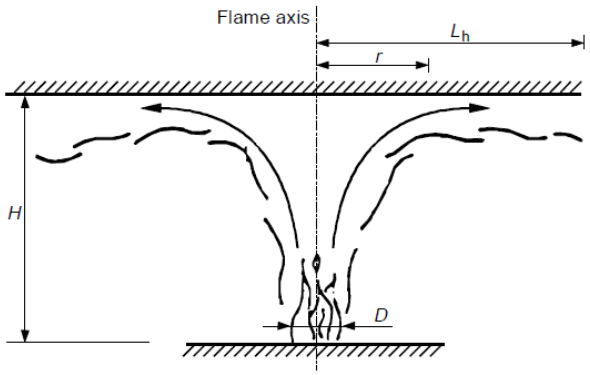


Figure 10- Localised fires impacting on ceiling of compartment (EN 1991-1-2, 2002).

EN 1991-1-2 (2002) only provides design formulas to determine the heat flux received by the surface area at the ceiling level, but not for calculating the ceiling jet temperatures. Considering a localised fire impacting the ceiling of the compartment as shown in Figure 10 ($L_f \geq H$), the horizontal flame length $L_h$ is given by:

$$L_h = (2.9H(Q_H^*)^{0.33}) - H \tag{2.28}$$

With:

$$Q_H^* = \frac{Q}{1.11.10^6.H^{2.5}} \tag{2.29}$$

Where:

$L_h$ is the horizontal flame length [m];
$H$ is the distance between the fire source and the ceiling [m];
$Q_H^*$ is a non-dimensional heat release rate;
$Q$ is the heat release rate of the fire [W].

The heat flux $\dot{h}$ (W/m$^2$) received by the fire exposed unit surface area at the ceiling level at the distance r from the flame axis is given by:

$$\dot{h} = \begin{cases} 100000 & \text{for } y \leq 0.30; \\ 136300\ to\ 121000y & \text{for } 0.30 < y < 1.0; \\ 15000y^{-3.7} & \text{for } y \geq 1.0. \end{cases} \tag{2.30}$$

With:

$$y = \frac{r + H + z'}{L_h + H + z'} \tag{2.31}$$

Where:

$r$ is the horizontal distance from the vertical flame axis to the point along the ceiling where the thermal flux is calculated [m];
$z'$ is the vertical position of the virtual heat source as given by equation (3.9) [m];
$D$ is the diameter of the fire [m].

The vertical position of the virtual heat source z' is given by:

$$Q_D^* = \begin{cases} 2.4D\left(Q_D^{*\frac{2}{5}} - Q_D^{*\frac{2}{3}}\right), & when\ Q_D^* < 1.0 \\ 2.4D(1.0 - Q_D^{*2.5}, & when\ Q_D^* \geq 1.0 \end{cases} \tag{2.32}$$

With:

$$Q_D^* = \frac{Q}{1.11.10^6.D^{2.5}} \tag{2.33}$$

The net heat flux $\dot{h}_{net}$ received by the fire exposed unit surface at the level of the ceiling is given by:

$$\dot{h}_{net} = \dot{h} - \alpha_c.(\theta_m - 20) - \phi\varepsilon_m\varepsilon_f\sigma((\theta_m + 273)^4 - 293^4) \tag{2.34}$$

Where:

$\alpha_c$ is the coefficient of heat transfer by convection [W/m$^2$K];
$\varepsilon_f$ is the emissivity of the fire;
$\varepsilon_m$ is the surface emissivity of the member;
$\phi$ is the configuration factor;
$\theta_m$ is the surface temperature of the member [°C];
$\sigma$ is the Stephan Boltzmann constant [5.67×10$^{-8}$ W/m$^2$K$^4$];
$\dot{h}$ is the heat flux received by the fire exposed unit surface area at the level of the ceiling.

In the case of several localised fires, the individual heat fluxes received by the fire exposed unit surface area, at the ceiling level, should be first calculated. The total heat flux is then taken as the summation of the contribution of all localised fires as follows:

$$\dot{h}_{hot} = \dot{h}_{hot} + \dot{h}_{hot} + \cdots \leq 100000 \qquad (2.35)$$

#### 2.2.3.2 Advanced fire models

Advanced fire models take into account the gas properties, mass and energy exchange processes associated with real compartment fires; so, they are able to predict compartment gas temperatures in a much more accurate way than simplified models. The advanced calculation models presented in EN 1992-1-2 (2002) normally include iterative procedures that may require considerable computational effort. For the calculation of fire load density, as well as the heat release rate, the methods previously described (see §2.2.3.1) are perfectly suitable. In the advanced fire models, unless more detailed information is available, the coefficient of heat transfer by convection should be taken as $\alpha_c$ = 35 W/m$^2$K.

The EN 1992-1-2 (2002) proposes two different advanced fire models:

- Zone models: i) One-zone models assuming a uniform, time dependent temperature distribution in the compartment; ii) two-zone models, assuming an upper layer with time dependent thickness and with time dependent uniform temperature, as well as a lower layer with a time dependent uniform and lower temperature.
- Computational Fluid Dynamics models, giving the temperature evolution in the compartment in a completely time dependent and space dependent manner.

##### *2.2.3.2.1 Zone models*

Zone models owe their name to the division of the fire compartment into one or two zones, in which the temperature is assumed to be uniform. The *one zone models* represent a post-flashover situation where the whole compartment is defined as a one single zone with a uniform, time dependent temperature distribution. The *two zone models* represent a pre-flash-over situation, where the compartment possesses a lower zone comprising cold air and an upper zone containing hot combustion products. Some two zone models computer programs produced by research institutions can be downloaded for free, namely CFAST from NIST, in the U.S.A., and OZone from the University of Liege in Belgium. These programs allow to compute the development of temperature in the fire compartment on the basis of differential

equations expressing mass balance and energy balance equilibrium (Franssen & Vila Real, 2010).

When modelling a compartment fire, the openings in the boundaries play a crucial role as they provide the air that feeds the fire and they can vent the compartment. Unlike in parametric models, in zone models each individual opening can be represented with its own dimensions and position. Forced ventilation can also be considered if needed. The energy absorbed by the walls is also of great importance and in zone models each wall can be represented individually, with all its layers. The amount of fuel present in the compartment is also of primary importance. For a zone model, the total fuel quantity present in the compartment must be given as a data and also the rate at which it will be released (heat release rate) as well as the associated burning rate (Franssen & Vila Real, 2010).

**One zone models -** According to Annex D of EN 1991-1-2 (2002), a one-zone model can be applied to post-flashover conditions and the temperature, density, internal energy and gas pressure in the compartment are assumed to be homogeneous. In a one zone model the temperature is calculated by considering the resolution of equations of mass and energy conservation.

The ideal gas law considered is:

$$P_{int} = \rho RT \ [N/m^2] \tag{2.36}$$

Where:

R is the ideal gas constant;
ρ is the gas density [kg/m$^3$];
T is the temperature [K].

The mass balance of the compartment gases is written as:

$$\frac{dm}{dt} = \dot{m}_{in} - \dot{m}_{out} + \dot{m}_{fi} \ [kg/s] \tag{2.37}$$

Where:

$\frac{dm}{dt}$ is the rate of change of gas mass in the fire compartment;
$\dot{m}_{in}$ is the rate of gas mass coming in through the openings;

$\dot{m}_{out}$ is the rate of gas mass going out through the openings;
$\dot{m}_{fi}$ is the rate of pyrolysis products generated.

The rate of change of gas mass and the rate of pyrolysis may be neglected, thus

$$\dot{m}_{in} = \dot{m}_{out} \tag{2.38}$$

These mass flows may be calculated based on static pressure due to density differences between air at ambient and high temperatures, respectively.

The energy balance of the gases in the fire compartment may be taken as:

$$\frac{dE_g}{dt} = Q - Q_{out} + Q_{in} - Q_{wall} - Q_{rad}\ [W] \tag{2.39}$$

Where:

$E_g$ is the internal energy of gas [J];
$Q$ is the heat release rate of the fire [W];
$Q_{out} = \dot{m}_{out} c T_f$;
$Q_{in} = \dot{m}_{in} c T_{amb}$;
$Q_{wall} = (A_t - A_{h,v})\dot{h}_{net}$ is the loss of energy to the enclosure surfaces;
$Q_{rad} = A_{h,v}\sigma T_f^4$ is the loss of energy by radiation through the openings;
c is the specific heat [J/kg K];
$\dot{h}_{net}$ is given by formula (3.1);
$\dot{m}$ is the gas mass rate [kg/s];
$T$ is the temperature [K].

**Two zone models** - According to Annex D of EN 1991-1-2 (2002), a two-zone model is based on the assumption of accumulation of combustion products in a layer beneath the ceiling, with a horizontal interface. In these models, different zones should be defined: i) an upper layer (corresponding to the part where the smoke and toxic gases accumulate, where uniform characteristics of the gas may be assumed), ii) a lower layer (where the temperature is lower), iii) the fire and its plume, iv) the external gas and v) the walls. Two-zone models allow the calculation of the exchanges of mass, energy and chemical substance between the different zones.

In a given fire compartment with a uniformly distributed fire load, a two-zone fire model may develop into a one-zone fire in the following situations: if the gas temperature obtained in the upper layer is greater than 500ºC; if the top layer grow up to 80% of the height of the compartment.

#### *2.2.3.2.2 Computational Fluid Dynamics models*

In the last decade, computational Fluid Dynamics models (CFD) have become increasingly popular in fire safety engineering. These models rely on a division of the compartment into a very high number of cells, in which the Navier-Stokes equations are solved and the values of pressure, temperature, velocity, chemical components and optical obstruction are obtained for each cell of the compartment. The application of CFD models requires specific software, powerful computers and highly experienced users (Franssen & Vila Real, 2010). The CFD models may be used to solve numerically the partial differential equations and to obtain the thermo-dynamic and aero-dynamic variables in all points of the compartment. As stated in Annex D of EN 1992-1-2 (2002), CFD models analyse systems involving fluid flow, heat transfer and associated phenomena, by solving the fundamental equations of the fluid flow which represent the mathematical statements of the conservation laws of physics.

### 2.3 Thermal exposure in steel elements - EN 1993-1-2 (2005) approach

The heating of unprotected or protected steel member is calculated by the EN 1993-1-2 (2005) method. The method is based on the assumption of a uniformly distributed temperature over the cross section and along the structure at each time of fire exposure. This condition invalidates its direct use for the case of columns exposed to localised fires, except for specific scenario of a column fully engulfed by a localised fire; even in this case scenario it is difficult to obtain a perfectly symmetric fire plume, as concluded by Byström and co-authors (Byström et al., 2012).

According to EN 1993-1-2 (2005), a massive section will heat up slowly (having a higher fire resistance) than a slender section. The influence of massiveness of cross section is considered by the "Section Factor" calculated through the following equation:

$$Section\ factor = \frac{A_m}{V} \tag{2.40}$$

Where:

$A_m$ is the lateral surface area of the steel profile exposed to fire [$m^2$];
V is the volume of the element exposed to fire [m].

For an equivalent uniform temperature distribution in the cross-section, the increase of temperature in an unprotected steel member during a time interval is determined by the following formula, from EN 1993-1-2 (2005):

$$\Delta\theta_{a,t} = k_{sh} \frac{A_m/V}{c_a.\rho_a}.h_{net,d}.\Delta t \quad [^oC] \tag{2.41}$$

Where:

$k_{sh}$ is the correction factor for the shadow effect;
$A_m/V$ is the section factor for unprotected steel members:
$c_a$ is the specific heat of steel [J/Kg.K];
$h_{net,d}$ is the design value of the net heat flux [W/m$^2$];
$\Delta t$ is the time interval [s];
$\rho_a$ is the unit mass of steel [Kg/m$^3$].

For I-sections under nominal fire actions the correction factor for the shadow effect may be determined from:

$$K_{sh} = 0.9\left[\frac{A_m}{V}\right]_b\left[\frac{A_m}{V}\right] \tag{2.42}$$

Where:

$\left[\frac{A_m}{V}\right]_b$ is the box value of the section factor.

In all other cases:

$$K_{sh} = \left[\frac{A_m}{V}\right]_b\left[\frac{A_m}{V}\right] \tag{2.43}$$

For cross sections with a convex shape fully engulfed in fire, the shadow effect does not play role and consequently the correction factor $k_{sh}$ may be considered equal to the unity. The shadow effect is related to the radiation interchange between surface areas during heat transfer. The quantification of the shadow effect is possible by using a configuration factor $\Phi$. This factor is the ratio between the radiated heat that reaches a given receiving surface and the total radiated heat leaving another surface. Its value depends on the size of the radiating surface, on the distance from the radiating surface to the receiving surface and on their

relative orientation. Methods for calculating the configuration factor are given in EN 1993-1-2 (2005).

EN 1993-1-2 provides a design method to evaluate the temperature development of steel members insulated with fire protection materials (sprays, boards and intumescent paint). Assuming uniform temperature along the steel member, the temperature increase is given by equation (2.44).

$$\Delta\theta_{a,t} = \frac{\lambda_p . A_p/V . (\theta_{g,t} - \theta_{a,t})}{d_p . c_a . \rho_a . (1+\phi/3)} . \Delta t - (e^{\phi/10} - 1) . \Delta\theta_{g,t} \quad [^oC] \qquad (2.44)$$

With:

$$\phi = \frac{c_p . \rho_p}{c_a . \rho_a} . d_p . A_p/V$$

Where:

$A_p/V$ is the section factor for steel members insulated by fire protection material;
$A_p$ is the appropriate area of fire protection material per unit length of the member [m²];
$V$ is the volume of the member per unit length [m³];
$c_a$ is the temperature dependant specific heat of steel, from section 3 [J/kgK];
$c_p$ is the temperature independent specific heat of the fire protection material [J/kgK];
$d_p$ is the thickness of the fire protection material [m];
$\Delta t$ is the time interval [s];
$\theta_{a,t}$ is the steel temperature at time t [°C];
$\theta_{g,t}$ is the ambient gas temperature at time t [°C];
$\Delta\theta_{g,t}$ is the increase of the ambient gas temperature during the time interval $\Delta t$ [K];
$\lambda_p$ is the thermal conductivity of the fire protection system [W/mK];
$\rho_a$ is the unit mass of steel [kg/m$^3$];
$\rho_p$ is the unit mass of the fire protection material [kg/m$^3$].

According to EN 1993-1-2 (2005), the value of Δt in equation (2.44) should not be taken as more than 30 seconds. Also, the area $A_p$ of the fire protection material should be taken as the area of its inner surface.

# 3 STATE-OF-THE-ART ON LOCALISED FIRES

## 3.1 Experimental research

The experimental research on columns subjected to localised fire actions was found to be sparse and relatively new. In 2003, Kamikawa and co-authors (Kamikawa et al., 2003) published, on the *Fire Safety Magazine 7*, the first experimental research on unprotected steel columns subjected to localised fires. Two different setups of steel columns exposed to fire were experimented: steel column surrounded by localised fire (4 tests) and steel column subjected to adjacent fires (5 tests). Figure 11 presents these two experimental layouts. The incident heat flux and the temperature on the steel column were measured. Square diffusion burners, with propane as the fuel, were used as the fire source. The tests were conducted on columns with 0.15 m x 0.15 m square hollow section, 4.5 mm thickness and 2.50 m tall. This columns were un-loaded and its interior was empty. In order to measure incident heat flux, a few columns were instrumented with one line of 15 mm diameter heat rate sensors (150 $kW/m^2$ range). For steel temperature measurement, different columns were instrumented with 0.20 mm diameter K-type Thermocouples (TC). The heat flux and the steel temperature measurements were conducted in distinct columns, subjected to the same fire condition, in order to avoid interference between measurement equipment. The upper end of each column was not closed in order to prevent excessive pressure rise in the column's cavity.

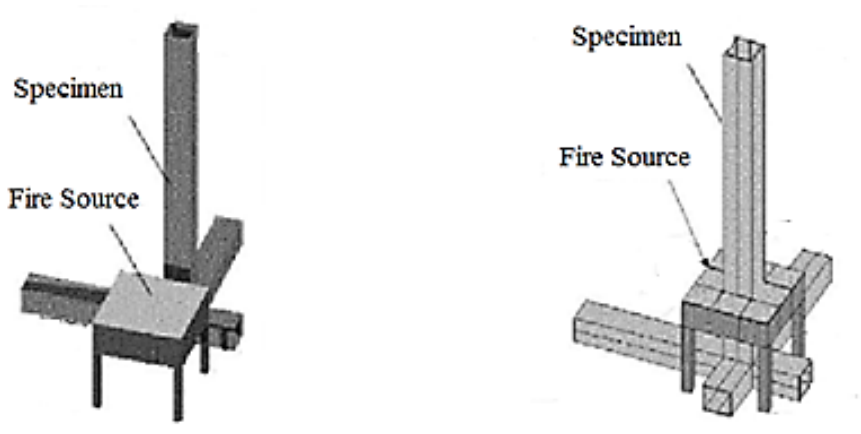


(a) (b)

Figure 11- Test setups: (a) steel column subjected to adjacent fires; (b) steel column surrounded by localised fire (Kamikawa et al., 2003)

Experimental results were compared with the scenario of uniform heating assumption, calculated according equation (3.1).

$$T_{fu} = \left(\frac{\dot{h}}{\varepsilon_m \sigma}\right)^{\frac{1}{4}} - 273.16 \qquad (3.1)$$

Where:

$\dot{h}$ is the heat flux [kW/m$^2$];
$\varepsilon_m$ is the surface emissivity of the member;
$\sigma$ is the Stefan-Boltzman Constant [5.67x10-11 kW/ s$^2$K$^4$].

The tests on columns subjected to adjacent fires demonstrated a notable decrease of surface heat flux with the increase of the column-source distance. Surface temperature of the column, in this configuration, was found to be notably lower than the estimate from heat flux data based on the uniform heating assumption, which, according the authors, suggests the significance of the conductive heat loss to unheated surfaces of the column. The tests with the surrounding fire configuration resulted in a heat flux evolution weakly dependent on heat release rate. This indicates that the high conductivity of steel no longer contributes to the relaxation of the heating of the column; surface temperature of the column with the surrounding fire configuration becomes very close to the estimated, based on the uniform heating.

Wald and his co-authors (Wald et al., 2009) reported an experimental programme to investigate the global structural behaviour of a compartment in a steel frame building, exposed to fire before demolition, performed on June 2006. Among other tests, one unprotected steel column was tested against localised fire. The test was designed to provide data for posterior numerical researches on the heat transfer into steel columns subjected to localised fire. In order to perform this test, a column of section IPE 200 was fixed to an IPN 300 secondary beam, as shown in Figure 12 (b). The internal dimensions of the fire compartment were 3.80 x 5.95 m with a height of 2.78 m. An opening, with dimensions 2.4 x 1.4 m, was created in order to ventilate the room during the fire test. Fire load was applied with an adjacent stack of wooden cribs 50 x 50 mm of length 1m. The development of the gas and column web temperatures was measured by 0.50 mm dia. K-type thermocouples according the distribution of Figure 12 (b). Steel temperatures were measured on the unexposed part of the column by thermocouples named TC13, TC14 and TC15, while to measure the gas temperature, thermocouples TG13, TG14 and TG15 were placed at the central axis of the fire plume. Results are depicted on Figure 12 (b).

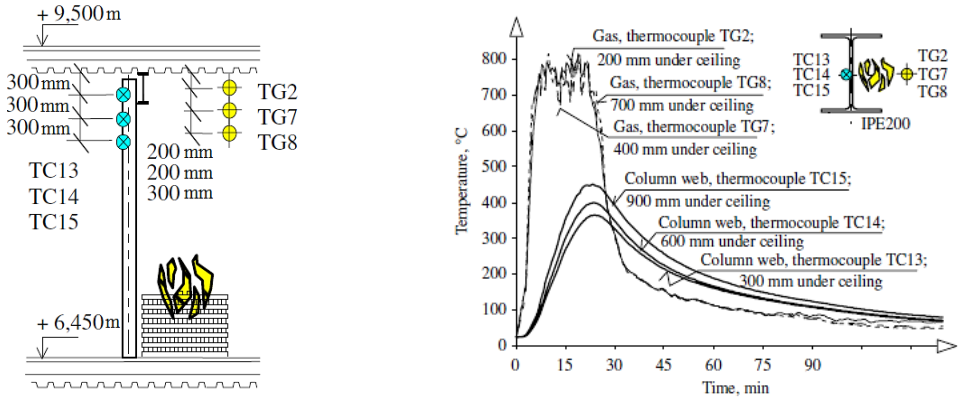


(a) (b)

Figure 12- (a) Experimental setup. (b) Measured temperatures on unprotected column during the localised fire (Wald et al., 2009)

The localised fire plume followed the model presented in Annex C of EN 1991-1-2 (2002), for larger fires impacting ceiling. A constant gas temperature was verified along the vertical axis of the fire plume whereas the steel temperature decreased in higher sections of the column. This occurrence is resultant from the radiative component of the heat flux, which is higher for surfaces closer to the burning surface.

More recently, Bystrom and co-authors (Byström et al., 2012) carried out a large scale test to explore thermal exposure of column exposed to localised fire. The experiments were carried out in the large fire hall of *SP Technical Research Institute* of Sweden with 20 x 20 x 20 m in size. A 6 m tall, CHS 200 x 10 circular unprotected steel column was exposed to three distinct circular pool fires: one 1.1 m dia. heptane pool and two diesel pools of diameters 1.1 and 1.9 m. The column was un-loaded and its interior was empty. The column was fixed in a secondary beam, 20 cm over the fuel containers under an exhaust hood, for ventilation (Figure 13).

Figure 13 - Experimental setup (Byström et al., 2012)

The temperatures of gas and steel were measured along height, and compared with estimates based on EC 1991-1-2 (2002), which in all cases overestimated the thermal impact. For the heptane pool action, results comparison is presented on Figure 14, as example.

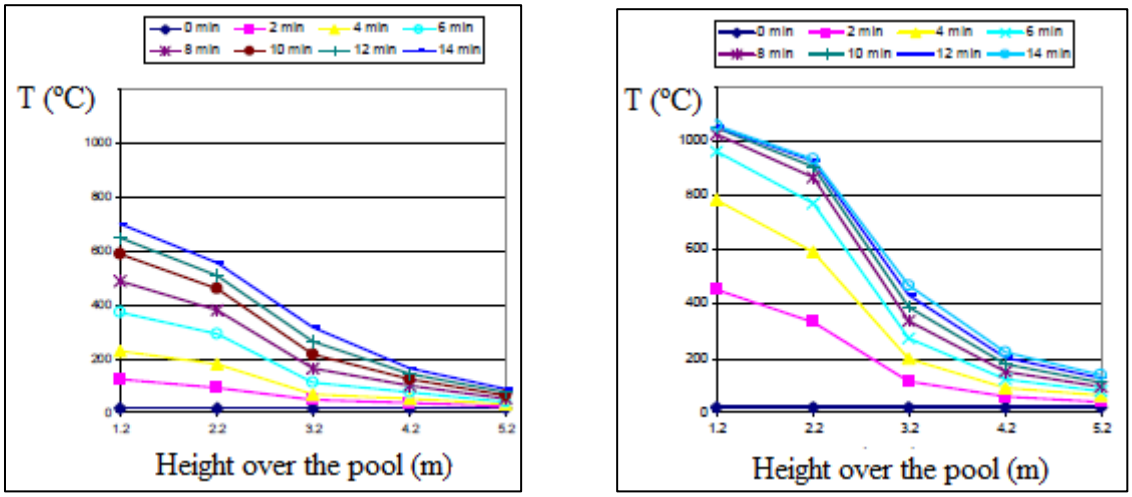


(a) (b)

Figure 14 - (a) Experimental steel temperature; (b) steel temperature prediction according EN 1991-1-2 (Byström et al., 2012)

As correction to the Eurocode results, it was assumed a flame emissivity lower than 1 (as suggested in EN 1991-1-2 (2002)), depending on flame thickness and absorption coefficient. The flame thickness was assumed as d/2 and the absorption coefficient 0.35 $m^{-1}$. With that correction, Eurocode results were clearly closer to the measured ones and still by the safety side, as shown in Figure 15.

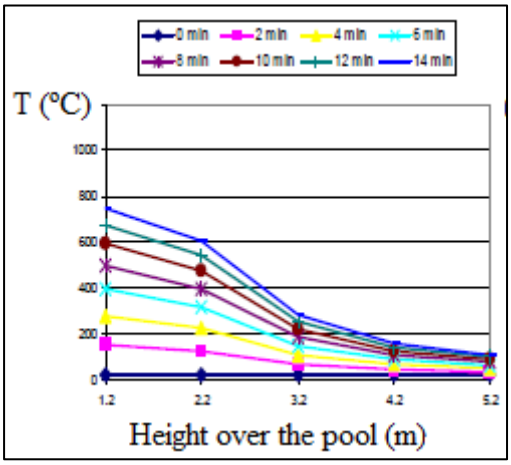


Figure 15 - Correction to the steel temperature prediction according to EN 1991-1-2 (2002) (Byström et al., 2012)

The studied fire scenario, where a steel column is fully engulfed by a localised fire, represents a simplified version of a localised fire action, once the uniform heating may be assumed due to symmetry of the fire load. This procedure cannot be applied to columns side by side with localised fires. However, the experimental procedures followed by (Byström et al., 2012) were proved to be accurate; based on the reliability of these results, the use of pool fires (as localised fire actions) was adopted in the experimental campaign described in this thesis.

## 3.2 Numerical and analytical research

In 2007, Sokol and Wald (Sokol and Wald, 2007) published a numerical study concerning steel columns subjected to localised fire based on Finite Element Method (FEM). The study focused on the heat transfer prediction, considering different column positions and distances from the localised fire, as shown in Figure 16.

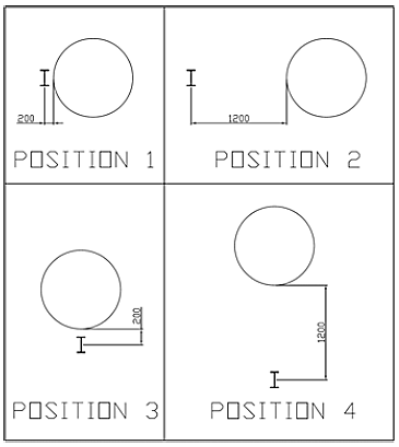


Figure 16 - Different column positions from a localised fire (Sokol, 2009)

The temperatures in the columns were predicted using the zone model *Ozone* software. The steel temperatures obtained by Wald et al., in the experimental program of 2006 (Wald et al., 2009), were used to calibrate this numerical model of heat transfer. The fire plume was replaced by a cylindrical surface modelled by shell elements; its diameter was equal to the fire diameter. The temperatures of the hot and cold zones were used for the convective heat flux; time dependent temperature and the height of the cylinder were used to derive the radiated heat flux. Heat transfer within cross sections of the column, was calculated using *Ansys* software. The column cross section was modelled using elements *SOLID 70: 3D* quadrilateral elements with one degree of freedom at each node; the column web was modulated with three layers, while for the flanges four layers were used.

As numerically verified, a localised fire leads a steel column to a non-uniform heating scenario. As result, asymmetric distribution of temperatures along the cross sections is verified. The thermal gradient between temperatures of column flanges is significant, for short distances of the column to the fire; for bigger distances, it becomes less significant.

Based on this previous numerical study, Sokol (Sokol, 2009) developed a simplified model for temperature prediction in columns exposed to localised fire. This model deals with the scenario used when the flames reach the ceiling. Through this model, it is possible to calculate the heat flux to the surface of a steel column. It is also possible to locate the section at which the maximum temperature is expected.

As shown in Figure 17, the flames are replaced by a cylindrical surface and the temperature of the flames is calculated according to EN 1991-1-2 (2002), Annex C. In this method, the non-uniform temperature within the steel sections is neglected.

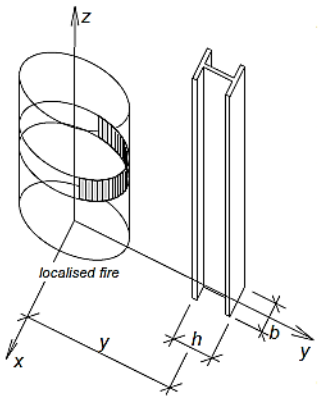


Figure 17- Simplified Method Scheme (Sokol, 2009)

The heat flux into the steel column is calculated as the radiation component obtained from the flames (the cylindrical surface), which is reduced due to losses by convection and radiation, according to equation (3.2).

$$h_{net} = h_{net\,,gain} - h_{net\,,loss} \tag{3.2}$$

The heat flux gained by radiation is given as total from the strips on the cylindrical surface:

$$h_{net\,,gain} = \Phi \varepsilon_{res} \sigma \left( (\theta_g(z) + 273)^4 - (\theta_m + 273)^4 \right) \tag{3.3}$$

Where:

$\varepsilon_m$ is the resultant emissivity of the flame.

The loss by convection and radiation is obtained from equation (3.4):

$$h_{net\,,loss} = (1-\Phi)\varepsilon_m\varepsilon_f\sigma((\theta_m+273)^4-(20+273)^4)+\alpha_c(\theta_m-20) \qquad (3.4)$$

The configuration factor $\Phi$ for each strip has to be evaluated numerically from the following formula:

$$\Phi = \frac{1}{A_1}\int_{A_1}\frac{\cos\varphi_1\cos\varphi_2}{\pi r^2}dA_1 \qquad (3.5)$$

It is derived for the front surface $\Phi_{front}$ (the exposed flange), and both side surfaces: $\Phi_{s1}$ and $\Phi_{sd2}$. Only the surface of the flames contributing to the radiation is taken into account, see Figure 17. The total configuration factor taking into account the radiation received on the whole column surface is given by:

$$\Phi = \frac{b\Phi_{front}+h(\Phi_{s1}\Phi_{s2})}{b+2h} \qquad (3.6)$$

The following formulas are used to predict the elevation $z$ (measured from the floor) at which the maximum column temperature is expected:

i) in the growing phase:

$$z = 0{,}1+\left(0{,}38-\frac{1}{x+1{,}97-0{,}45D^2}\right)L_f,\ L_f \le H \qquad (3.7)$$

ii) during uniform burning:

$$z = 0{,}1+\frac{x}{50}+\left(\frac{L_f}{20x}\ln(t')\right),\ L_f \le H \qquad (3.8)$$

The temperatures in the steel section may be calculated according to EN 1993-1-2 (2005) approach (see equation (2.41)), once uniform heating scenario is assumed. However this assumption is not in accordance with a localised fire and may not be conservative in the design of steel columns. Further studies are required in order to determine the effects of non-uniform temperatures in steel columns.

More recently, Li and Zhang (Li & Zhang, 2010) presented a Computational Fluid Dynamics (CFD) model adopted to predict the thermal behaviours of steel columns exposed to localised fires. *Fire Dynamics Simulator* (FDS) software was used for this numerical research. The aim of this paper was to investigate FDS capacity of predicting the thermal response of steel columns exposed to localised fires. For this purpose, the same models experimented by Kamikawa and co-authors (Kamikawa et al., 2003), were modelled in FDS: a steel column surrounded by localised fire and steel column subjected to adjacent fires. In the simulations, 255 kW heat release rate was used for adjacent fire test, while 81 kW was used for surrounding test. Experiment and numerical results are compared and very good agreement between predicted and measured results was found in surrounding fire case. However, same did not happen in the case of adjacent fire condition: FDS gives acceptable prediction of heat fluxes to front and back surfaces of the column, but fails to predict heat fluxes to side surface, as shown in Figure 18.

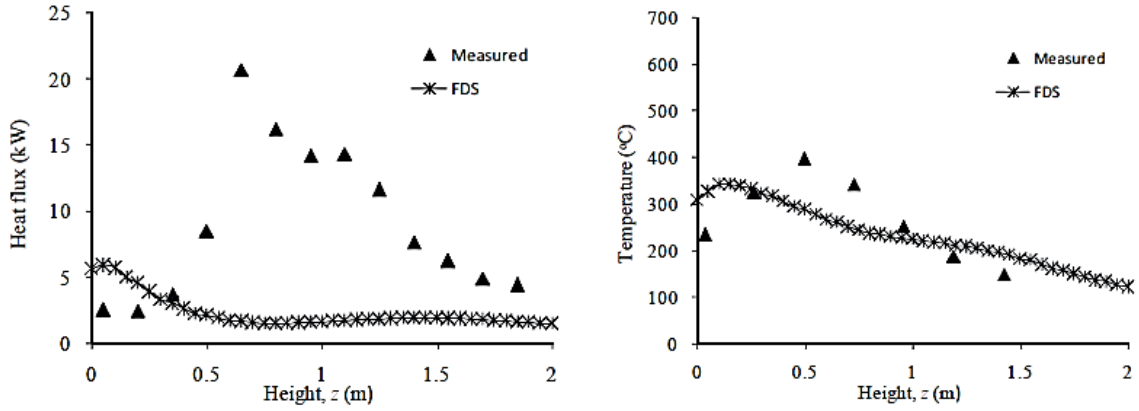


Figure 18 - Temperatures at the side surface of the column (Li & Zhang, 2010)

This study revealed the uncertainty level associated with the heat transfer into steel columns. The measured heat flux to the side surfaces during experimental tests was much higher than the one predicted by FDS, which had influence in the associated steel temperatures. It was proved that an estimation of heat fluxes according to the fundamental properties of the fuel and steel column may underestimate the thermal action caused by a localised fire. Therefore, experiments need to be carried out in order to provide a proper knowledge on the effect of external factor in the heat flux to steel columns. Effects of wind actions and enclose effects in the heat release rate were proved to be significant and their evaluation is under the scope of this thesis.

# 4 ESTIMATION OF HEAT RELEASE CHARACTERISTICS IN LOCALISED FIRE SCENARIO

## 4.1 Introduction

In accordance with Annex C of EN 1991-1-2 (2002), an estimation of the heat release rate (Q) is the most important requirement for the application of the localised fire models (see equations (2.25) and (2.26)). Other prerequisites, such as the fire diameter and the distance between the fire source and the ceiling are geometric parameters, with no problems in measurement. In order to estimate heat release rate in localised fires, Annex E of EN 1991-1-2 (2002) proposes an evaluation according to compartment occupancy. This proposal results in a uniform temperature within the fire compartment which is characteristic of fully engulfed fire scenarios. However, the use of average temperatures may not be safe to verify localised fire occurrence. If only a limited part of a structure is exposed to fire, its fire resistance may be significantly different from that obtained assuming uniform temperature distribution. This can lead to very conservative or even incorrect fire design. Moreover, columns heated from one side usually develop an important temperature gradient across the cross-section, which will lead to the deflection of the member towards the heat source. The overall thermal expansion will also lead to the development of restraint forces at the ends of the member. This will cause additional normal moments and subsequently also second-order moments into the member (Outinen et al., 2010).

Various studies have reported heat release rate values for the most current fire sources, such as furniture, combustibles and car explosions: see for example Bukowski and Peacock (1989), Karlsson and Quintiere (2000) and Babrauskas (2002). Figure 19 shows the heat released from various fire sources, according to the particular experiments published by Bukowski and Peacock (Bukowski & Peacock, 1989). Figure 20 presents heat released from burning of typical class 3 vehicles (trucks with more than 2 axles) as an example of extreme localised fire action (Haremza et al., 2013).

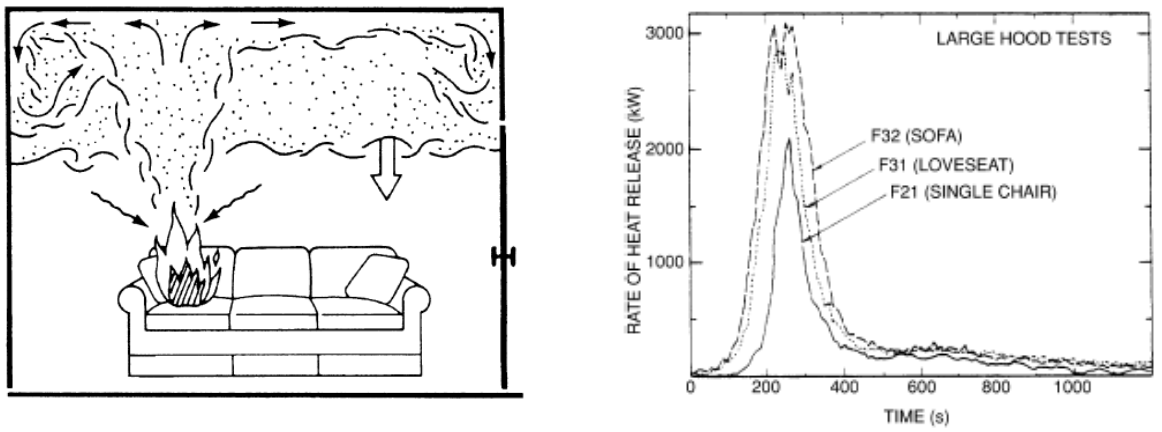


(a) (b)

Figure 19- (a) Illustration of a localised fire ignition in a sofa (Karlsson & Quintiere, 2000); (b) Heat release rate according to the particular experiments published by Bukowski and Peacock (Bukowski & Peacock, 1989)

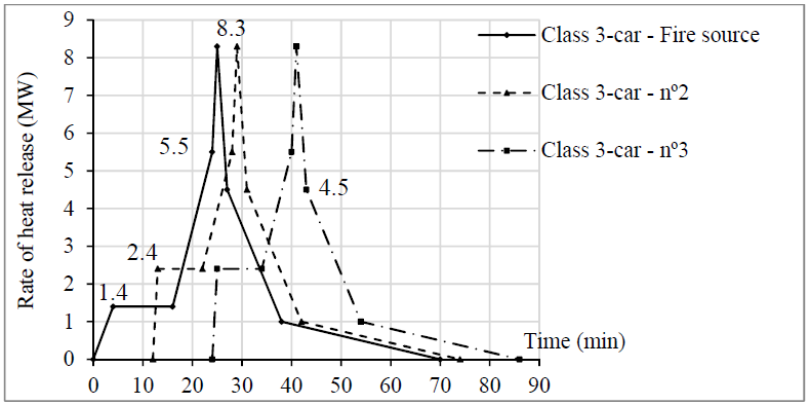


Figure 20- Curves of rates of heat release from burning of 3 vehicles, class 3 (Haremza et al., 2013)

## 4.2 Heat release rate measurement methods

The most common method to assess materials heat release rate is the Cone Calorimeter test (see Figure 21), which follows the procedure given in international standard ISO 5660-1 (1993). The basis of this method is that most gases, liquids, and solids release a constant amount of energy for each unit mass of oxygen consumed (13.10 kJ/kg). After ignition, all of the combustion products are collected in a hood and removed through an exhaust duct, in which the flow rate and composition of the gases is measured, in order to determine how much oxygen has been used. This way, it is possible to assess heat release as a function of the consumed oxygen.

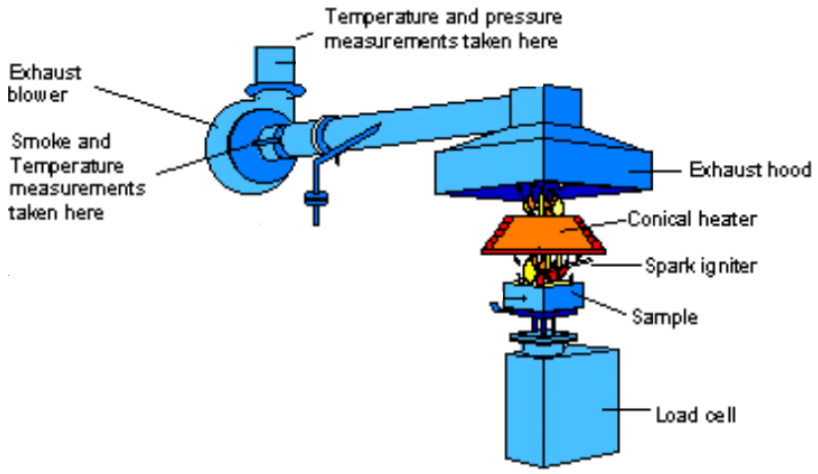


Figure 21- Cone Calorimeter test, according to ISO 5660-1 (1993) (Efectis Nederland BV, 2011)

Another common method of assessing the heat release rate is to measure the burning rate, which is also known as the mass loss rate, as suggested by Babrauskas, in the *SFPE Handbook of Fire Protection Engineering* (Babrauskas, 2002). This may be done by weighing the material as it burns, using weighing devices or load cells. Estimating the heat release rate based on the burning rate requires knowledge of the material effective heat of combustion ($\Delta H_{c,eff}$):

$$Q = \dot{m}\Delta H_{c,eff} \tag{4.1}$$

Where:

| | |
|---|---|
| Q | is the heat release rate [MW]; |
| $\dot{m}$ | is the burning rate [kg/sec]; |
| $\Delta H_{c,eff}$ | is the effective heat of combustion [kJ/kg]. |

The average burning rates for many products and materials have been experimentally determined in free-burning tests. For many materials, the burning rate is reported per horizontal burning area (kg/m$^2$-sec). If the horizontal burning area of the fire source ($A_f$) and the effective heat of combustion ($\Delta H_{c,eff)}$ are known, the above equation becomes:

$$Q = \dot{m}^{"}\Delta H_{c,eff} A_f \tag{4.2}$$

Where:

$\dot{m}"$ is the burning rate per unit area and time [kg/m$^2$-sec];
$A_f$ is the horizontal burning area of the fire source [m$^2$].

However, burning rate per unit area and time ($\dot{m}"$) is not constant for smaller burning areas. This is explained by the fact that (radiative) heat flux, from the flame toward the fuel surface, is lower for smaller fire plumes. Figure 22 shows a decrease on burning rate for circular fires with diameter lower than 2 m.

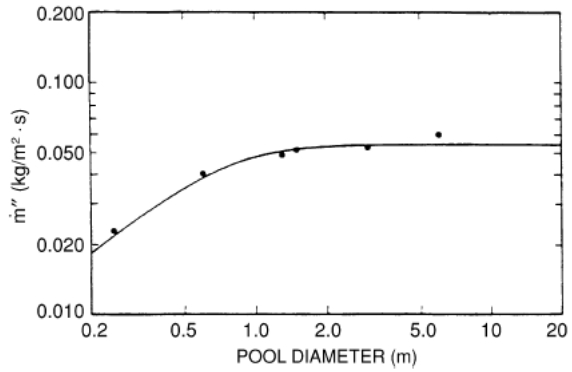


Figure 22- Burning rate per unit area and time for gasoline pools of various diameters (Karlsson & Quintiere, 2000)

In equation (4.3), burning rate is presented as a function of fire diameter, respecting the curve presented in Figure 22 .

$$\dot{m}" = \dot{m}"_{\infty}\left(1 - e^{-k\beta D}\right) \tag{4.3}$$

Where:

$\dot{m}"_{\infty}$ is the maximum burning rate per unit area and time [kg/m$^2$-sec]
kβ is the empirical constant [m$^{-1}$];
D is the diameter of burning area [m].

In order to take into account the dependence of burning rate (per unit area and time) on burning area, Babrauskas (2002) presented equation (4.4):

$$Q = \dot{m}"_{\infty}\, \Delta H_{c,eff} A_f (1 - e^{-k\beta D}) \tag{4.4}$$

Table 2 summarizes the burning characteristics of the fuels, determined by Babrauskas (2002) and analysed in the context of present thesis. Note that the heat of combustion given in Table 2 corresponds to the complete heat of combustion.

Table 2- Burning characteristics of fuel materials (Babrauskas, 2002)

| **Fire load** | Density [kg/m$^3$] | Mass Burning Rate ($\dot{m}''_\infty$) [kg/m$^2$-sec] | Heat of Combustion ($\Delta H_c$) [kJ/kg] | Empirical Constant $k\beta$ [m$^{-1}$] |
|---|---|---|---|---|
| Petroleum Products | | | | |
| Diesel | 918 | 0.045 | 44.4 | 2.1 |
| Benzene | 740 | 0.048 | 44.7 | 3.6 |
| Crude oil | 855 | 0.0335 | 42.6 | 2.8 |
| Fuel oil, heavy | 970 | 0.035 | 39.7 | 1.7 |
| Gasoline | 740 | 0.055 | 43.7 | 2.1 |
| Kerosene | 820 | 0.039 | 43.2 | 3.5 |
| Transformer oil | 760 | 0.039 | 46.4 | 0.7 |
| Cellulose Material | | | | |
| Wood | 420-640 | 0.055 | 13-15 | - |

Finally, the equation (4.5) given by Babrauskas (2002) is used to estimate the heat release rate in the context of this thesis:

$$Q = \dot{m}''_\infty \chi \Delta H_c A_f (1 - e^{-k\beta D}) \quad (4.5)$$

Where:

$\chi$ is the efficiency of combustion; For sootier flames, such as those that appear when diesel burns, the diameter dependence should be considered and the combustion efficiency is lower than 100%. According to (Karlsson & Quintiere, 2000), combustion efficiency may be considered around 60 to 70% for free burn experiments. Byström and co-authors considered combustion efficiency to be in a 70 % to 80% range;

$\Delta H_c$ is the heat of combustion [kJ/kg].

## 4.3 Enclosure Effects on the Burning Rate

In accordance with equation (4.1), when a fire source burns inside a compartment, the heat release rate is directly dependent on the burning rate, which represents the fuel mass loss per unit time. So, the enclosure effects on the burning rate may be significant in the heat release rate. The size of the compartment and the opening factor were found to be the most relevant compartments characteristics with effects on the burning rate.

When a fire source starts burning in a compartment, the smoke and hot gases will accumulate at the compartment ceiling level and heat the compartment boundaries. In smaller compartments, these boundary surfaces and the hot gases may radiate heat toward the fuel surface, increasing the burning rate and consequently the heat release rate (Karlsson & Quintiere, 2000), see Figure 23. Also, the compartment openings may not guarantee the oxygen needed for combustion, decreasing the amount of fuel consumed and increasing the concentration of unburned gases. For small ventilation rates, the limited availability of oxygen causes incomplete combustion, thereby decreasing the burning rate (Babrauskas, 2002).

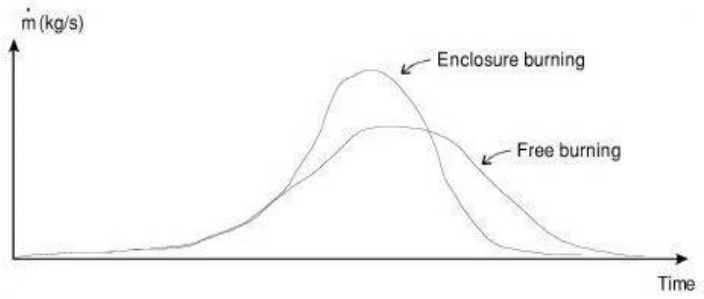


Figure 23- Comparison between an enclosure burning in a small compartment and a free burning (Karlsson & Quintiere, 2000)

## 4.4 Pool Fires

### 4.4.1 Introduction

Different procedures have been used, in order to simulate a localised fire: pool fires (Byström et al., 2012); wood cribs (Wald et al., 2009) and gas diffusion burners (Kamikawa et al., 2003). In this research work it was decided to use pool fires as fire source, once burning characteristics of liquid fuel have been widely studied. The use of wood cribs would imply in-situ measurements of density and moisture content as moisture content of wood has strong influence on its burning characteristics, as shown in Table 2. On the other hand, the use of diffusion burners was considered be a more dangerous process than the use of pool fires.

Looking into the bibliography, a pool fire may be defined as “a buoyant diffusion flame in which the fuel is configured horizontally” (Hamins & Burch, 1996). In this context, a pool

fire may be the result of a spilled combustible (gas, liquid or solid) of any shape and thickness, and may be controlled by a confinement such as a container. For a given amount of fuel, spills with a large surface area burn with a higher heat released for a short duration, and spills with a smaller surface area burn with a lower heat released for a longer duration (Babrauskas, 2002).

The ignition of liquid fuels may result from leakage of containers, oil spill from electrical transformers or fuel sprays from pipe flanges on equipment such as gasoline generators. Fuels such as liquids used for cleaning and painting are examples of possible localised fire sources. Therefore, pool fires may directly simulate a liquid fuel burning; on other hand, adjusting the diameter and the type of liquid fuel used as fire source, pool fires may simulate a large range of other fire sources such as car explosions or burning furniture.

### 4.4.2 Burning Duration of a Pool Fire

In accordance with Babrauskas (Babrauskas, 2002), the burning duration ($t_b$) of a pool fire for a fixed mass or volume of liquid fuel is estimated using following formula:

$$t_b = \frac{4V}{\pi D^2 \nu} \tag{4.6}$$

Where:

V is the volume of liquid [$m^3$];
D is the pool diameter [m];
$\nu$ is the regression rate [m/sec].

The regression rate (ν) is defined as “a volumetric loss of liquid per unit surface area of the pool per unit time” (Babrauskas, 2002), as illustrated by the formula:

$$\nu = \frac{\dot{m}''}{\rho} \tag{4.7}$$

Where:

$\dot{m}''$ is the burning rate per unit area and time [$kg/m^2$-sec] given by equation (4.3);
$\rho$ is the liquid fuel density [$kg/m^3$].

# 5 EXPERIMENTAL EVALUATION OF HEAT TRANSFER IN LOCALISED FIRE SCENARIO

## 5.1 Introduction

This chapter presents the details of the experimental investigation on the heat transfer phenomenon into steel columns subjected to localised fires, carried out under research project *Impactfire – Robust Connections for Impact and Fire Loading*, within the Workpackage 1 – *Accidental Loading Scenario*. Experimental tests were performed with technical assistance provided by Laboratory of Testing Materials and Structures of the University of Coimbra. The main goal of the experimental research was to create heat transfer correlations for the specific case of steel columns subjected to localised fires. Full-scale fire tests were performed in a large fire compartment, where a steel column was exposed to distinct localised fire scenarios.

## 5.2 Experimental setup

A large compartment was required in order to perform full-scale natural fire tests. After legal authorization and approbation by a fire fighting unit, the tests were performed in the former ceramic industry *Cerâmicas Estaco* located in Coimbra, Portugal (Figure 24).

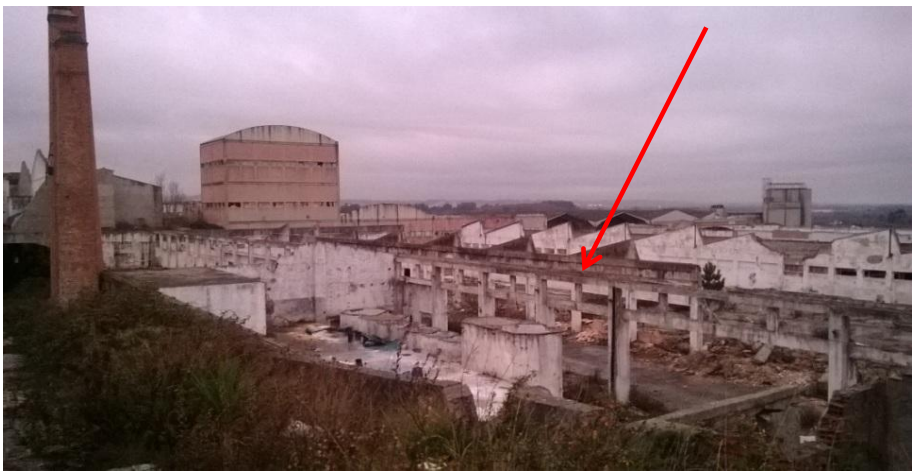

Figure 24- *Cerâmicas Estaco*, Coimbra

### 5.2.1 Fire compartment characteristics

The experiments were carried out in a large compartment located in a basement, with the configuration presented in Figure 25. The compartment internal dimensions were 10 m x 9.75 m and 3 m high. A concrete beam with a 0.30 m x 0.45 m rectangular cross-section supported the compartment celling slab at mid-spam. The beam was supported by a concrete column at mid-span, with a 0.30 m dia. circular section. The compartment ceiling consisted in a one-way concrete joist slab with 0.20 m thickness and the floor was a basement concrete floor slab with reduced thickness. The walls surrounding the compartment were 0.20 m masonry walls. In its initial configuration, the fire compartment presented two openings: a 4.65 m x 2.2 m door opening and a 0.60 m x 0.40 m window opening. In order to study different opening factors, various compartment openings configurations were tested along the experimental program, in order to study different opening factors; namely the door opening was gradually closed along the experimental programme and a ceiling opening was provided, with increasing dimensions through the experimental programme.

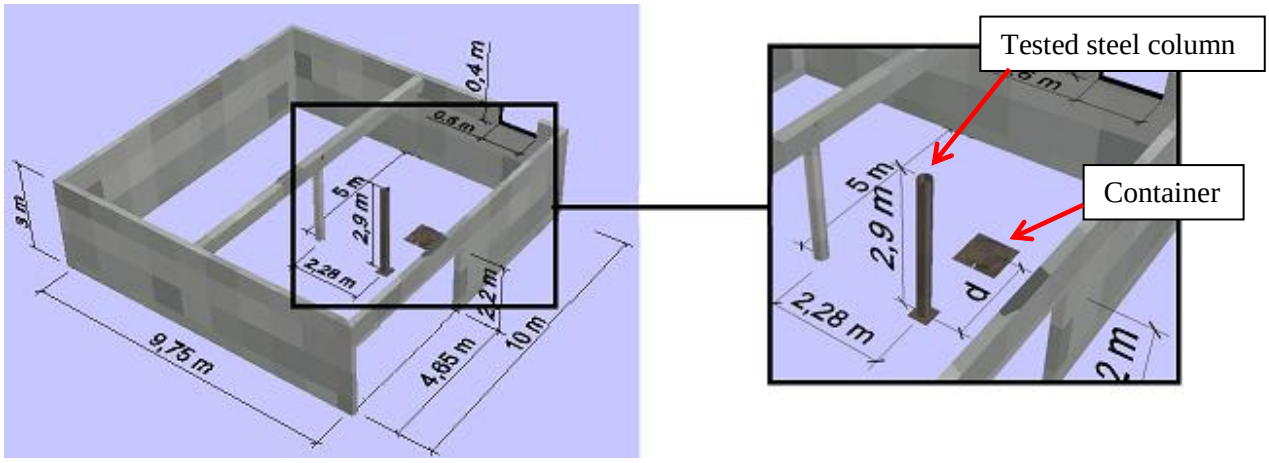


Figure 25- Localised fire test compartment configuration

### 5.2.2 Steel column characteristics

During the fire experiments, a circular hollow steel column was subjected to distinct localised fire scenarios. In order to avoid irreversible deformations during fire exposure through all the fire tests, a robust column, in steel grade S355, with circular hollow section with 245 mm dia. and 10 mm thickness, was used. The column high of 2.90 m, slightly lower than compartment height (3 m), was established in order to avoid deflection and additional bending moments induced in the member by restrained thermal elongation. According to the values given in EN 1993-1-2 (2005) for thermal elongation of carbon steel and present in Figure 3, a 2.90 m column would expand 5 cm in the worst case scenario (a uniform heating of 1200 ºC).

The column was unloaded and its circular interior was left empty. The lower and upper ends of the column were sealed in order to avoid gas exchanges, as it happens in a real situation. The column was simply supported by base plate in order to guarantee the stability of the column.

Once the steel column could not be placed in the centre of compartment due to a pre-existent concrete column, it was decided to locate it at the exact mid distance from the pre-existent column and the wall possessing the opening. This position would guarantee adequate ventilation, providing a faster exhausting of burning gases. The steel column was positioned according to Figure 25.

### 5.2.3 Containers characteristics

The thermal action was applied through pool fires. The pool fires were effected with two distinct steel circular containers filled with a liquid fuel (see §5.4.1) and placed in distinct positions inside the fire compartment.

The pool fires were defined as two containers in steel grade S235 were designed: a 0.70 m dia. container with 12 l capacity and a 1.10 m fire container with 30 l capacity, as illustrated in Figure 26. It was intended to build robust containers ensuring that burning area would stay constant along the pool fire. For that purpose, 15 mm steel plates were used for containers grounding whereas 25 mm thick hollow sections were used for lateral confinement, reinforced with triangular stiffeners in order to avoid lateral deformation.

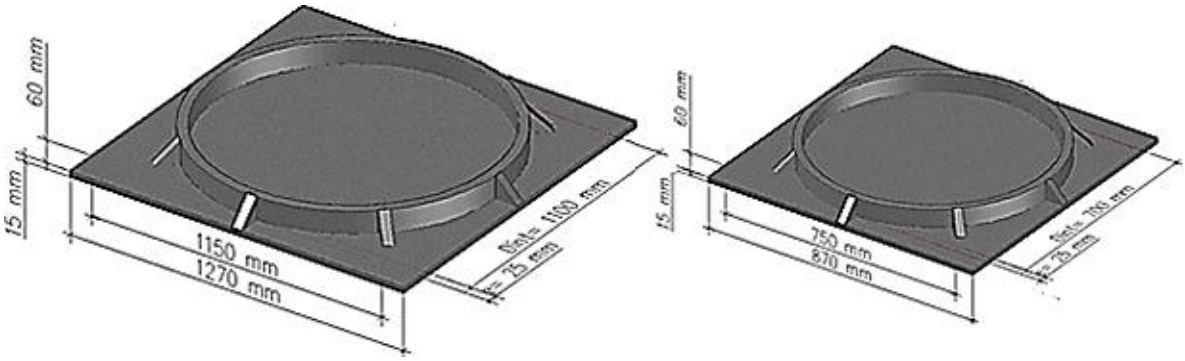


(a) (b)

Figure 26- Steel containers: (a) 1.10 m dia. steel container; (b) 0.70 m dia. container

These two distinct pool fires were used in order to simulate both localised fire models presented in Annex C of EN 1991-1-2 (2002): i) not impacting the ceiling; ii) impacting the

ceiling. Its diameter was chosen according the required thermal action to simulate both scenario (§5.4.2).

Firstly, the pool fires were placed in an adjacent position to the steel column: for the 0.70 m dia. pool, the distance between geometrical centres of the steel column and the circular pool was set as 0.60 m; for the 1.10 m dia. pool, this distance corresponded to 0.80 m. A schematic view of the pools positioning in the fire compartment is presented in Figure 27. Secondly, it was intended to place the pool fires in a further distance in order to study the effects of distance on the heat transfer to the steel column. Aiming to simulate a real fire situation, as a car fire, the pools were placed 1.20 m away from the column: being 2.40 m x 4.80 m the recommended dimensions for a car space (Vehicular Access Standards, 1999), the gravity centre of a car engine may be positioned at 1.20 m from a limiting column. A schematic view of the pools positions in this case scenario is presented in Figure 28.

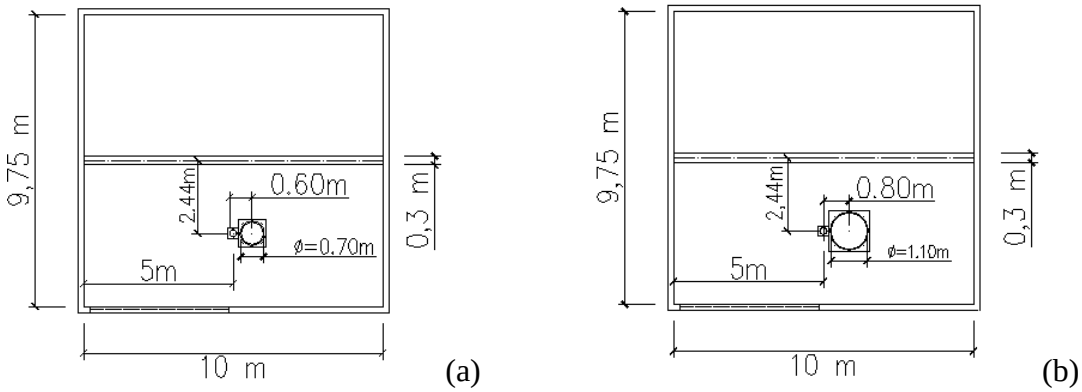


Figure 27- Test configuration: (a) 0.70 m pool at adjacent position; (b) 1.10 m pool at adjacent position

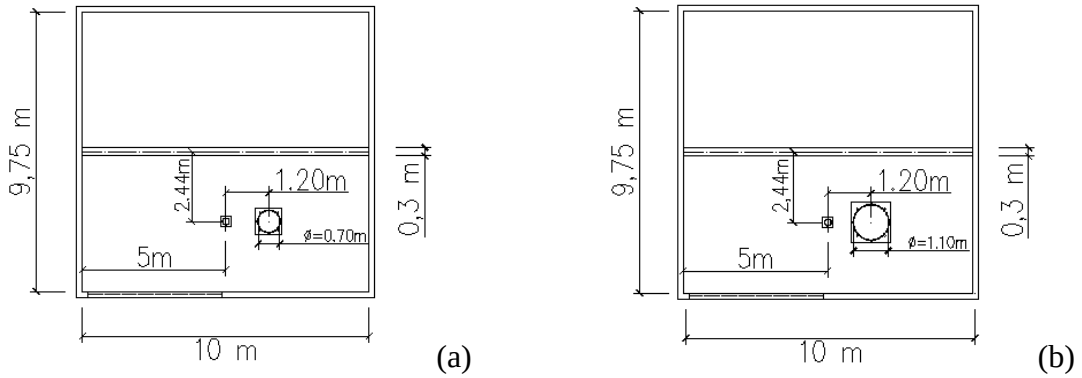


Figure 28- Test configuration: (a) 0.70 m pool at 1.20 m distance; (b) 1.10 m pool at 1.20 m distance

## 5.3 Experimental programme

The experimental programme of this research is presented in Table 3 . The CHS column was exposed to a total of height fire tests, each of them simulating a distinct fire scenario. For comparison purposes, the fire tests were divided in 3 different groups, in accordance with Table 3 . Group 1 includes four fire tests using the 0.70 m pool at adjacent fire position, performed in distinct ventilation conditions. Group 2 includes two fire tests using the 0.70 m pool positioned 1.20 m away from the steel column, in distinct ventilation conditions. Group 3 includes two fire tests using the 1.10 m pool, with the two distinct positions mentioned before and the same ventilation conditions.

Table 3- Test planning

| Group | Test | Pool Diameter D [m] | Pool Distance d [m] | Openings [m] |
|---|---|---|---|---|
| 1 | 1(*) | 0.70 | 0.60 | 4.50 m x 2.55 m door |
| | | | | 0.60 m x 0.40 m window |
| | 2 | 0.70 | 0.60 | 1.90 m x 2.55 m door |
| | | | | 0.60 m x 0.40 m window |
| | | | | 0.36 m x 0.30 m celling opening |
| | 3 | 0.70 | 0.60 | 1.90 m x 2.55 m door |
| | | | | 0.60 m x 0.40 m window |
| | | | | 0.36 m x 0.60 m celling opening |
| | 4 | 0.70 | 0.60 | 1.90 m x 2.55 m door opened 37º |
| | | | | 0.60 m x 0.40 m window |
| | | | | 1.10 m x 0.60 m celling opening |
| 2 | 5 | 0.70 | 1.20 | 1.90 m x 2.55 m door |
| | | | | 0.60 m x 0.40 m window |
| | | | | 0.36 m x 0.60 m celling opening |
| | 6 | 0.70 | 1.20 | 1.90 m x 2.55 m door opened 53 % |
| | | | | 0.60 m x 0.40 m window |
| | | | | 1.10 m x 0.60 m celling opening |
| 3 | 7 | 1.10 | 0.80 | 1.90 m x 2.55 m door opened 53 % |
| | | | | 0.60 m x 0.40 m window |
| | | | | 1.10 m x 0.60 m celling opening |
| | 8 | 1.10 | 1.20 | 1.90 m x 2.55 m door opened 53 % |
| | | | | 0.60 m x 0.40 m window |
| | | | | 1.10 m x 0.60 m celling opening |
| (*) In this test, it was used 15 l of fuel instead of 12 l (by measurement error). The effects of this exception are taken into account in the analysis of experimental results. | | | | |

## 5.4 Thermal actions

### 5.4.1 Fuel selection

A pool fire may be the result of burning combustible of any shape and thickness, and may be controlled by a confinement such as a container. Using previous knowledge on pool fires, it was decided to create localised fires using a liquid combustible controlled by steel containers with a circular shape. These containers (see §5.2.3) insure a constant burning area during a fire. Based in this assumption, equation (4.5) may be used in order to calculate the heat release rate.

The choice of liquid combustible was accomplished through two small scale burning tests. The aim of these tests was to compare burning characteristics of the two most common fuel combustibles in the market: diesel and gasoline. A square steel container with dimensions 0.25 m x 0.25 m was prepared to perform burning tests (Figure 29 (a)). The mass loss was measured along the fire test, in order to compare the burning characteristics of diesel and gasoline (95 octanes). The density of diesel and gasoline was measured as 0.838 kg/l and 0.739 kg/l, respectively. One litter of fuel was burned in each test. Comparison of both tests is presented in Figure 29 (b).

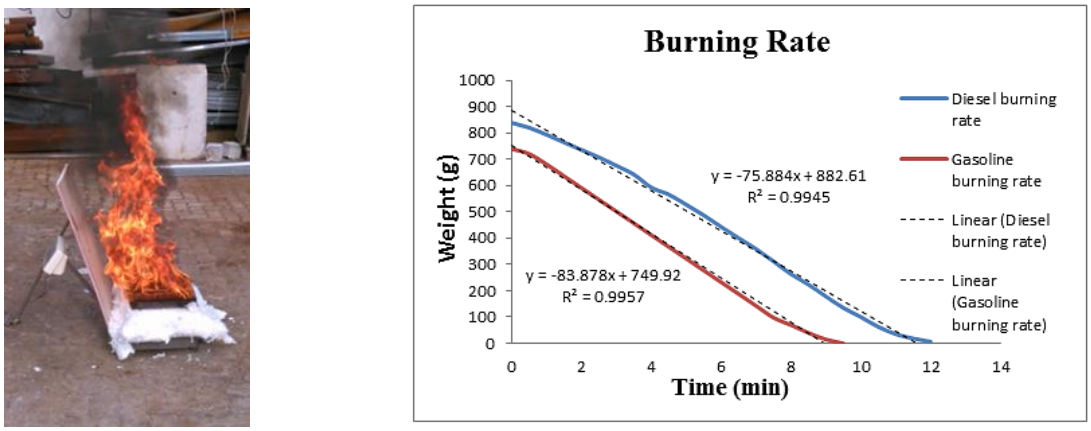


(a) (b)

Figure 29- (a) Small scale fire test; (b) Burning rates comparison for fuels: diesel and gasoline

The burning rate (per unit area per unit time) was estimated to be 0.021 kg/m$^2$-sec for diesel and 0.023 kg/m$^2$-sec for gasoline.

The burning rate for gasoline was compared with the simplified method presented in Figure 23. For that purpose, equivalent diameter of the used container was calculated according to formula (5.1).

$$D = 2\sqrt{\frac{A}{\pi}} = 2\sqrt{\frac{0.25 * 0{,}25}{\pi}} = 0.282\ m \qquad (5.1)$$

For a pool fire with equivalent diameter of 0.282 m, the obtained burning rate for gasoline was found to be in accordance with the simplified methods, as shown in Figure 30.

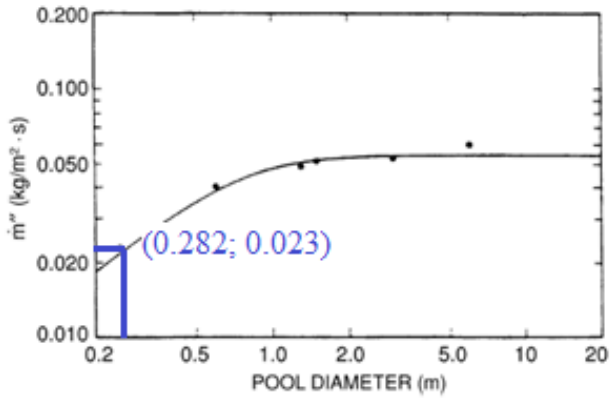


Figure 30- Comparison between experimental and theoretical burning rates

Table 4 compares the experimental burning rates, obtained in the small scale tests, with estimations obtained by equation (4.3): $\dot{m}" = \dot{m}"_{\infty}\left(1 - e^{-k\beta D}\right)$. The resulting deviations are small enough to validate this simplified approach. Burning characteristics ($\dot{m}"_{\infty}$ and kβ) of fuel materials may be found in Table 2.

Table 4- Estimations for burning rate per unit area and time

| | **Diesel** | **Gasoline** |
|---|---|---|
| $\dot{m}"_{\infty}$ [kg/m$^2$-sec] | 0.045 | 0.055 |
| kβ | 2.1 | 2.1 |
| D [m] | 0.282 | 0.282 |
| $\dot{m}"$ [kg/m$^2$-sec] | 0.020 | 0.025 |
| **Deviation** | **- 4.24 %** | **+ 6.87 %** |

As diesel and gasoline have similar heat of combustion (Table 2), the thermal action resulting from the heat release rate on combustion is directly proportional to burning rate. So, the use of gasoline would provide higher heat release rate for the same burning area. However, for the

same fuel volume, diesel provided a fire with longer duration, as shown in Figure 29 (b). The diesel lower burning rate and its higher density are the reasons for this to happen. Therefore, it would be necessary a bigger volume of gasoline to guarantee the same time of exposure. Consequently, the cheaper price of diesel together with its higher density and longer fire duration turned the use diesel as combustible for the full-scale fire tests of this work.

### 5.4.2 Thermal actions in experimental tests

EN 1991-1-2 (2002) presents two distinct localised fire models: smaller fires not impacting the celling and larger fires impacting the celling (see Figure 9 and Figure 10). In order to simulate both scenarios, an estimation of thermal action was required. According to equation (2.25), the total length of a fire plume is given by $L_f = -1.02D + 0.0148Q^{2/5}$. Being the heat release rate $Q = \dot{m}''\chi\Delta H_c A_f(1 - e^{-k\beta D})$ as shown in equation (4.5), the total length of a fire plume ($L_f$) may be expressed as a function of the pool diameter:

$$L_f = -1.02D + 0.0148.\left[\dot{m}''\chi\Delta H_c\pi\frac{D^2}{4}\left(1 - e^{-k\beta D}\right)\right]^{2/5} \quad (5.2)$$

Once all the burning characteristics for diesel are known (see Table 2), total length of the fire plume becomes directly dependent on fire diameter. In order to simulate both localised fire scenarios presented in Annex C of EN 1991-1-2 (2002), two distinct pool fires were defined: i) one leading to a fire plume with total length lower than the height of compartment ($L_f < 3$ m) and ii) another leading to a plume reaching the ceiling ($L_f > 3$ m). These pool fires were intended to be controlled by containers and the containers dimensions were chosen from a large range of possible diameters as shown in Table 5.

In order to simulate a real localised fire situation using the smallest fuel quantity, burning duration was set to be approximately 10 min. The burning duration was defined according to real fire situations as shown in Figure 19, where a single chair actively burns for about 10 minutes. Estimations for heat release rate were made for total efficiency of combustion ($\chi = 1$) - conservative approach. Volume estimations were made for a corrected fuel density 0.838 kg/l, as measured in previous small scale tests. Consequently, two pool fires were defined in accordance with Table 6.

Table 5 - Definition of thermal actions

| D [m] | $L_f$ [m] Equation (5.1) | $L_f$ < Celling [= 3 m] | Q [MW] Equation (4.5) | V [l] | Burning Duration [min] Equation (4.6) |
|---|---|---|---|---|---|
| 0.70 | 2.28 | not impacting ceiling | 0.58 | 15 | 13.85 |
| | | | | 12 | 11.08 |
| | | | | 10 | 9.24 |
| 0.80 | 2.59 | not impacting ceiling | 0.80 | 15 | 10.04 |
| | | | | 12 | 8.03 |
| | | | | 10 | 6.69 |
| 0.90 | 2.89 | not impacting ceiling | 1.06 | 30 | 7.60 |
| | | | | 20 | 6.08 |
| | | | | 10 | 5.07 |
| 1.00 | 3.18 | impacting ceiling | 1.36 | 40 | 15.88 |
| | | | | 30 | 11.91 |
| | | | | 20 | 7.94 |
| 1.10 | 3.46 | impacting ceiling | 1.68 | 40 | 12.79 |
| | | | | 30 | 9.59 |
| | | | | 20 | 6.39 |
| 1.20 | 3.73 | impacting ceiling | 2.05 | 40 | 10.53 |
| | | | | 30 | 7.90 |
| | | | | 20 | 5.26 |

Table 6 - Designed pool fires

| D [m] | $L_f$ [m] Equation (5.1) | $L_f$ < Celling [= 3 m] | Q [MW] Equation (4.5) | V [l] | Burning Duration [min] Equation (4.6) |
|---|---|---|---|---|---|
| 0.70 | 2.28 | not impacting ceiling | 0.58 | 12 | 11.08 |
| 1.10 | 3.46 | impacting ceiling | 1.68 | 30 | 9.59 |

## 5.5 Testing procedure and instrumentation

In order to perform the experimental test, the containers were positioned according to Figure 27 and Figure 28, and filled with fuel, which was ignited in order to perform a localised fire.

As specified in the experimental programme, the steel CHS 245 X 10 column was subjected to distinct localised fire actions, through the consideration of different pool diameters, fuel volumes and compartment openings.

The pool diameter and fuel volumes were determined according to §5.4.1 and §5.4.2.

Concerning the compartment boundaries, several opening sets were tested in order to verify enclosure effects on the fire development. In addition to the original openings, a ceiling opening was created, in order to simulate distinct ventilation conditions. Variations on the opening areas were considered as well. Concerning the door opening, the real situation of half-open door was also tested (opening angles of 37 % and 53 %).

Figure 31 shows the smoke evacuation, during a fire test. The smoke evacuated through the door opening spread to surrounding compartments, being released through the main entrance of the building (Figure 31 (a)). The smoke evacuated by the window opening was released into the ceiling level (Figure 31 (b)).


Figure 31- Smoke evacuation: (a) Building main door; (b) Compartment ceiling

The temperatures were registered using wire thermocouples. 60 K-type thermocouples with two 0.5 mm dia. wires were used to monitor steel and gas temperatures in each test. Thermocouples measuring gas temperatures presented an exposed bare junction while thermocouples measuring steel temperatures presented a grounded junction. Figure 32 illustrates the specimen and the positioning of thermocouples. In order to study the evolution of temperatures along the column height, measurements were made in 6 sections equally spaced by 0.47 m, as represented in Figure 32 a). In each section, four equally spaced thermocouples were welded to the column, monitoring the steel temperature ($TS_{ji}$, where $j$ is the section number and $i$ the position number according to Figure 32 (b)). In addition, gas temperatures were monitored by four thermocouples placed 5 cm away from the ones welded to the column ($TG_{ji}$). At the same levels, temperatures were also measured along the vertical axis of the fire plumes ($TFj$).

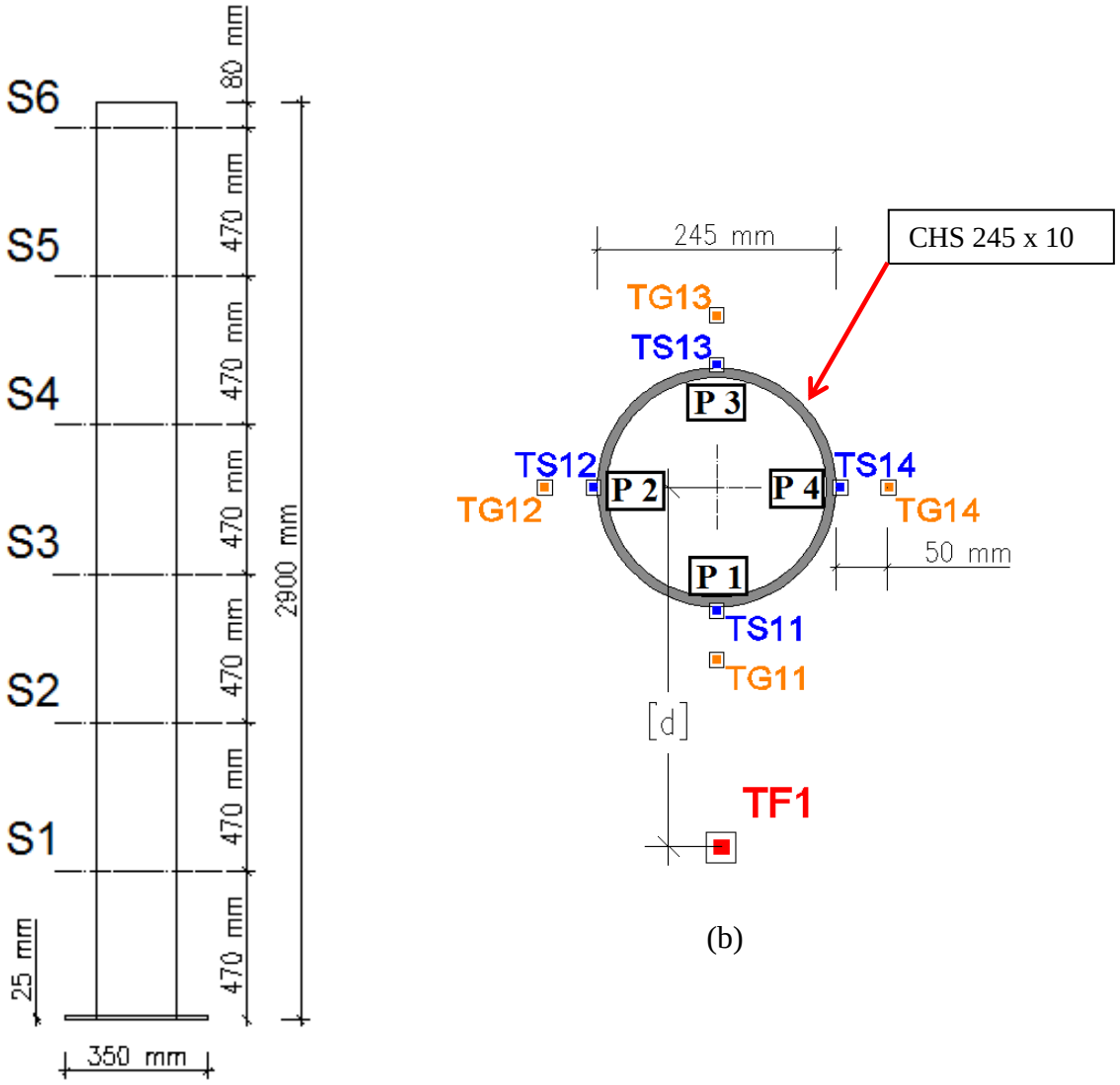


Figure 32- Steel specimen with positioning of the thermocouples: (a) View and definition of measured sections [mm]; (b) Section 1: top view with positioning of thermocouples [mm]

## 5.6 Results

### 5.6.1 Fire development and plume total heights

During fire tests, the flames were clearly tilted towards lateral positions. During the tests, the position of thermocouple wires along the column height (as seen in Figure 34), allows the definition of the column sections S1 to S4, in accordance to Figure 32 (a), creating a scale for experimental measurement of fire length. Within the three groups of tests performed in the experimental study (see Table 3), different fire developments were observed.

In the first and second groups of tests, flames were flickering to an average height between 1 and 2 m. In the third group of tests, the increase of the pool diameter from 0.7 m to 1.1 m enlarged the size of the flames considerably, but even within this group different fire scenarios were accomplished.

Figure 33 presents a series of pictures from test 1 at different instants during fire exposure. Figure 34 (a) presents the fire plume on its theoretical position with a measured length of 1.88 m (corresponding to column section S4). On the other hand, as represented in Figure 33 (b) and (c), at a measured length of 0.47 m (corresponding to column section S1), the flame was most of the time tilted towards lateral positions. The convective mass flows within the compartment (due to the air heating) together with the wind flows (due to openings), were the other main factors responsible for flame tilting.

In some fire scenarios, like the one presented in Figure 34, in which a series of pictures from test 2 is presented, the flame tilted to the position shown in Figure 34 (b) for almost the entire test. It was noticed that the plume development changes according to the nearest oxygen source, as shown in Figure 34 (c); in this test, the fire plume tilted to the position closer to the door opening, causing the fire to overlap the steel column.

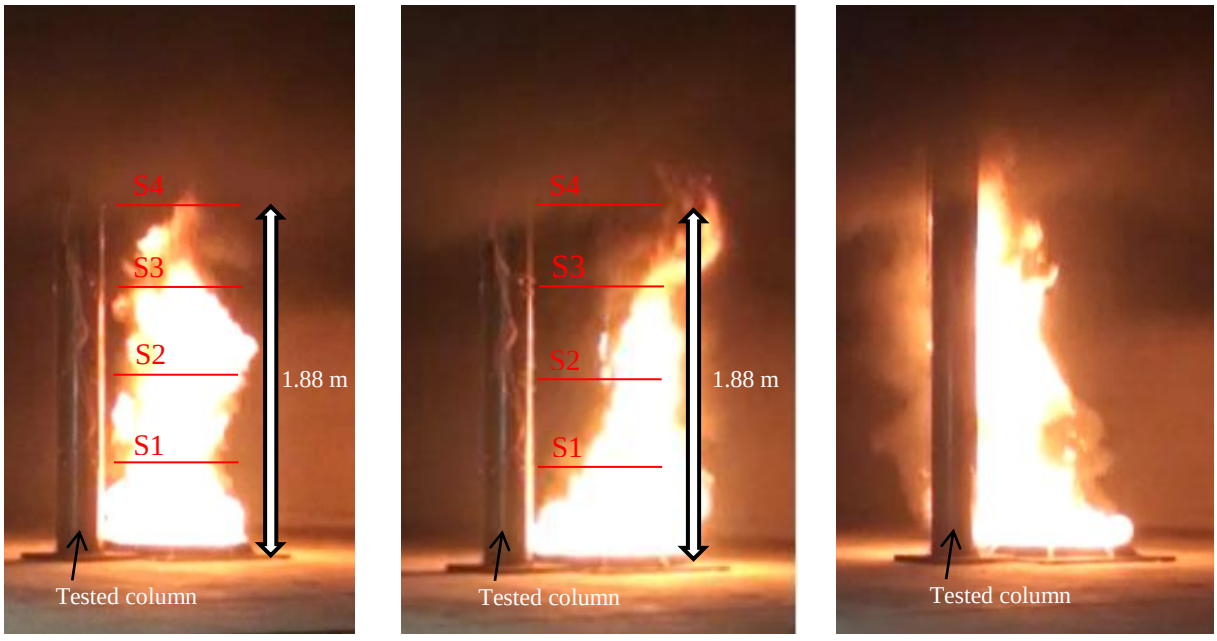


(a) (b) (c)

Figure 33- Fire plume resulting from test 1

(a) (b) (c)

Figure 34- Fire plume resulting from test 2

The increase of the pool diameter from 0.7 m to 1.1 m, which characterizes the third group of tests, enlarged the size of the flames considerably. Different fire scenarios were accomplished in tests 7 and 8: in test 7, the fire plume reached the ceiling, representing a large fire impacting the ceiling, while test 8 represented a small localised fire, similar to the ones observed in tests groups 1 and 2.

Detailed explanation about the fire developments in experimental tests are presented in the following items.

### 5.6.2 Analysis of tests results within Group 1

#### 5.6.2.1 Temperatures along the vertical axis of the fire plume

Within the first group of tests, the CHS 245 x 10 steel column was exposed to the same thermal action (0.70 m dia. pool fire at 0.60 m distance), according to different opening sets, as described in Table 3. Monitored gas temperatures at the vertical axis of the fire plume during tests 1 to 4 are reported in Figure 35 and Figure 36.

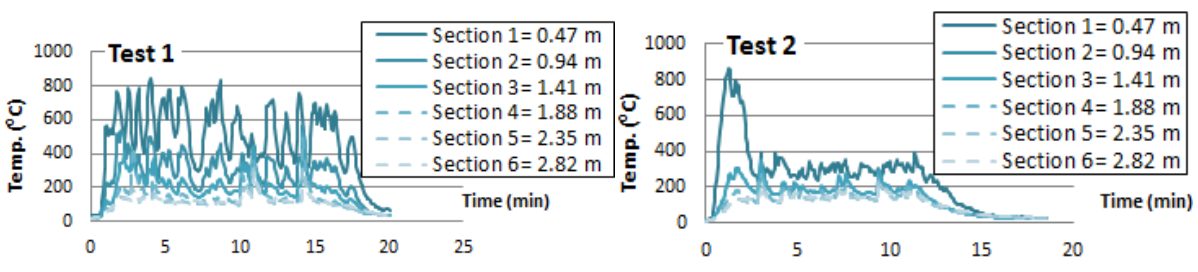


(a) (b)

Figure 35- Temperatures along the vertical axis of the fire plume: (a) test 1; (b) test 2

During test 1, it was observed a strong plume turbulence, which is verified by intermittent measurements in the lower sections (section 1 to 3). At upper sections, specifically over 1.88 m (section 4), the temperature remained uniform, indicating a fire plume maximum height lower than 1.88 m. Test 1 presented the longest fire duration (approximately 20 min); however, this duration will not be compared within the results of test group 1, once it is the result of the use of an exceptional fuel volume (15 l). It is also worth mentioning that the fire compartment in test 1 presented the greatest opening area within the experimental programme.

Test 2 was performed under distinct opening conditions: door opening area was reduced to less than a half and a small opening was created at the ceiling level. A notable fact during the test was the continuously tilting of the fire plume after the first minutes of fire development (see Figure 34). This is supported by the measured temperatures in section 1 of the fire plume (see Figure 35 (b)). After 3 min, the monitored temperature decreased substantially indicating a non-vertical development of the fire plume towards the door opening, which was the nearest oxygen source.

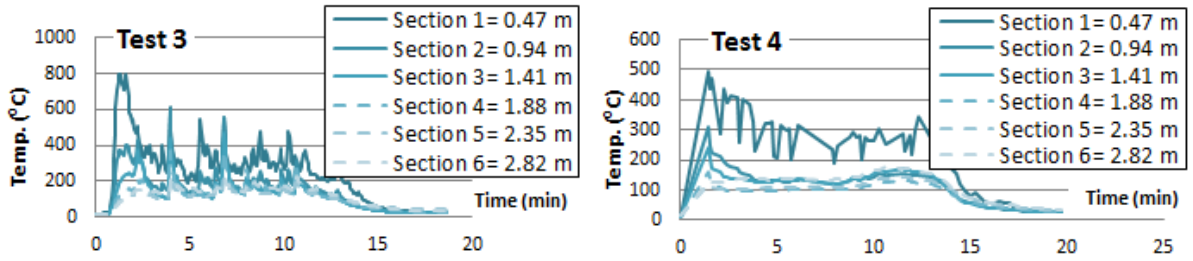


(a) (b)

Figure 36- Temperatures along the vertical axis of the fire plume: (a) test 3; (a) test 4

Test 3 was performed in very similar conditions to test 2. However, the ceiling opening area was increased. Being the ceiling vent placed 8 m away from the compartment door, the flame tilting was less significant, as depicted in Figure 36- however, the global behaviour of the flame was similar to the one observed during test 2.

Test 4 was performed under distinct enclosure scenario: a half-open fire resistant door was assembled with an opening angle of 37º, whereas the ceiling opening area was increased once more. As a result, the burning time was slightly higher than the burning time verified in tests 2 and 3. Besides, lower temperatures were measured along the fire plume, during the entire test, which could be justified with the occurrence of a lower heat release rate in test 4. Another plausible explanation would be the effects of wind action, causing a tilting of the fire plume during the entire test. These possibilities are discussed in the following sub-chapter.

#### 5.6.2.2 Average steel temperature along the vertical axis of the column

Average steel sections temperatures, as a function of exposure time, are depicted in Figure 37 and Figure 38, for tests 1 to 4.

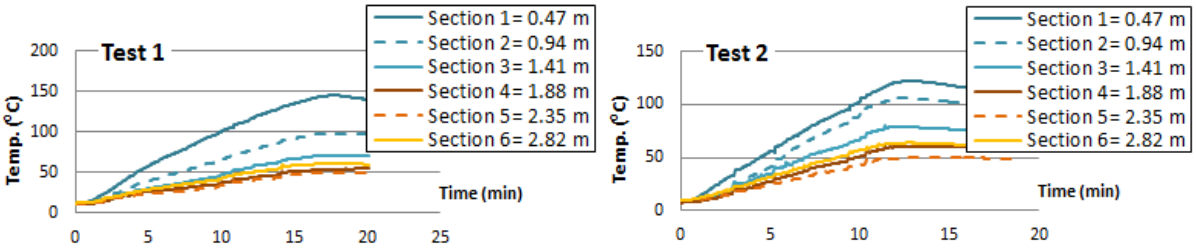


(a) (b)

Figure 37- Average steel temperature along the vertical axis of the column: (a) test 1; (b) test 2

Through the analysis of average steel temperatures on tests 1 and 2 in Figure 37, it was noticed a direct relationship between fire exposure time and measured steel temperatures. For 13 minutes of fire exposure, the steel column presents similar steel temperatures at section 1. However, in sections 2 and 3, higher temperatures were measured in test 2, for lower times of fire exposure, resulting of the tilting of the top flames towards the column, as shown in Figure 34 (c).

Concerning the evolution of temperature along the total height of the column measured during these tests, it was verified that the average steel temperature decreases along the height of the member. A notable variation in the average steel temperature was observed in section 1 to 3; which demonstrates the predominance of heat transfer by radiation at high levels within the total height of the fire plume. For steel sections higher than the total length of the plume, the heat transfer is performed mainly due to convective heat flux (see equation (2.2)). This fact is in accordance with section 6 measurements: the accumulation of hot gases at the ceiling level (due to convective mass flows) leads to higher steel temperatures than the ones measured in section 5.

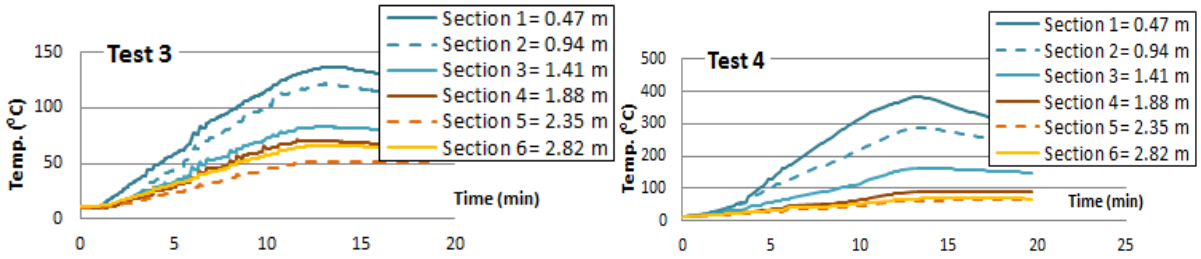


(a) (b)

Figure 38- Average steel temperature along the vertical axis of the column: (a) test 3; (b) test 4

The comparison between the results presented in Figure 38 (b) and Figure 39 (a) shows the similarity in the measured steel temperatures in tests 2 and 3, in accordance with the similar gas temperatures (along the fire plume) measured in these two tests. This similarity can be explained with the compartment ventilation conditions, very similar in both tests.

The average steel temperatures measured during test 4 present a distinct exposure scenario. The effects of the wind action (resulting from exterior wind flows) were pointed as a possible explanation for the low gas temperatures measured along the vertical axis of the plume, an explanation supported by the measured steel temperatures in Figure 39 (b): in all steel sections, the temperatures were found to be incredibly higher than the ones measured in tests 1 to 3, indicating a total rotation of the central axis of the plume.

#### 5.6.2.3 Average temperatures in the vicinity of the steel column

Average temperatures in the vicinity of the steel column are presented in Figure 40 and Figure 41. Gas temperatures were measured in the vicinity of the steel column by K-type thermocouples with two 0.5 mm wires placed 5 cm away from the steel column. Due to the upwards convective mass flows, the measured gas temperatures were barely uniform during tests 1, 2 and 3. Besides, higher temperatures were measured in section 6 of the steel column due to the accumulation of hot gases at the ceiling level. Test 4 presented a distinct scenario. Due to the wind action, thermocouples in the vicinity of the column measured gas temperatures inside the fire plume; this scenario changed the expected distribution of temperatures. The comparison between Figure 42 (b) and Figure 36 (b), shows that the gas temperatures measured in the vicinity of the steel column were higher than the ones measured in the vertical axis of the plume.

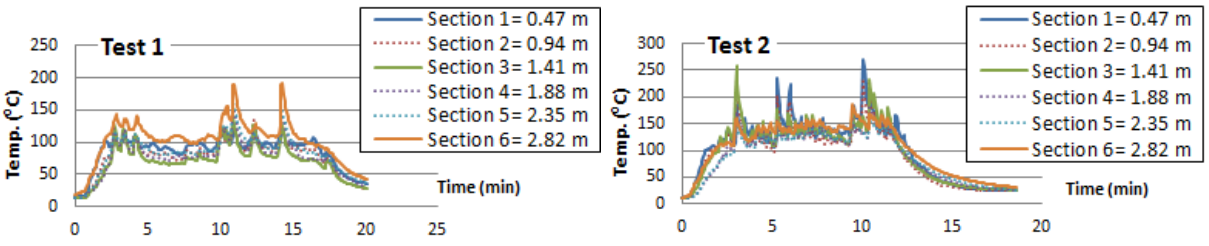


(a) (b)

Figure 39- Average temperatures in vicinity of the steel column: (a) test 1; (b) test 2

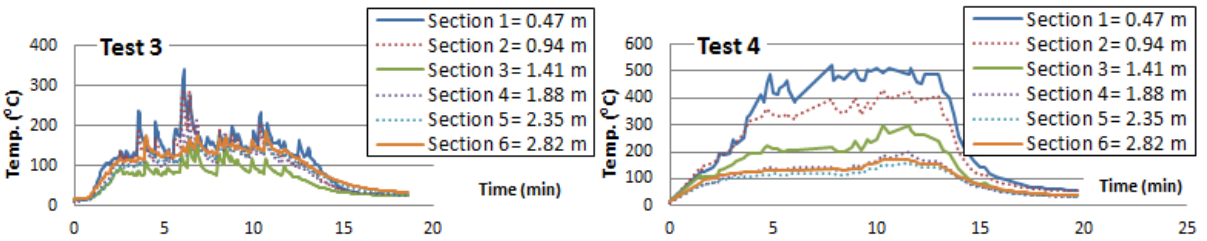


(a) (b)

Figure 40- Average temperatures in vicinity of the steel column: (a) test 3; (b) test 4

#### 5.6.2.4 Thermal gradient in the steel cross sections

Measured temperatures along the steel sections were not uniform. As expected, fire exposed surfaces presented higher temperatures due to the radiative component of heat flux (see equation (2.3)) than unexposed surfaces, which were heated mainly due convection and conduction through the steel column, due to shadow effect.

Figure 41 presents the evolution of steel section temperature gradient in the two extreme sections along the height of the column, namely section 1 and 6, during test 1. As shown in Figure 41 (a), the temperatures in steel section 1 presented a huge variation between exposed (position 1) and unexposed surfaces (position 3). The plume tilting towards lateral position is also reflected in the asymmetric temperatures measured in positions 2 and 3. It was also observed that he temperature gradient decreases along the column height. In steel sections closer to the compartment ceiling (section 6), the temperature gradient is no longer significant, as shown in Figure 41 (b). Monitored steel temperatures for section 1 to 6, during test 1 can be found in Annex 1. In tests 2 to 4, the steel sections temperature gradient was found to be very similar to the one observed in test 1.

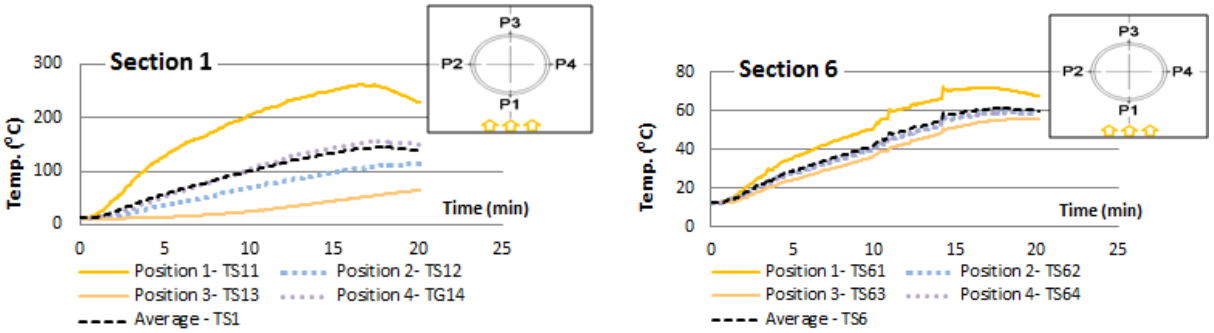


(a) (b)

Figure 41- Thermal gradient in the steel sections during test 1: (a) section 1; (b) section 6

#### 5.6.2.5 Thermal gradient in the vicinity of the steel sections

The gas temperatures in the vicinity of the steel column during test 1 are presented in Figure 42 for sections 1 and 6. At lower heights of the steel column, the gas temperatures in position 3 (corresponding to the side of the steel column opposed to the fire source) remain almost constant during the entire test; this is explained by the upward convective mass flows. Another notable fact concerns the gas temperatures measured in position 4 which are higher than the gas temperatures in position 1. This reveals an asymmetric heating of the column, explaining the asymmetric steel temperatures previously observed in Figure 41 (a).

As verified in the gas temperatures measurements presented in Figure 42, the thermal gradient decreases along the height of the column. In Figure 42 (b), the section temperature becomes uniform at the ceiling level, due to the hot gases accumulated.

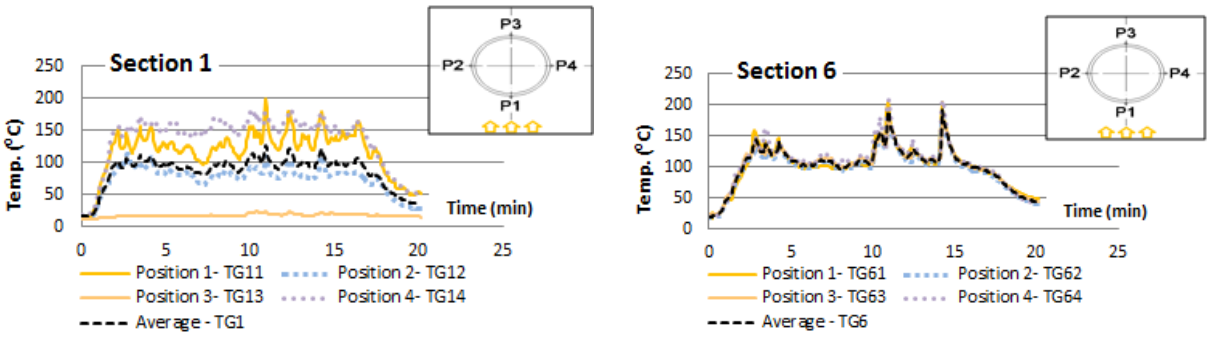


(a) (b)

Figure 42- Thermal gradient in vicinity of the steel sections during test 1: (a) section 1; (b) section 6

### 5.6.3 Analysis of tests results within Group 2

#### 5.6.3.1 Temperatures along the vertical axis of the fire plume

Within the second group of tests, the CHS 245 x 10 steel column was exposed to the same thermal action (0.70 m dia. pool fire at 1.2 m distance), considering different opening sets, as described in Table 3. Monitored gas temperatures at the vertical axis of the fire plume during tests 5 and 6 are reported in Figure 43.

The flame presented the same behaviour in both 5 and 6 fire tests, exhibiting continuous tilting after the first minutes of fire development. However, the burning duration was considerable higher during test 6, reflecting the smaller ventilation area and consequent decrease in oxygen density near the fire source.

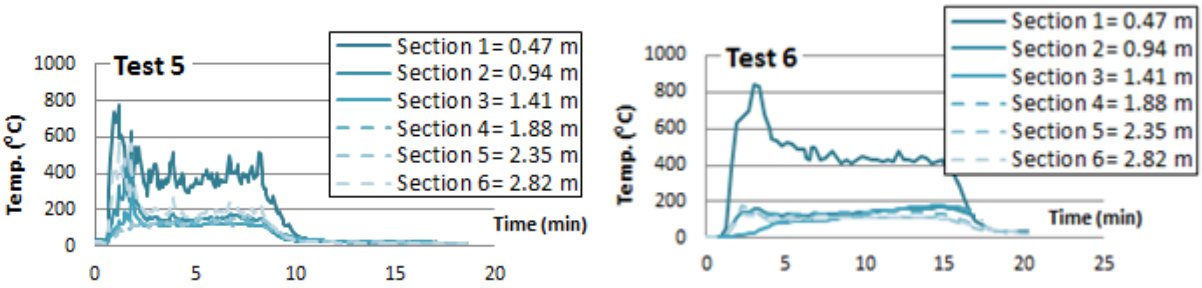


(a) (b)

Figure 43- Temperatures along the vertical axis of the fire plume: (a) test 5; (b) test 6

#### 5.6.3.2 Average steel temperature along the vertical axis of the column

Average steel temperatures along the column height are depicted in Figure 44 for tests 5 and 6. As observed for Group 1, the analysis of average steel temperatures noticed direct relationship between fire exposure time and measured steel temperatures was noticed. For 8 minutes of fire exposure, the steel column presents similar steel temperatures in both tests.

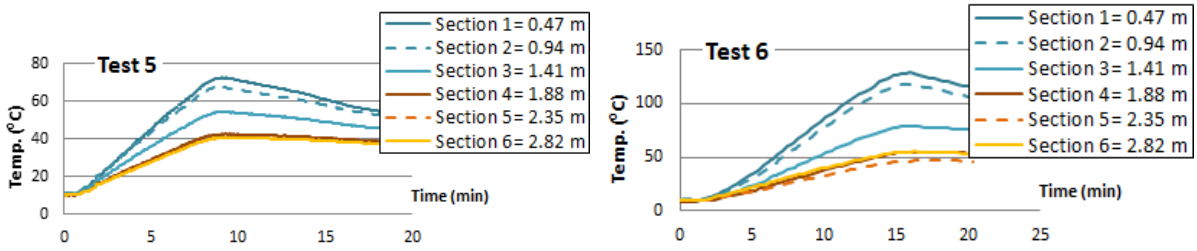


(a) (b)

Figure 44- Average steel temperature along the vertical axis of the column: (a) test 5; (b) test 6

#### 5.6.3.3 Average temperatures in the vicinity of the steel column

Due to the upwards convective mass flows, the measured gas temperatures during tests 5 and 6 were barely uniform in all column section, as shown in Figure 45. A similar observation was made during tests 1, 2 and 3. However, in test 6, higher temperatures were measured in section 1, which may be justified by flame tilting in later stages of fire development.

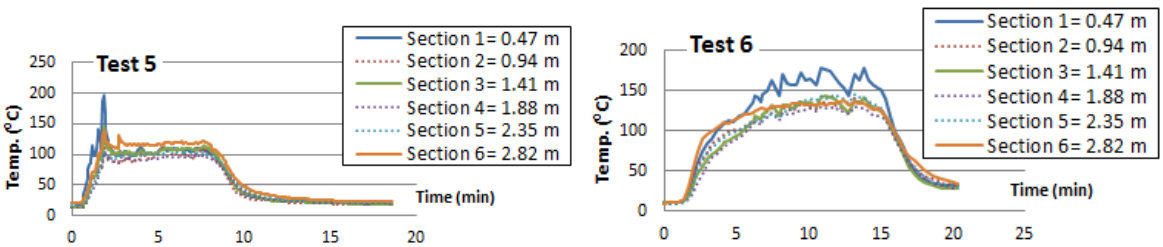


(a) (b)

Figure 45- Average temperatures in vicinity of the steel column: (a) test 5; (b) test 6

#### 5.6.3.4 Thermal gradient in the steel cross sections

Figure 46 presents the evolution of steel section temperature gradient in the two extreme sections along the height of the column, namely section 1 and 6, during test 5. According to Figure 48 (a), a huge temperature variation between exposed (position 1) and unexposed surfaces (position 3) was verified in section 1, in accordance with the results of the first group of tests. The plume tilting is also reflected in the asymmetric temperatures measured in positions 2 and 3. The temperature gradient decreases along the column height, in accordance with results obtained for the first group of tests. Monitored steel temperatures for section 1 to 6, during test 5 can be found in Annex 1. Concerning test 6, the steel sections temperature gradient was found to be very similar to the one observed in test 5.

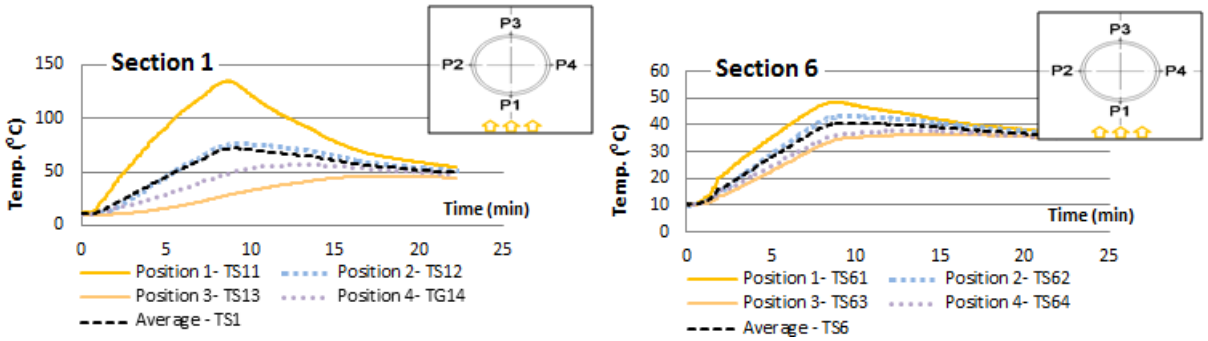


(a) (b)

Figure 46- Thermal gradient in the steel sections during test 5: (a) section 1; (b) section 6

#### 5.6.3.5 Thermal gradient in the vicinity of the of the steel sections

Monitored gas temperatures during test 5 are presented in Figure 47. Temperature evolution in the vicinity of each section followed the exact same principles verified during the first group of tests.

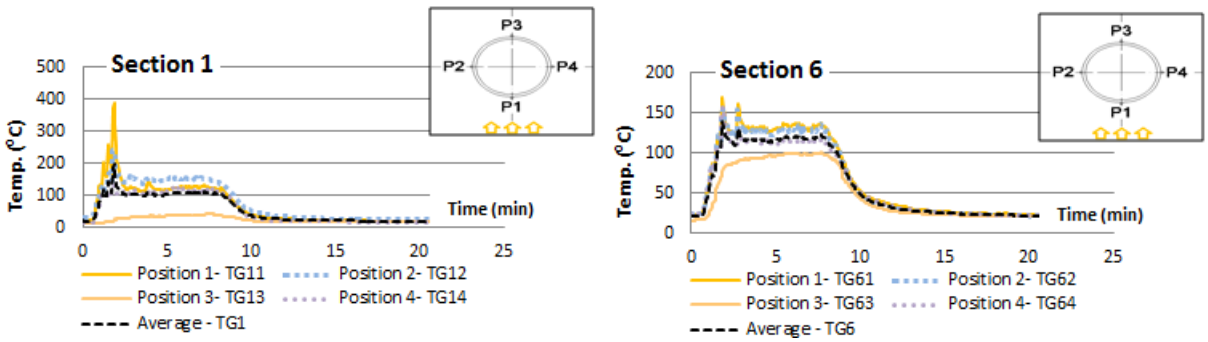


(a) (b)

Figure 47- Thermal gradient in vicinity of the steel sections during test 5: (a) section 1; (b) section 6

### 5.6.4 Analysis of tests results within Group 3

#### 5.6.4.1 Temperatures along the vertical axis of the fire plume

Within the third group of tests, the CHS 245 x 10 steel column was exposed to the same thermal action (1.10 m dia. pool fire at 1.20 m distance), according to different opening sets. Monitored gas temperatures at the vertical axis of the fire plume during tests 7 and 8 are reported in Figure 48.

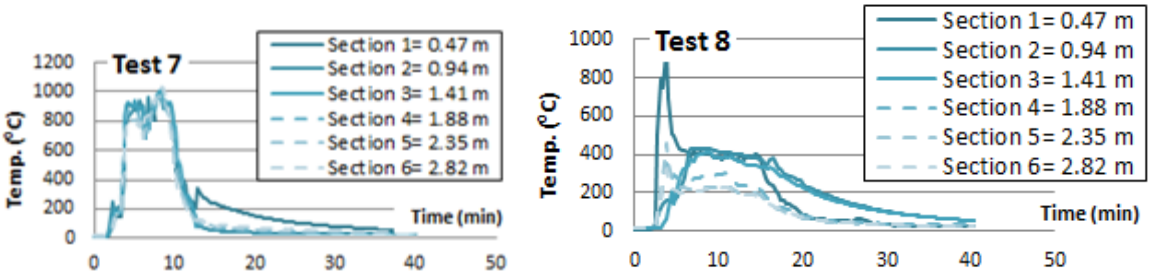


(a) (b)

Figure 48- Temperatures along the vertical axis of the fire plume: (a) test 7; (b) test 8

Localised fire tests within group 3 were intended to simulate localised fire models when the flames reach the compartment ceiling. However, different fire scenarios were accomplished in tests 7 and 8. In test 7 (see Figure 48 (a)), uniform temperatures were measured along the vertical axis of the fire plume, indicating a fire model where the flame reaches the ceiling. In the final stage of test 7 fire development, the gas temperature remained more elevated closer to the fuel surface due to the progressive extinguishment of the fire plume, which no longer reaches the ceiling. On the other hand, temperature measurements during test 8 indicate the occurrence of a fire plume characteristic of small fires not impacting the ceiling, similar to the ones observed during tests 1 to 6.

#### 5.6.4.2 Average steel temperature along the vertical axis of the column

In accordance with the gas temperatures measured along the fire plume, the average temperatures on the steel column shown in Figure 51 are indicative of the distinct fire plumes obtained in tests 7 and 8. In test 7, average steel temperatures increased along the column height; in this scenario, the flames at the ceiling level directly heated the column top, explaining the higher temperatures measured in the top of the steel member. In test 8, the temperatures evolution followed the same behaviour observed in tests 1 to 6. Comparing both situations, higher temperatures were measured in sections 4 to 6 during test 7, whereas higher temperatures were measured in sections 1 to 3 during test 8.

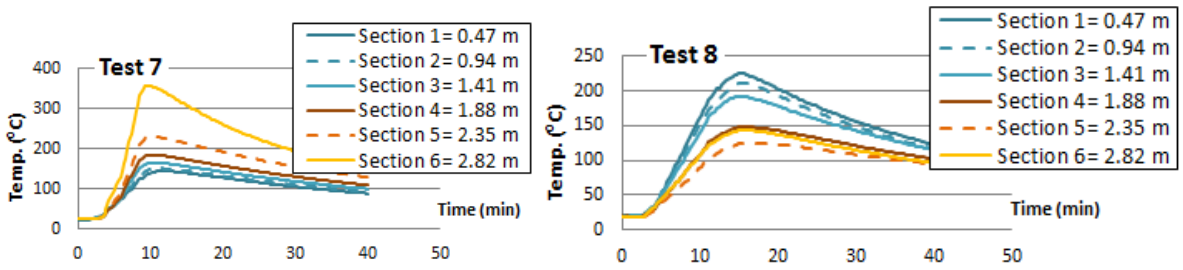


(a) (b)

Figure 49- Average steel temperature along the vertical axis of the column: (a) test 7; (b) test 8

#### 5.6.4.3 Average temperatures in the vicinity of the steel column

In accordance with the measured steel temperatures, temperatures in the vicinity of the steel column during test 7 increased along the column as observed in Figure 52 (a). During test 8, the temperatures in the vicinity of the column presented some uniformity as shown in Figure 52 (b), similarly to the results obtained in the first and second groups of tests.

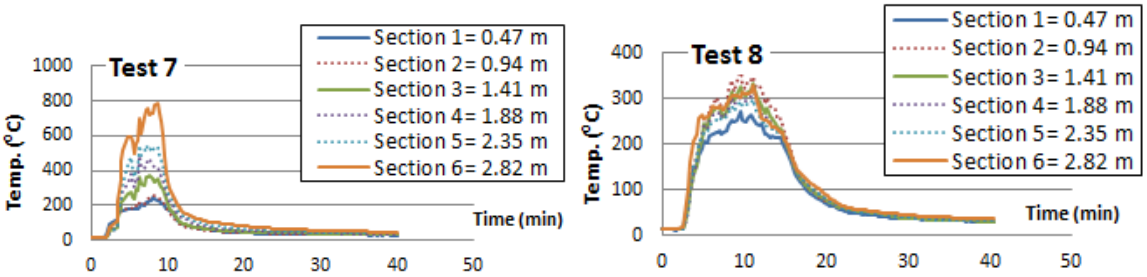


(a) (b)

Figure 50- Average temperatures in vicinity of the steel column: (a) test 7; (b) test 8

#### 5.6.4.4 Thermal gradient in the steel cross sections

Figure 51 presents the evolution of steel section temperature gradient along the column height, during test 7. In section 1, a huge temperature variation between position 1 and position 3 was verified, in accordance with the results obtained in the first and second groups of tests. However, the temperature gradient along the column height presented distinct evolution from the one observed in the first and second groups of tests: in test 7, as the flames impact the ceiling, the temperature gradient is evident along the total column height. For a higher heat released rate, the measured steel temperatures in section 6 could be uniform; for that to happen, the fire layer at the ceiling level would need to be ticker.

Monitored steel temperatures in column sections 1 to 6 during test 7 may be found in Annex 1. Concerning test 8, the monitored temperatures followed the thermal behaviour verified in tests group 1 and 2.

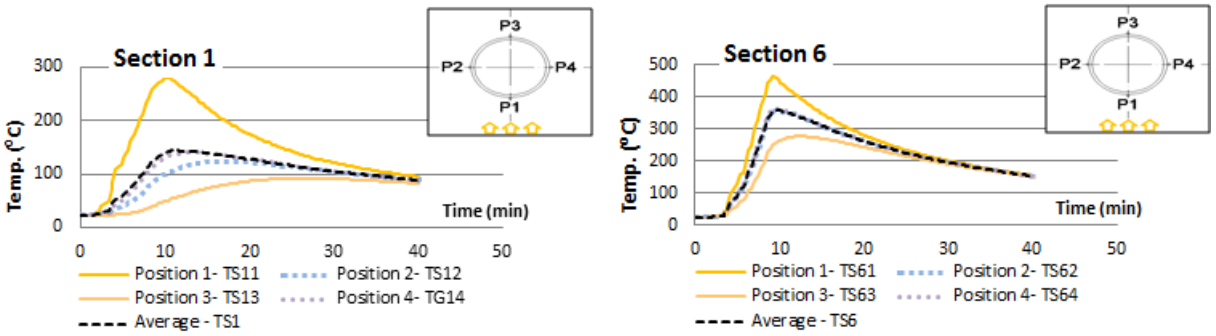


(a) (b)

Figure 51- Thermal gradient in the steel sections during test 7: (a) section 1; (b) section 6.

#### 5.6.4.5 Thermal gradient in the vicinity of the of the steel sections

Concerning the thermal gradient in the vicinity of the steel column during test 7 presented in Figure 52, a few changes were noticed relatively to the first group of tests, where the fire load was positioned at an adjacent position: i) the gas temperature measured in position 3 did not remain constant at the lower section (see Figure 52 (a)), due to the high rate between container and pool diameter, which exposed a bigger part of the column to convective heat flows; and ii) the temperature in the vicinity of section 6 did not reach an uniform configuration, due to the presence of fire at the level of the ceiling.

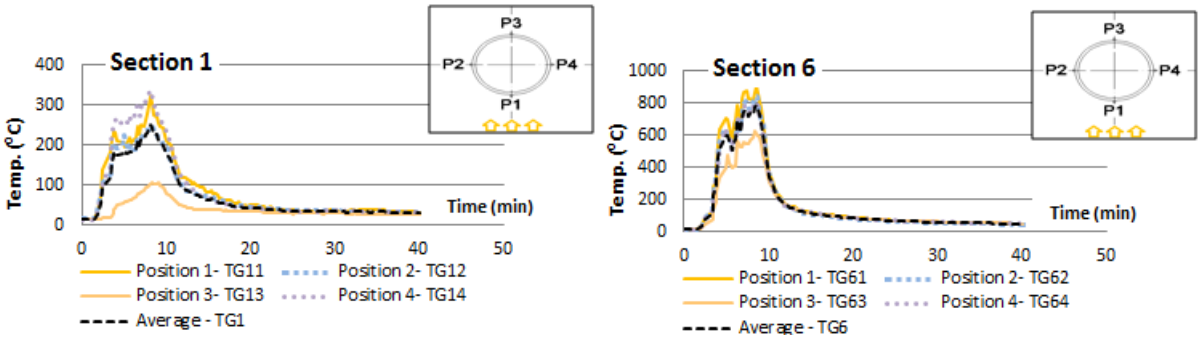


(a) (b)

Figure 52- Thermal gradient in vicinity of the steel sections during test 7: (a) section 1; (b) section 6

## 5.7 Result Analysis

According to the global results, the estimations presented in Table 6 were not accurate. The verified plume heights resulting for pool dia. 0.70 m and pool dia. 1.10 m were in fact lower than 2.28 and 3.46 m respectively (see §5.6.1); this fact indicates an overestimation to the released rate, resulting from the considered efficiency of combustion ($\chi = 1$). But, even if this approach resulted in a conservative estimation, the burning duration was completely

underestimated, once it was verified to be dependent on the ventilation conditions. This fact leaded the CHS steel column to distinct exposure times, each one dependent on the compartment openings set, and consequently more elevated steel temperatures were observer. These estimations are analysed and calibrated according experimental results, in Chapter 6.

Regarding tests group 1, in which the column was exposed to the 0.70 m dia. localised fire under distinct fire compartment openings, the fire development was dependent on the ventilation level: major burning durations occurred for smaller opening areas. Higher burning durations leaded the column to higher exposition time and consequently to higher average steel temperatures. Within group 2, where 0.70 m dia. localised fire was positioned at further distance from the steel column, the fire development was once more conditioned by ventilation conditions, presenting the same behaviour observed in tests group 1.

Comparing the average steel temperatures between groups 1 and 2, a considerable decrease on the average steel temperatures is verified for localised fire at further distance. As observed in all tests from groups 1 and 2, a localised fire exposure leaded the steel column to a non-uniform heating scenario. As a result, an asymmetric distribution of temperatures along the column height was verified. Concerning the relative position between the column and the localised fire, it was noticed that for short distances between the column and the fire (tests group 1) the thermal gradient in the cross sections is significant; whereas for larger distances it becomes less significant (tests group 2). This may be explained by characteristics of radiated heat transfer (see equation (2.3)). For short distances, surfaces exposed to fire received an elevated heat flux by radiation while the unexposed side of the section received a residual flux due to shadow effect. For larger distances, the effect of radiation in the column becomes less significant in the exposed surfaces and thereby, lower gradients were verified.

Concerning tests group 3, in which the steel column was exposed to the 1.10 m dia. localised fire, the temperature evolution along the height of the column was proved to be dependent on the plume model (impacting or not impacting the ceiling). For columns exposed to fires impacting the ceiling, average temperature is constant along the height of the column, with a maximum value at the ceiling level. For columns exposed to small fires not impacting the ceiling, the maximum temperatures are reached in the lower part of the column.

Concerning the specific case scenario of test 4, the wind action may have effects on the heat flux from the localised fire source to the steel column. In the presence of wind, the flame may not remain vertical, changing the thermal radiation to the surrounding column and consequently increasing the thermal exposure. This effect has strong effect into the steel temperatures. Figure 53 illustrates the effects of the wind on a fire plume.

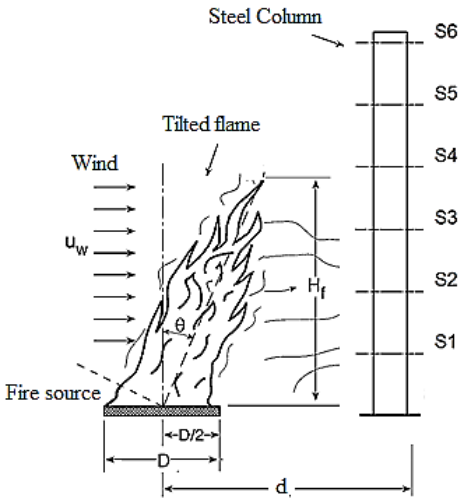


Figure 53- Wind action on a fire plume

## 5.8 Experimental setups after test

During the experimental programme no deformations were observed in the steel column as the highest temperature measured in steel sections during tests did not exceeded 400 ºC. However, the effects of fire exposure were evident in the fire compartment. Figure 54 presents the experimental setup after tests 5 and 7. In test 5, the 0.70 m dia. fire container was positioned 1.20 m away from the steel column whereas in test 7, the 1.10 m dia. fire container was localised at adjacent position to the steel column. The effects of the flame impacting the ceiling during test 7 are evident in Figure 54 (b).

(a) (b)

Figure 54- Experimental setups after tests: (a) test 5; (b) test 7

The effect of the colour variation in the compartment walls, ceiling and in the steel column, caused by fire exposure during the experimental tests, was neglected during the experimental programme. However, this factor may have marginal influence in the heat transfer through radiation.

# 6 VALIDATION OF EXPERIMENTAL RESULTS

## 6.1 Overview

Based on the analytical estimations and numerical tools available in literature, this chapter intends to provide a proper validation and understanding of the experimental results. Estimations for heat release rate were calibrated and compared with experimental results. The distinct burning durations obtained during the tested scenarios, which lead steel columns to higher durations of fire exposure, and consequently to the development of higher steel temperatures, are explained in accordance to a numerical analysis performed by software Ozone (Cadorin, 2003).

## 6.2 Calibration of analytical estimations for thermal actions

The experimental program is based in analytical estimations of thermal actions presented in §5.4. These estimations were based on pool fire theories and presented in Table 6. Using a conservative approach, calculations were made for an ideal combustion efficiency equal to 100 % (corresponding to the assumption of $\chi$=1). However, the temperatures measured during the experimental programme were lower than the ones predicted and the assumption of a 100% combustion efficiency seems unrealistic. So, in order to calibrate the estimated results, combustion efficiency was considered to be around 60% to 80% as suggested by several authors (Byström et al., 2012; Karlsson & Quintiere, 2000). Table 7 presents the calibration of results based on the consideration of different combustion efficiencies: $\chi$=0.6, $\chi$=0.7 and $\chi$=0.8.

Table 7- Calibration of analytical estimations

| D [m] | $\chi$ | $L_f$ [m] Equation (5.1) | $L_f$ < Celling [= 3 m] | Q [MW] Equation (4.5) | V [l] | Burning Duration [min] Equation (4.6) |
|---|---|---|---|---|---|---|
| 0.70 | 0.6 | 1.73 | not impacting ceiling | 0.35 | 12 | 11.08 |
| | 0.7 | 1.88 | not impacting ceiling | 0.41 | | |
| | 0.8 | 2.03 | not impacting ceiling | 0.47 | | |
| 1.10 | 0.6 | 2.61 | not impacting ceiling | 1.01 | 30 | 9.59 |
| | 0.7 | 2.85 | not impacting ceiling | 1.18 | | |
| | 0.8 | 3.07 | impacting ceiling | 1.35 | | |

Table 7 shows that the total length of the flames is much lower for lower rates of combustion effectiveness. In fact, the consideration of 70% of combustion effectiveness leads to the exact total length of flames experimentally measured, L = 1.88 m, for the 0.70 m dia. pool (Figure 33). Concerning the 1.10 m dia. pool, only a rate of combustion higher than 80%, leads the plume to a total length higher than 3 m, situation which represents the localised fire scenario where the flames are impacting the ceiling. This fact justifies the different fire scenarios accomplished (impacting and not impacting the ceiling) in tests 7 and 8, where the same 1.10 m dia. pool fire was used.

According to these calculations, the combustion efficiency was estimated to be 70 % within the first and second groups of tests. Concerning the third group of test, combustion efficiency was estimated as 80 % for test 7 and 70 % for test 8. Based on previous calculations, it was proved that the use of higher combustion efficiency does not necessary lead to a conservative approach of the heat transfer into steel columns. For example, when comparing tests 7 and 8 it is observed that the lower combustion efficiency in test 8 resulted in a completely different plume model due to the reduced flames height. Consequently, the temperature distribution along the steel column is totally different for the two distinct plume models, which may be important for design purposes.

Concerning the burning duration, no direct relationship was found to combustion efficiency. However, the burning time was calculated assuming a fuel controlled burning or, in other words, a fire where the oxygen needed for combustion is constant along the burning duration. This prediction was not verified, due to the range of exposure times verified along the experimental programme.

## 6.3 Numerical analysis of enclosure effects

In order to compare enclosure effects on the burning rates (see §4.3) obtained during the experimental programme, tests 1 to 6 were computed with the zone fire model software *Ozone* (Cadorin, 2003). Tests 7 and 8 were not computed once they were performed with the same fire action, under equal compartment boundaries.

As a zone model, this software uses the equations of mass and energy conservation. These equations allow calculations of mass exchange between the internal gas and the external gas through compartment openings. The energy exchange between the fire, the internal gas, the walls and openings are considered as well. Concerning the localised fires, *Ozone* presents a localised fire model, but only to the specific case of beams subjected to a localised fire impacting the ceiling, as specified in EN 1991-1-2 (2002).

As input, compartment data was introduced into the models: i) compartment dimensions, ii) walls, floor and ceiling thermal and geometrical characteristics, iii) opening areas and locations and iv) thermal action. Concerning the thermal action, the localised fire was introduced into the models according to: i) burning area; ii) heat released rate (Q); iii) combustion efficiency (χ), and iv) heat of combustion ($\Delta H_c$= 44.4 [kJ/kg] for diesel). The burning rate was calculated by the software according to the relations between inputted parameters (see equation (4.2)). The thermal actions were computed according to the previous considerations on the combustion efficiency: 70 % for the all the considered tests. Table 8 presents the parameters applied in each simulation. As input requirements, celling openings [$m^2$] were defined according to equivalent diameters [m]; on the other hand, pool fire diameters [m] were converted into the equivalent burning area [$m^2$].

Table 8- Input data

| Group | Test | Openings [m] | Burning area [$m^2$] | Q [MW] | Burning duration [s] |
|---|---|---|---|---|---|
| 1 | 1 | 4.50 m x 2.55 m door | 0.38 | 0.41 | 665 |
| | | 0.60 m x 0.40 m window | | | |
| | 2 | 1.90 m x 2.55 m door | 0.38 | 0.41 | 665 |
| | | 0.60 m x 0.40 m window | | | |
| | | 0.37 m dia. celling opening | | | |
| | 3 | 1.90 m x 2.55 m door | 0.38 | 0.41 | 665 |
| | | 0.60 m x 0.40 m window | | | |
| | | 0.53 m dia. celling opening | | | |
| | 4 | 1.90 m x 2.55 m door opened 37 % | 0.38 | 0.41 | 665 |
| | | 0.60 m x 0.40 m window | | | |
| | | 0.92 m dia. celling opening | | | |
| 2 | 5 | 1.90 m x 2.55 m door | 0.38 | 0.41 | 665 |
| | | 0.60 m x 0.40 m window | | | |
| | | 0.53 m dia. celling opening | | | |
| | 6 | 1.90 m x 2.55 m door opened 53 % | 0.38 | 0.41 | 665 |
| | | 0.60 m x 0.40 m window | | | |
| | | 0.92 m dia. celling opening | | | |

*Ozone* software combines both one and two zone models, as standard procedure. As starting point, the software follows a two-zone fire model but it may develop into a one-zone fire for the following situations according to conditions defined by the software; in the case of study, the lower layer grown up to 80 %, due mainly to the low heat release rates computed, which

represented a criteria of transition from two to one zone model. Therefore, tests were modelled according to a one-zone fire.

One-zone models assume a uniform, time dependent temperature distribution in the compartment. Although this uniform temperature does not simulate a localised fire action in a compartment, the calculation of the oxygen mass balance during each fire test was important in order to study the enclosure effects on the burning rates.

Through the test simulations, a notable decrease in the total oxygen mass of the compartment was verified. However, the oxygen mass loss is logically bigger near the localised fire. Figure 55 presents the variation of oxygen mass during test 1: the initial oxygen mass within the compartment is 80 kg, being reduced until the minimum peak of 70.82 kg. This peak is controlled by ventilation, being lower for compartments with smaller ventilation areas. After the fire exposure, oxygen mass is e re-established within the compartment.

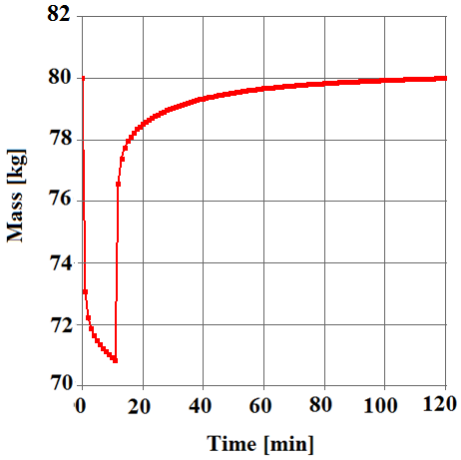


Figure 55- Evolution of Oxygen Mass along test 1

The minimum oxygen peaks obtained by *Ozone* were compared with the experimental burning duration, as presented in Table 9. Through the analysis of results, a direct relationship was found between lower levels of oxygen and higher burning durations, within test groups 1 and 2. The exception was test 1, due to the exceptional volume of fuel used in this test (15 l). Therefore, the enclosure effects on the burning duration are supported by the zone model Ozone.

Table 9- Comparison between minimum oxygen mass and burning duration

| Group | Test | Minimum Oxygen Mass [kg] | Experimental Burning Duration [min] |
|---|---|---|---|
| 1 | 1 | **70.82** | **19.70(*)** |
| | 2 | 67.56 | 15.6 |
| | 3 | 67.65 | 15.6 |
| | 4 | 64.53 | 17.2 |
| 2 | 5 | 67.65 | 9.4 |
| | 6 | 65.72 | 16.5 |
| * Exceptional test where a different volume of fuel was used. | | | |

# 7 CONCLUSIONS AND FUTURE WORKS

## 7.1 Conclusions

The two fire models considered in EN 1991-1-2 (2002) for localised fires scenario allow the quantification of thermal actions for steel beams but not for vertical elements.

The first model, representing a fire plume not impacting the compartment ceiling, allows determining the temperatures along the vertical axis of the plume. However, in a real structural scenario, a column and respective plume are likely to be positioned side by side. Therefore, the temperature estimated by the first model is unlikely to be the boundary temperature of a column subjected to a localised fire. In order to use this plume model, a configuration factor is needed to estimate the radiative heat flux, from the plume to the steel column. Moreover, in the studied case scenarios, the gas temperature in the vicinity of the column was proved to be not uniform as a result of conductive and convective heat flows in the compartment. As the estimation of gas temperatures in the vicinity of the column is a prerequisite for application of the Newton law of cooling, presented in equation (2.2), the heat flux by convection cannot be estimated by Eurocode procedures.

The second model, representing a plume impacting the ceiling, leads to the direct calculation of net heat flux of a structural member placed at the ceiling level. However, the thermal action must be defined along the vertical axis of the column for an accurate design; temperature gradient in the cross sections and along the total height of the column may cause imperfections due to thermal elongation, having effects on the buckling of a load bearing column.

In order to define a localised fire, estimations for heat released rate and burning duration are necessary. Even though the heat released rate may be conservatively estimated according burning properties of the fuel (assuming a total efficiency of combustion($\chi = 1$)), the estimation of burning duration offers bigger problems, once it was verified to be dependent on the ventilation conditions.

According to the global experimental results, a localised fire leads a steel column to a non-uniform heating scenario. As result, an asymmetric distribution of temperatures along the column height is verified. Concerning the relative position between the column and the

localised fire action, it was verified that, for short distances between the column and the fire, the thermal gradient in the cross sections is significant; whereas for larger distances it becomes less significant. This may be explained by characteristics of radiated heat transfer. For short distances, surfaces exposed to fire received an elevated heat flux by radiation, while the unexposed side of the section received a residual flux due to shadow effect. For larger distances, the effect of radiation in the column becomes less significant in the exposed surfaces and thereby, lower temperature gradients were verified.

The temperature evolution along the height of the column was proved to be dependent on the plume model (impacting or not impacting the ceiling). For columns exposed to fires impacting the ceiling, average temperature is constant along the height of the column, with a maximum value at the ceiling level. For columns exposed to small fires not impacting the ceiling, the maximum temperatures are reached in the lower part of the column.

The localised fire development, inside a compartment, was proved to be dependent on the ventilation level: major burning durations occurred for smaller opening areas. Major burning durations leaded the column to higher exposition time and consequently to more elevated steel temperatures. The wind action may have effects on the heat flux from the localised fire source to the steel column. In the presence of wind, the flame may not remain vertical, changing the thermal radiation to the surrounding column and consequently increasing the thermal exposure.

## 7.2 Future works

Eurocode presents general expressions for determination of the heat flux. These expressions derive from the well-known equations for the calculation of the radiative heat flux (Stefan–Boltzmann law) and the convective heat flux (Newton law of cooling). Analytical validation of the experimental results should be performed trough these laws. The most important prerequisites for application of the general expression of net heat flux ($\dot{h}_{net,c}$) presented in EN 1991-1-2 (2002) is the configuration factor; in Annex G it is presented a method to calculate the configuration factor in columns exposed to external fires. Similar studies must be made in order to estimate the configuration factor in localised fire scenario. Figure 56 presents the results of an analytical approach aimed to estimate the configuration factor. This Figure depicts the average steel temperature evolution during test 1 together with its predictions based on the equation of net heat flux ($\dot{h}_{net,c}$) presented in EN 1991-1-2 (2002) – see equation (2.1) – and on the equation of the increase of temperature ($\Delta\theta_{a,t}$) in an unprotected steel member from EN 1993-1-2 (2005) – se equation (2.41). The experimental gas temperatures were used as an input in these formulas, in order to estimate the steel temperature.

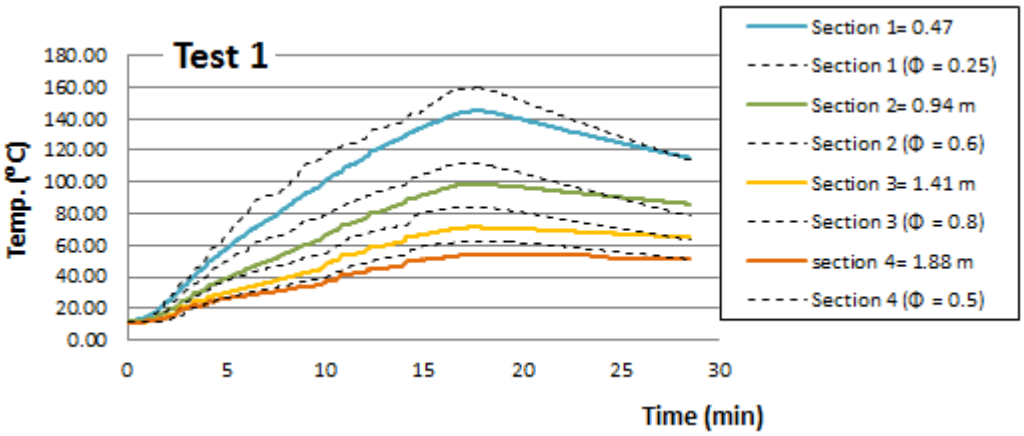


Figure 56- Configuration factors

This simplified approach shown that the configuration factor may be taken as a constant for each section. However it changes according to the height of the column. From this on, parametrical studies must be done in order to evaluate the heat flux into steel columns subjected to localised fires.

Concerning the experimental research, different thermal loads, steel columns and fire locations may be tested in order to evaluate the impacts of these parameters in the thermal response of steel structures subjected to localised fires. It would be interesting to carry out more tests in columns at serviceability state in order to study the effects of non-uniform fire exposure into the deflection of the steel columns.

Furthermore, CFD models may be developed and validated, in order to perform a numerical analysis and subsequent parametrical studies.

# REFERENCES

Babrauskas, V., 2002. Chapter 3 - Heat release rate. In: *SFPE Handbook of Fire Protection Engineering, 3rd edition.* Quincy, MA, EUA: National Fire Protection Association.

Buchanan, A., 2008. The Challenges of Predicting Structural Performance in Fires. *10th International Association for Fire Safety Science Symposium*, pp. 79-90.

Bukowski, R. & Peacock, R., 1989. *Example Cases for the hazard- Fire Hazard Assessment Methot.* U.S.A.: U.S. Department of Commerce.

Byström, A., Sjöström, J., Wickström, U. & Veljkovic, M., 2012. Large scale test to explore thermal exposure of column exposed to localized fire. *Congress: Structures in Fire 2012,* pp. 185-194.

Cadorin, J., 2003. *Compartment fire models for structural engineering,* Université de Liège: Doctorat Thése, Faculté des Sciences Appliqués.

Correia, A., 2011. *Fire resistance of steel and composite steel-concrete columns,* Coimbra: PhD Thesis.

Correia, E., 2007. *Comportamento, análise e procedimentos de automatização no dimensionamento ao fogo de estruturas de aço.* Vitória, Brazil, Master Thesis, pp. 1-5.

Drysdale, D., 1999. *An introduction to fire dynamics.* 2nd ed. New york: John wiley & Sons.

Duff, M. & Towey, J., 2010. *http://www.analog.com.* [Online] Available at: http://www.analog.com/library/analogdialogue/archives/44-10/thermocouple.pdf [Accessed 12 th January 2014].

Efectis Nederland BV, 2011. *http://www.efectis.com.* [Online] Available at: http://www.efectis.com/images/page/1306_summary.PDF [Accessed 6th January 2014].

EN 1990, 2009. *Eurocode - Basis of structural design.* Brussels, CEN.

EN 1991-1-1, 2009. *Eurocode 1 - Design of steel structures – Part 1-1: General actions, Densities, self-weight, imposed loads for buildings.* Brussels: CEN.

EN 1991-1-2, 2002. *Eurocode 1 - Basis of Design and Actions on Structures – Part 1-2: Actions on Structures Exposed to Fire.* Brussels: CEN.

EN 1993-1-2, 2005. *"Eurocode 3 - Design of steel structures – Part 1.2: General rules - Structural fire design".* Brussels: CEN.

EN 1993-1-2, 2005. *Eurocode 3 - Design of steel structures – Part 1.2: General rules - Structural fire design.* Brussels: CEN.

Franssen, J.-M. & Vila Real, P., 2010. *Fire Design of Steel Structures.* 1st edition ed. s.l.:ECCS.

Gutiérrez-Montes, C., Sanmiguel-Rojas, E., Viedma, A. & Rein, G., 2009. Experimental Data and Numerical Modelling of 1.3 and 2.3 MW Fires in a 20 m Cubic Atrium. *Building and Environment 44,* p. 1827–1839.

Haller, M. et al., 2008. *Dissemination of structural fire safety engineering knowledge (DIFISEK),* Brussels: RFCS publications.

Hamins, A. & Burch, R. R., 1996. Introduction. In: *Characteristics of pool fire burning.* Indianapolis, USA: s.n., pp. 1-5.

Haremza, C., Santiago, A. & Silva, L. S. d., 2013. Design Of Steel And Composite Open Car Parks. *Advanced Steel Construction, Vol. 9, Nº 4,* December, pp. 350-368.

Hasemi, Y., 1986. Thermal Modeling Of Upward Wall Flame Spread. *Fire Safety Science 1,* pp. 87-96.

Hasemi, Y., Yoshida, M., Yasui, N. & Parker, W., 4-385. Upward Flame Spread Along A Vertical Solid For Transient Local Heat Release Rate. *Fire Safety Science 4,* pp. 385-396.

Hasemi, Y., Yoshida, M., Yokobayashi, Y. & Wakamatsu, T., 1997. Flame Heat Transfer And Concurrent Flame Spread In A Ceiling Fire. *Fire Safety Science 5,* pp. 379-390.

Hesketad, G., 1998. *Dynamics of the fire plume.* 2815-2833 ed. UK: The Royal Society of London.

ISO 5660-1, 1993. *Fire tests on building materials and structures - Method for measuring the rate of heat release of products.* UK: BSI Bristish Standards.

ISO 834-1, 1999. *Fire-resistance tests - Elements of a building constructions - Part 1: General requirements.* UK: BSI Bristish Standards.

Kamikawa, D., Hasemi, Y., Wakamatsu, T. & Kagiya, K., 2003. Experimental Flame Heat Transfer Correlations For A Steel Column Adjacent To And Surrounded By A Pool Fire. *Fire Safety Science 7,* pp. 989-1000.

Karlsson, B. & Quintiere, J., 2000. Chapter 3 - Energy Release Rates. In: *Enclosure Fire Dynamics.* United States of America: CRC Press LLC.

Lennon, T., 2008. *"Eurocodes: Background and applications" workshop.* Brussels, European Commission press release.

Li, G. & Zhang, C., 2010. *Thermal Response of Steel Columns Exposed to Localized Fires—Numerical Simulation and Comparison with Experimental Results.* Michigan State, United States of America, DEStech Publications, Inc., pp. 35-42.

Outinen, J. et al., 2010. *Seminar on steel structures: design of cold-formed steel structures,* Helsinki: Helsinki University of Technology.

Pchelintsev, A., Hasemi, Y., Wakamatsu, T. & Yokobayashi, Y., 1997. Experimental And Numerical Study On The Behaviour Of A Steel Beam Under Ceiling Exposed To A Localized Fire. *Fire Safety Science 5,* pp. 1153-1164.

PD 6688-1-2, 2007. *Background paper to the UK National Annex to BS EN 1991-1-2.* s.l.:BSI British Standards.

PD 7974-1, 2003. *Application of fire safety engineering principles to the design of buildings.* s.l.:BSI Bristish Standard.

Portas, N., 1964. Industrialização da Construção. *Análise Social*, pp. 90-103.

Pultar, M., Sokol, Z. & Wald, F., 2010. *Temperature of External Column During Fire Test.* Michigan State, United States of America, DEStech Publications, Inc., pp. 83-90.

Santiago, A., 2008. *Behaviour of beam-to-column steel joints under natural fire,* Coimbra: PhD Thesis - Universidade de Coimbra.

Shannon, K. S. & Butler, B., 2003. *A review of error associated with thermocouple temperature measurement in fire environments.* Missoula, Montana, Proceedings of the 2nd International Wildland Fire Ecology and Fire Management Congress and the 5th Symposium on Fire and Forest Meteorology. 7B.4. 16 November 16-20, 2003. American Meteorological Society.

Simões da Silva, L., Simões, R. & Gervásio, H., 2010. Introduction. In: *Design of Steel Structures.* s.l.:ECCS, pp. 1-28.

Sjöström, J., Byström, A., Lange, D. & Wickström, U., 2012. *Thermal exposure to a steel column from localized fires*, Sweden: SPT Report.

Sokol, Z., 2009. *Report 3.2.2.2-13 Simplified Model For Temperature Prediction Of Columns,* Prague: CIDEAS.

Sokol, Z. & Wald, F., 2007. *Report 3.2.2.3-4 Column Temperature In A Localized Fire,* Prague: CIDEAS.

Sugawa, O. & Tobari, M., 2000. *Behavior of Flame/Plume Flow in and near Corner Fire - Entrainment Coefficient For Corner Fire.* San Antonio, U. S., Sheilda L. Bryner, pp. 489-493.

Vehicular Access Standards, 1999. *Parking Standards.* 2nd Edition ed. UK: Department of the Environemnt.

Wald, F. et al., 2009. Temperatures during fire tests on structure and its prediction according to Eurocodes. *Fire Safety Journal*, p. 135–146.

Xhuan Dat, P. & Kang Hai, T., 2011. Membrane actions of RC slabs in mitigating progressive collapse of building structures. *Engineering Structures*, pp. 120-140.

Zhang, C., Li, G.-Q. & Usmani, A., 2013. Simulating the Behavior of Restrained Steel Beams to Flame Impingement from Localized-Fires. *Journal of Constructional Steel Research*, pp. 120-151.

Zhao, Z., 2006. Steel columns under fire - A neural network based strength model. *Advances in Engineering Software 37*, pp. 97-105.

# ANNEX 1- INDIVIDUAL SECTION MEASUREMENTS

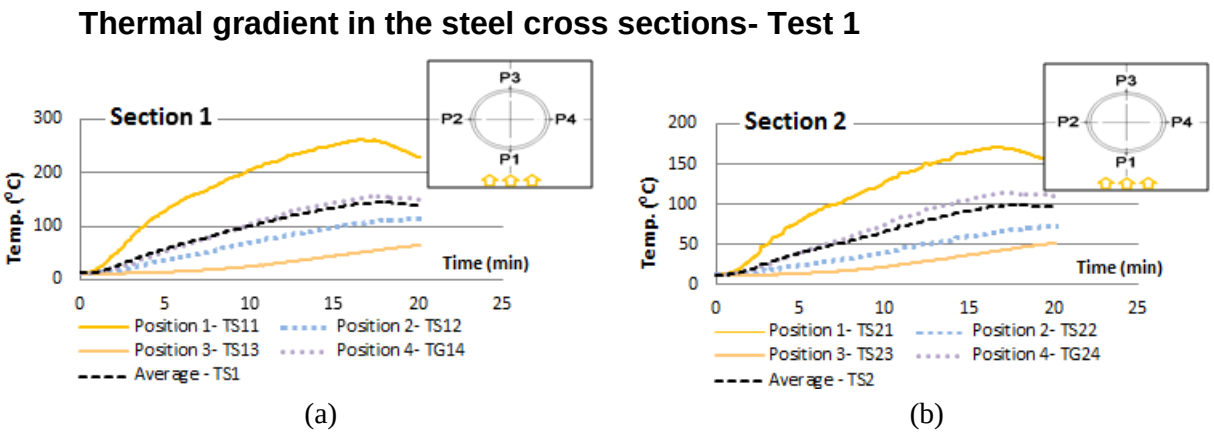


(a) (b)

Figure A1.1- Thermal gradient in the steel sections during test 1: (a) section 1; (b) section 2

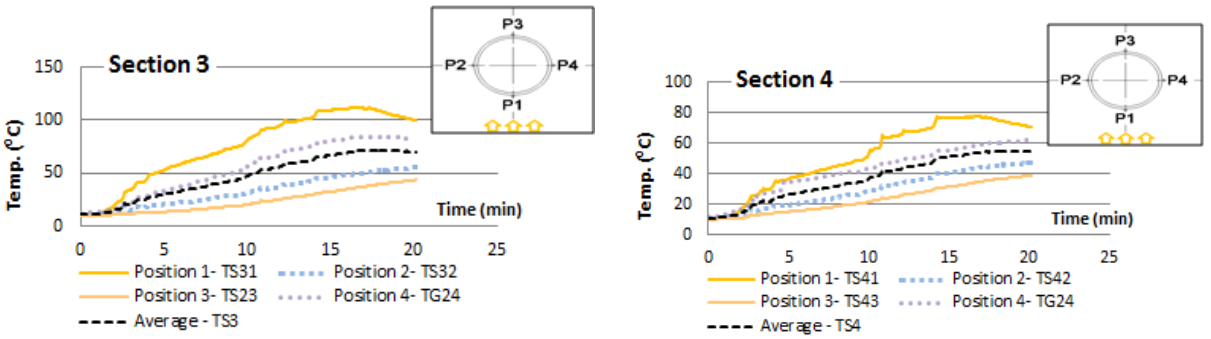


(a) (b)

Figure A1.2- Thermal gradient in the steel sections during test 1: (a) section 3; (b) section 4

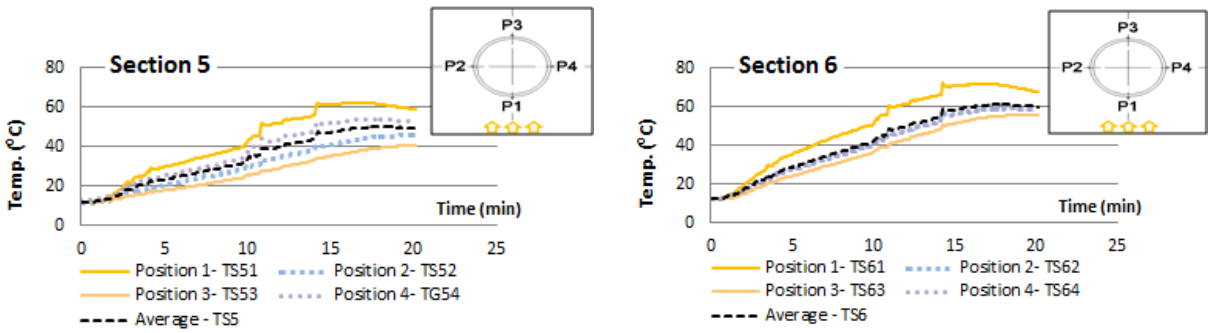


(a) (b)

Figure A1.3- Thermal gradient in the steel sections during test 1: (a) section 5; (b) section 6

## Thermal gradient in the steel cross sections- Test 5

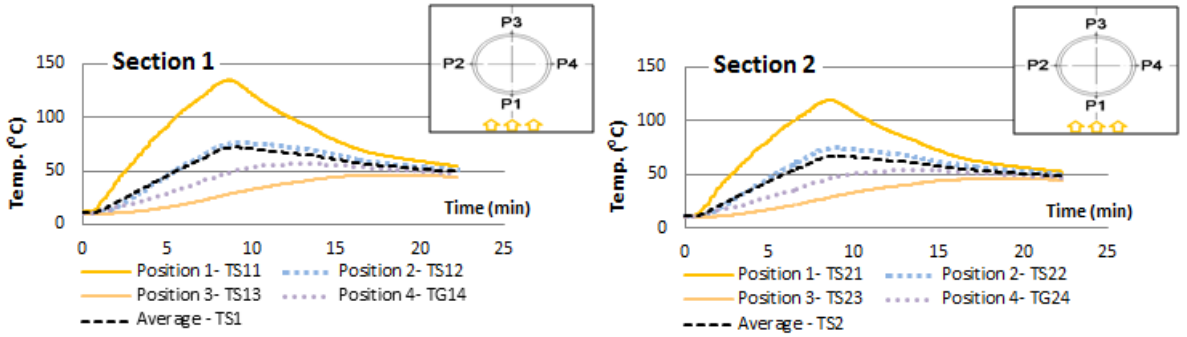


(a) (b)

Figure A1.4- Thermal gradient in the steel sections during test 5: (a) section 1; (b) section 2

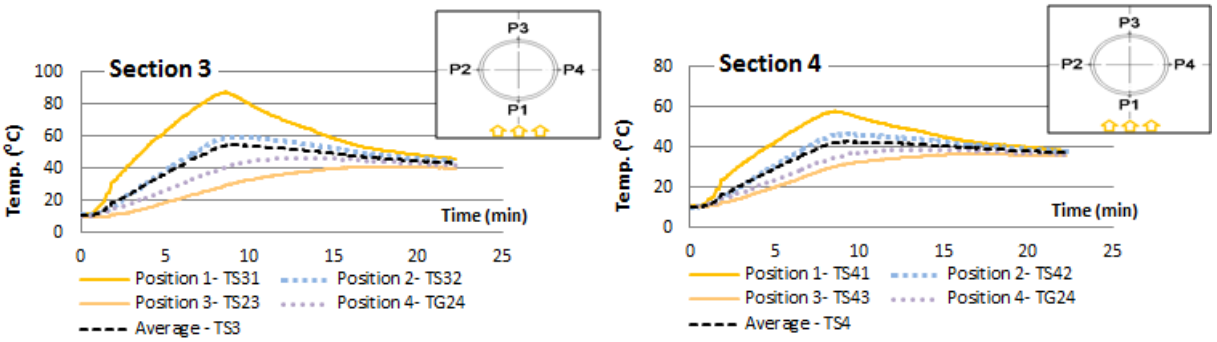


(a) (b)

Figure A1.5- Thermal gradient in the steel sections during test 5: (a) section 3; (b) section 4

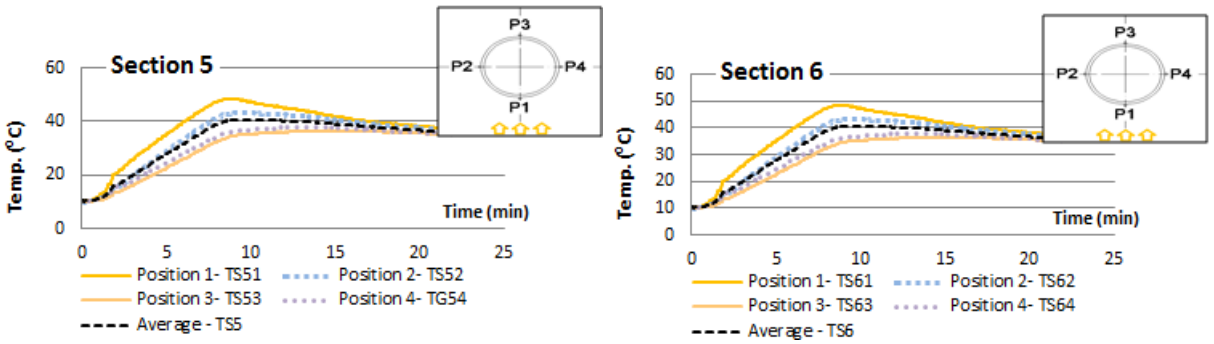


(a) (b)

Figure A1.6- Thermal gradient in the steel sections during test 5: (a) section 5; (b) section 6

## Thermal gradient in the steel cross sections- Test 7

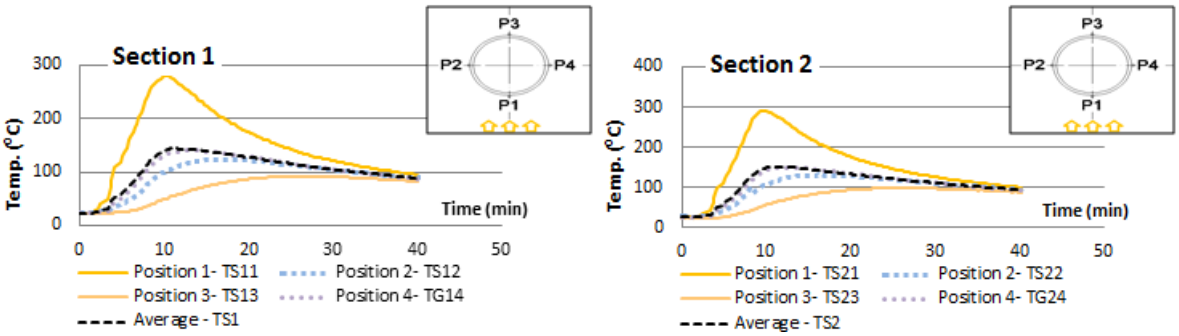


(a) (b)

Figure A1.7- Thermal gradient in the steel sections during test 7: (a) section 1; (b) section 2

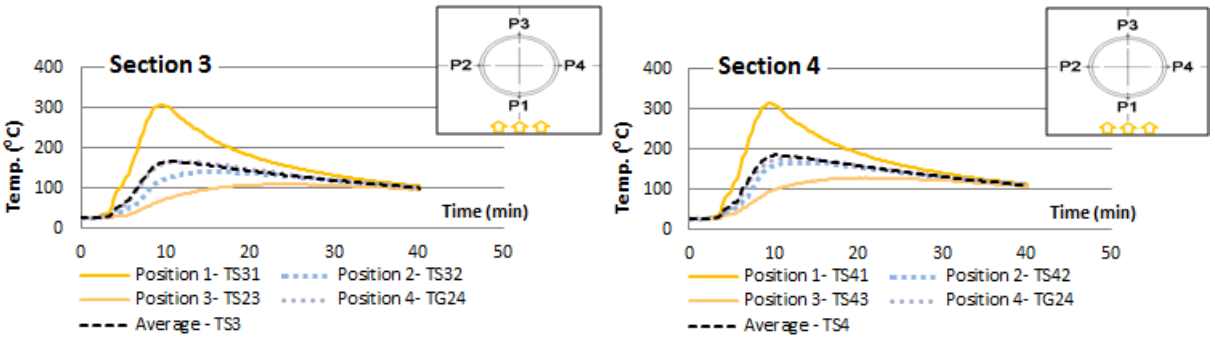


(a) (b)

Figure A1.8- Thermal gradient in the steel sections during test 7: (a) section 3; (b) section 4

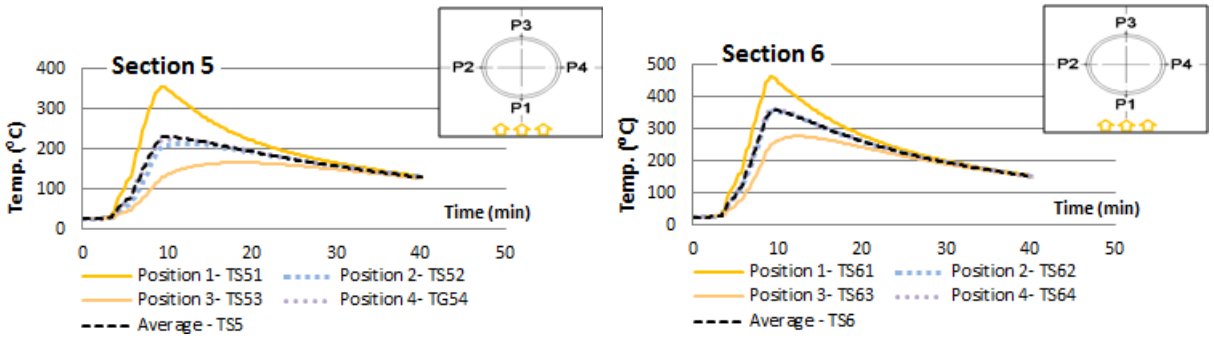


(a) (b)

Figure A1.9- Thermal gradient in the steel sections during test 7: (a) section 5; (b) section 6

## Thermal gradient in vicinity of the steel sections- Test 1

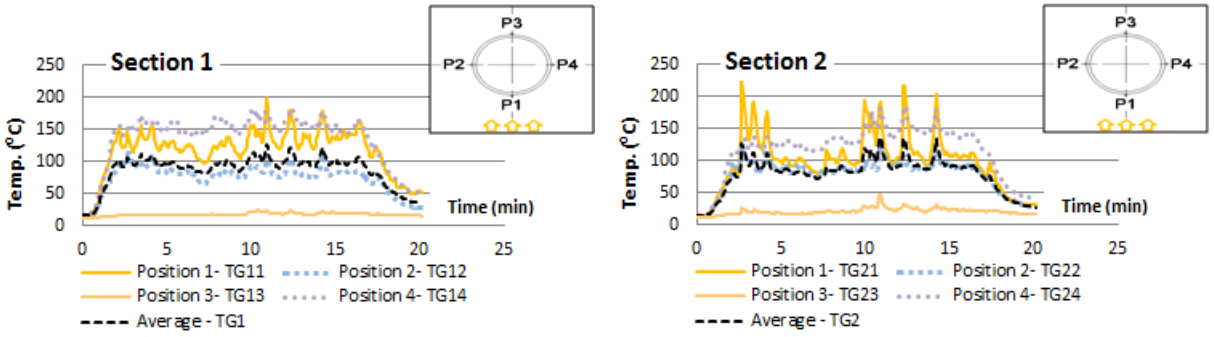


(a) (b)

Figure A1.10- Thermal gradient in vicinity of the steel sections during test 1: (a) section 1; (b) section 2

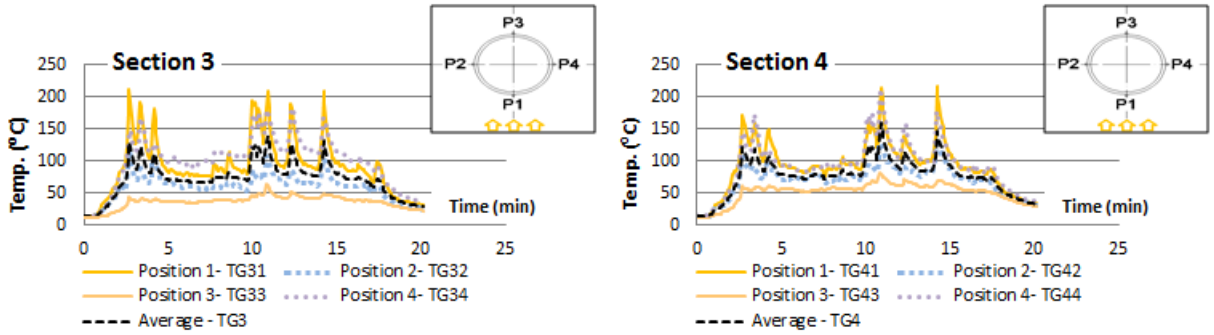


(a) (b)

Figure A1.11- Thermal gradient in vicinity of the steel sections during test 1: (a) section 3; (b) section 4

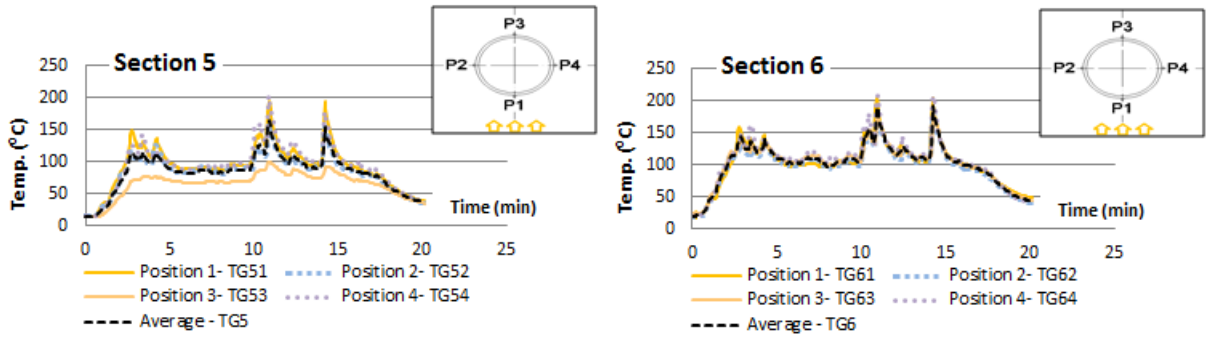


(a) (b)

Figure A1.12- Thermal gradient in vicinity of the steel sections during test 1: (a) section 5; (b) section 6

## Thermal gradient in vicinity of the steel sections- Test 5

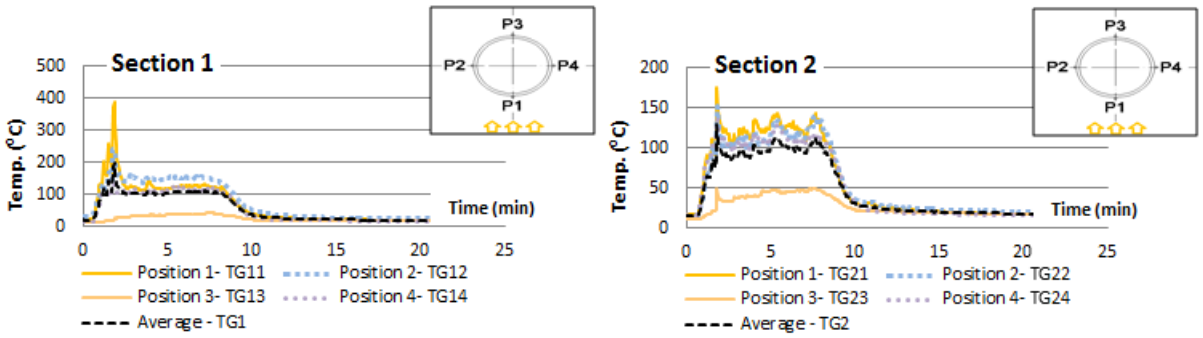


(a) (b)

Figure A1.13- Thermal gradient in vicinity of the steel sections during test 5: (a) section 1; (b) section 2

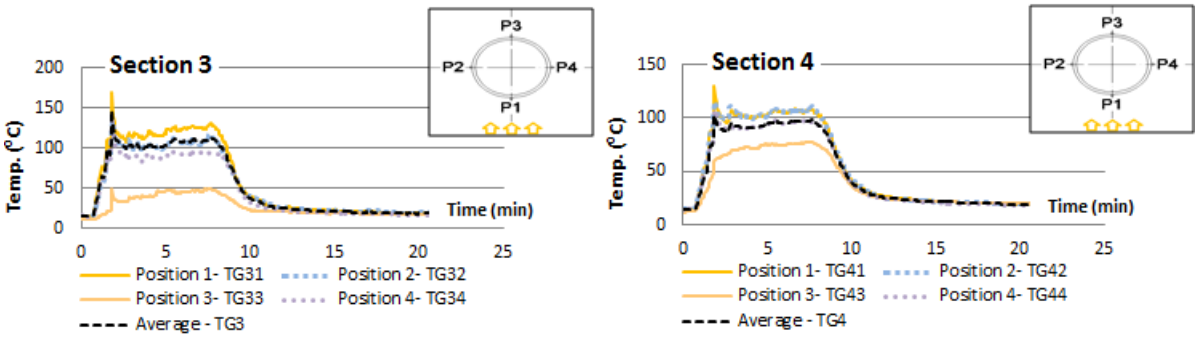


(a) (b)

Figure A1.14- Thermal gradient in vicinity of the steel sections during test 5: (a) section 3; (b) section 4

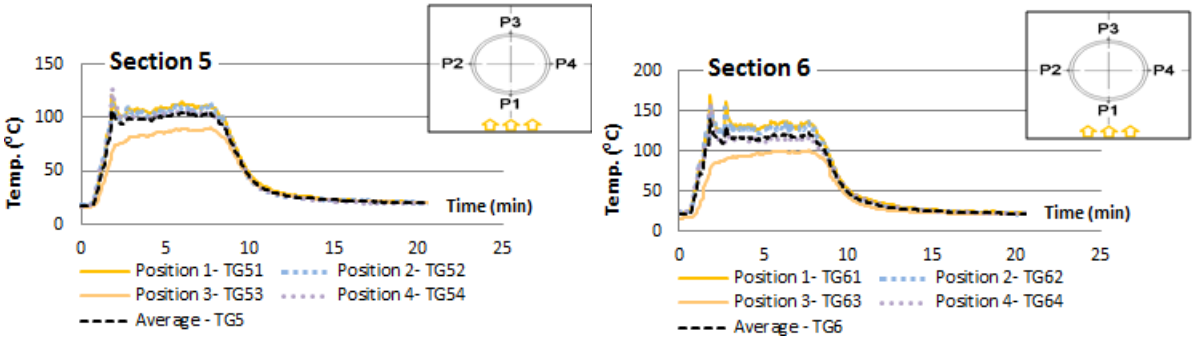


(a) (b)

Figure A1.15- Thermal gradient in vicinity of the steel sections during test 5: (a) section 5; (b) section 6

## Thermal gradient in vicinity of the steel sections- Test 7

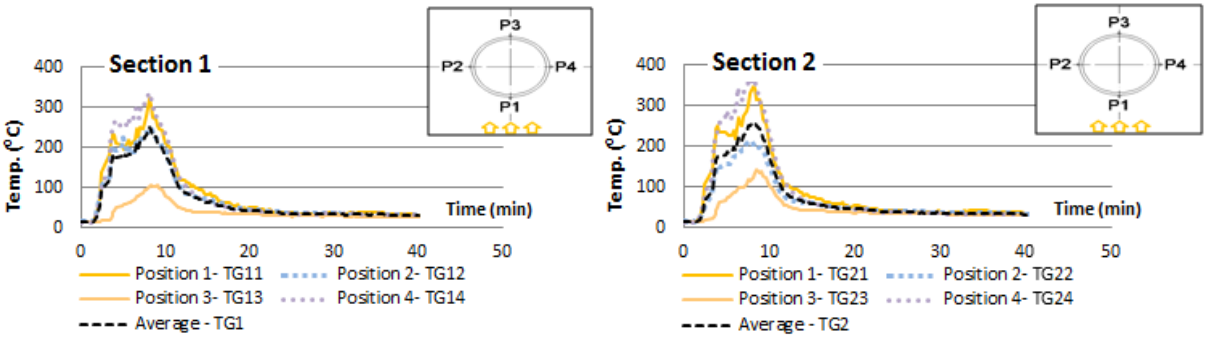


(a) (b)

Figure A1.16- Thermal gradient in vicinity of the steel sections during test 7: (a) section 1; (b) section 2

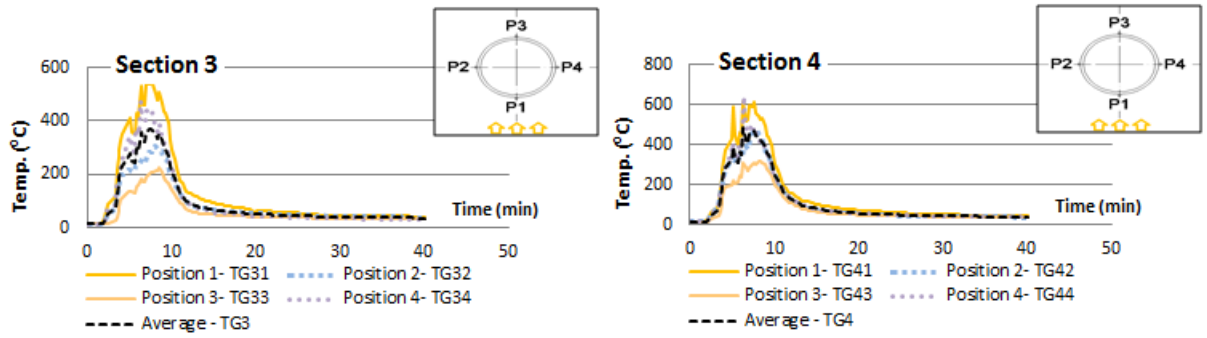


(a) (b)

Figure A1.17- Thermal gradient in vicinity of the steel sections during test 7: (a) section 3; (b) section 4

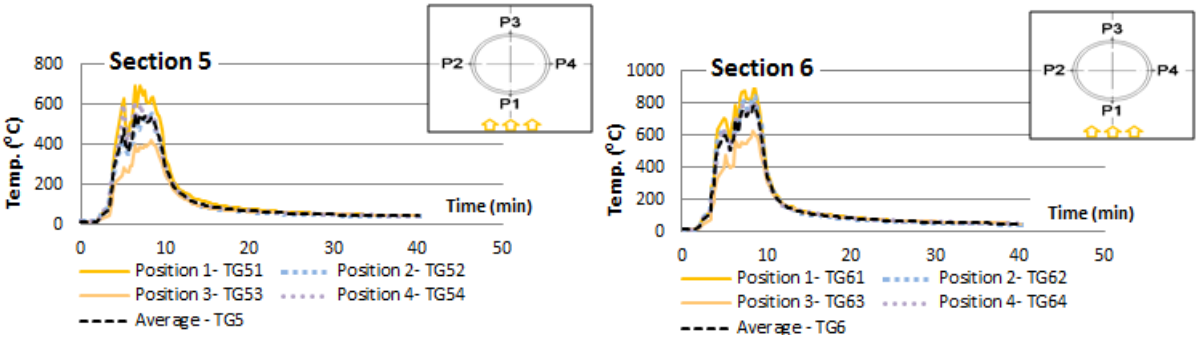


(a) (b)

Figure A1.18- Thermal gradient in vicinity of the steel sections during test 7: (a) section 5; (b) section 6